The many phases of QCD_3 and dualities

Abdullah Khalil Hassan Ibrahim

Department of Mathematical Sciences

University of Liverpool

Thesis submitted in accordance with the requirements of the University of Liverpool for the degree of Doctor of Philosophy in

Theoretical Physics

February 2022

I would like to dedicate this thesis to my wife, Hager.

Declaration

I hereby declare that except where specific reference is made to the work of others, the contents of this dissertation are original and have not been submitted in whole or in part for consideration for any other degree or qualification in this, or any other University. This dissertation is the result of my own work and includes nothing which is the outcome of work done in collaboration, except where specifically indicated in the text.

Abdullah Khalil Hassan Ibrahim

February 2022

Acknowledgements

This project would not have been possible without the support of many people. Many thanks to my adviser, Radu Tatar, who read my revisions and helped make the project possible through his suggestions. I would also like to thank the University of Liverpool and the department of Mathematical Sciences for providing me with the financial means to complete this project. And finally, thanks to my wife, parents, and friends who endured this long process with me, always offering support.

The many phases of QCD_3 and dualities

Abdullah Khalil Hassan Ibrahim

Abstract

We investigate the low-energy physics of QCD-like theories in $2+1$ dimensions coupled to a Chern-Simons term and fermion(s) in various representations of the gauge group ($SU(N)$). The level/rank dualities and Boson/Fermion dualities provide access to such theories.

We first discuss the phase diagram of QCD_3 with fermions in the fundamental representation and a Chern-Simons term with level k [1]. The theory is well-described via topological field theories in the semiclassical limits. For sufficiently low k values, a new quantum phase is introduced for small fermion mass to cover the entire phase diagram. The quantum phase is conjectured to be a non-linear sigma model. We also discuss the extension of this work by including two sets of fermions with different masses, resulting in a two-dimensional phase diagram [2].

We add to these previous studies the analysis of the phase diagrams of a theory with three distinct groups of fermions described in my work [3]. The phase diagram becomes three-dimensional, with multiple topological field theories and different shapes of quantum regions: cuboid, planar, and linear sigma models. We discuss the consistency of the phase diagrams with boson/fermion dualities, in addition to their reduction to one and two-family diagrams.

We consider in detail the analysis of QCD_3 with a Majorana fermion in the adjoint representation [4]. The theory has an $\mathcal{N}=1$ supersymmetry for a particular choice of the fermion mass. Supersymmetry is spontaneously broken for a certain k limit, and the infrared description requires a new quantum phase to fill the phase diagram with the right symmetries and anomalies. We also address the possibility of building a two-dimensional phase diagram with the adjoint matter, which is the subject of a forthcoming publication [5]. The phases of this theory on the diagonal line of the two-dimensional phase diagram have also been investigated [6].

Table of contents

List of figures

List of tables

Chapter 1

Introduction

Quantum Field Theory (QFT) has become the centrepiece of theoretical physics for the past fifty years. Originally, QFT was developed to describe the dynamics of elementary particles. It has since become an indispensable tool in modern physics fields such as statistical physics, condensed matter physics, cosmology and has influenced certain advances in pure mathematics.

However, QFTs are exceptionally difficult to handle. There are extremely few explicit computations that can be performed, and those that can are often simply asymptotic approximations to physical observables. For a long time, symmetries were the most significant tool for understanding systems within the QFT framework, and supersymmetry, in particular, has played an essential part in these studies. Of contrast, the fundamental problems in quantum field theory usually address the dynamics of strongly interacting systems. In many cases, especially outside of supersymmetry, this renders exact computations unfeasible. One of these strongly-coupled systems is the interaction of quarks and anti-quarks, which can be adequately explained by Quantum Chromodynamics (QCD).

Moving from strongly to weakly coupled systems has thus been the key to simplifying computations and providing access to some physical observables. This is possible within the framework of dualities, particularly S-dualities in which two theories might flow to the same fixed point in the infrared (IR). The most well-

known S-duality is the Seiberg duality, which is a four-dimensional duality between two supersymmetric theories. Theory A is an $\mathcal{N} = 1$ supersymmetric quantum chromodynamics (SQCD) with $SU(N)$ gauge group coupled to F flavours of fundamental chiral multiplets and F flavours of antifundamental chiral multiplets. The dual theory B is a $\mathcal{N} = 1$ theory with gauge group $SU(F - N)$ (i.e. $F - N$ colours) and F flavours [7–9]. The original theory is strongly coupled with electric description, whereas the dual description is weakly coupled and represents a magnetic phase.

Many supersymmetric dualities in 4d have developed since the conjecture of Seiberg duality and their generalization to three dimensions has also been of significant interest [10–18]. The success of these supersymmetric dualities in both three and four dimensions motivates theoretical physicists to seek non-supersymmetric dualities, particularly in three dimensions. In 3d, one may consider adding the Chern-Simons term, which provides a topological feature for three-dimensional theories. In the last five years, the search for dualities inside theories with a topological phase in the IR has been an important direction of research. The success in finding dualities in $2 + 1$ dimensions has advanced our understanding of the dynamics and phases of strongly coupled theories such as QCD_3, which is the central focus of this thesis.

The remainder of this chapter offers an outline of the dynamics and topological nature of the Chern-Simons theories. We also look at the dualities between $2 + 1$-dimensional Chern-Simons theories, such as the level/rank dualities and Aharony dualities. We also go through how to analyze QFT in $2 + 1$ dimensions. In chapter 2, we review the work done to investigate the phases and transitions that occurs in the phase diagram of a QCD-like theory in $2+1$ dimensions coupled to a number of flavours in the fundamental representation of the gauge group. A symmetry-breaking scenario to the global symmetry is used to obtain the complete phase diagram. We also go over the tests that have been undertaken to ensure that the phase diagram is legitimate in cases where the phase diagram is only

conjectural. In chapter 3, we extend the work in chapter 2 to include three families of fundamental flavours with three different masses where the phase diagram becomes three-dimensional. We discuss all the phases in the three-dimensional phase diagram and the consistency checks for validity. In chapter 4, we discuss the analysis and phases of QCD in $2+1$ dimensions when adjoint matter (Majorana fermion) is introduced. We also go through the process of adding another fermion of the same mass and explain the duality chain notion. We discuss the possibility of obtaining a two-dimensional phase diagram when the extra adjoint fermion has a different mass. Finally, we summarise our study and provide suggestions for further research on this topic of interest.

1.1 Aspects of quantum field theories in $2+1$ dimensions

In $2+1$ dimensions, the Dirac fermions are two-component spinors defined by the equations

$$(i\gamma^\mu\partial_\mu - e\gamma^\mu A_\mu - m)\,\psi = 0 \quad \text{or} \quad i\partial_0\psi = \left(-i\vec{\alpha}\cdot\vec{\nabla} + m\beta\right)\psi\,, \tag{1.1}$$

where $\vec{\alpha} = \gamma^0\vec{\gamma}$, $\beta = \gamma^0$. γ^μ are the γ-matrices satisfying the following commutation relations

$$\begin{aligned} \{\gamma^\mu, \gamma^\nu\} &= 2\eta^{\mu\nu}\,, \\ \gamma^\mu\gamma^\nu &= \eta^{\mu\nu} - i\epsilon^{\mu\nu\sigma}\gamma_\sigma\,, \\ \mathrm{tr}\,(\gamma^\mu\gamma^\nu\gamma^\sigma) &= -2i\epsilon^{\mu\nu\sigma}\,. \end{aligned} \tag{1.2}$$

The Minkowskian metric $\eta^{\mu\nu}$ has the following signature

$$\eta^{\mu\nu} \equiv diag(1,-1,-1)\,. \tag{1.3}$$

In $2+1$ dimensions, there is no notion of chirality, where one can not find a γ^5 that commutes with all the γ-matrices since $i\gamma^0\gamma^1\gamma^2 = \mathbb{1}$. The γ-matrices can be expressed in two different representations: the Dirac representation with γ-matrices

$$\gamma^0 = \begin{pmatrix} 1 & 0 \\ 0 & -1 \end{pmatrix}, \gamma^1 = \begin{pmatrix} 0 & i \\ i & 0 \end{pmatrix}, \gamma^2 = \begin{pmatrix} 0 & 1 \\ -1 & 0 \end{pmatrix}. \tag{1.4}$$

The Dirac fermions are specified by $\bar{\psi} = \left(\psi^\dagger\right)^T \gamma_0$, where T and $\dagger$ denote the transpose and the hermitian adjoint respectively. The other representation describes the Majorana fermion where equation (1.1) has an imaginary β and real α. The γ-matrices become

$$\gamma^0 = \begin{pmatrix} 0 & -i \\ i & 0 \end{pmatrix}, \gamma^1 = \begin{pmatrix} i & 0 \\ 0 & -i \end{pmatrix}, \gamma^2 = \begin{pmatrix} 0 & i \\ i & 0 \end{pmatrix}. \tag{1.5}$$

The Majorana fermion λ is a real two-component fermion field with the conjugation operation $\bar{\lambda} = \lambda^T\gamma_0$. The Lagrangian of the massive Majorana fermion is then

$$\mathscr{L}_\lambda = \frac{i}{2}\bar{\lambda}\gamma^\mu\partial_\mu\lambda + \frac{m}{2}\bar{\lambda}\lambda\,. \tag{1.6}$$

In $2+1$ dimensions, the actions of the discrete symmetries $\mathcal{T}$, $\mathcal{C}$, and $\mathcal{P}$ (time-reversal, charge conjugation, and parity) are described as follows:

- **Parity** $\mathcal{P}$: Performing the reflection in two spatial dimensions is equivalent to rotation. As a result, the parity transformation is specified by a reflection on only one of the spacial components in $2+1$ dimensions. The parity transformation then takes the form

$$\begin{aligned} \mathcal{P}: \quad (x^0, x^1, x^2) &\longrightarrow (x^0, -x^1, x^2)\,, \\ (A^0, A^1, A^2) &\longrightarrow (A^0, -A^1, A^2)\,, \end{aligned}$$

$$\psi \longrightarrow \gamma^1 \psi \,,$$
$$\lambda \longrightarrow i\gamma^1 \lambda \,. \tag{1.7}$$

A very important term that we will discuss later takes the form of $\epsilon^{\mu\nu\rho} A_\mu A_\nu A_\rho$, where A_μ is a gauge field. This term becomes $-\epsilon^{\mu\nu\rho} A_\mu A_\nu A_\rho$ under parity transformations, which means that it breaks parity symmetry. We also notice that the mass term breaks parity where $\bar{\lambda}\lambda \to -\bar{\lambda}\lambda$.

- **Charge conjugation** $\mathcal{C}$: Charge conjugation is a transformation under which a Dirac fermion becomes anti-fermion. The Dirac equation of the anti-particle is then

$$(i\gamma^\mu \partial_\mu + e\gamma^\mu A_\mu - m)\,\psi_c = 0 \,, \tag{1.8}$$

where $\psi_c = \mathcal{C}\gamma^0 \psi^*$, $\mathcal{C}$ is the charge conjugation matrix which is chosen to be γ^2 for the Dirac representation. The mass term preserves the charge conjugation symmetry.

- **Time-reversal** $\mathcal{T}$: The time-reversal is a transformation $x^0 \to -x^0$. However, one would avoid taking $p^0 \to -p^0$ when performing this transformation, so we also take $i \to -i$. The transformations under time-reversal are specified by

$$\begin{aligned} \mathcal{T}: \quad (x^0, x^1, x^2) &\longrightarrow (-x^0, x^1, x^2) \,, \\ (A^0, A^1, A^2) &\longrightarrow (A^0, -A^1, -A^2) \,, \\ \psi &\longrightarrow \gamma^2 \psi \,, \\ \lambda &\longrightarrow i\gamma^0 \lambda \,. \end{aligned} \tag{1.9}$$

The fermion mass term also breaks time-reversal.

We notice that the fermion mass term breaks both parity and time-reversal symmetries. Some discrete anomalies are introduced when parity and time-reversal

symmetries are broken; matching these anomalies is crucial for verifying suggested quantum field theories phases.

1.2 Chern-Simons Theories

The Chern-Simons (CS) theory is a quantum gauge theory with a surprisingly subtle action that describes the dynamics of quantum field theories in two spatial dimensions. The topological structure of the Chern-Simons theories gives access to non-trivial examples of quantum field theories. It also has a wide range of applications in different aspects of theoretical physics, most notably within condensed matter and String Theory, where it is used to explain the quantum hall effect [19–23].

Chern and Simons started to study the three-form in three dimensions [24]. The integral of the Chern-Simons three-form on a given manifold is used to formulate a gauge theory, which added a physical significance to the Chern-Simons term. In [25], an abelian gauge theory with a pure Chern-Simons term was introduced, followed by the formulation of the non-abelian Chern-Simons theory in [26–28]. The latter becomes of interest when Stanley Deser, R. Jackiw, and S. Templeton [28, 29] found that the gauge field in $2+1$ dimensions acquires a mass from the Chern-Simons term. Later on, Witten endorses the significance of Chern-Simons theory by arguing that it is exactly solvable and describing its implications for three-dimensional geometry, particularly the understanding of the Jones polynomials of knot theory in three-dimensions [30]. Witten was also able to develop a two-dimensional conformal field theory (CFT) based on his understanding of the Chern-Simons theory.

The main idea is that in $2+1$ dimensions, a new term can be added to the Lagrangian without violating gauge invariance. This is known as the Chern-Simons term, and it takes the form $A_\mu \partial_\nu A_\sigma$ with its permutations, where A_μ is the gauge field (the photon in this case). In this section, we provide a brief overview of

the kinematics and dynamics of Chern-Simons theories, based primarily on the discussions in these review articles [22, 23, 31].

1.2.1 Dynamical mass generation for the photon

Let us begin with the most basic scenario, in which a gauge field gets a dynamical mass from the CS term. Consider a pure Maxwell gauge theory with a Lagrangian $-\frac{1}{4e^2} f_{\mu\nu} f^{\mu\nu}$, where $f_{\mu\nu} = \partial_\mu A_\nu - \partial_\nu A_\mu$ is the abelian field strength, and e^2 is the electromagnetic coupling constant. In 2+1 dimensions, we add the CS term to the Lagrangian with a coupling κ to be

$$\mathscr{L}_{CS}^{U(1)} = -\frac{1}{4e^2} f_{\mu\nu} f^{\mu\nu} + \kappa \epsilon^{\mu\nu\sigma} A_\mu \partial_\nu A_\sigma \,, \tag{1.10}$$

where $\epsilon^{\mu\nu\sigma}$ is the antisymmetric Levi-Civita tensor. The equations of motion are not $\partial_\mu f^{\mu\nu} = 0$, but rather

$$\partial_\mu f^{\mu\nu} + 2\kappa e^2 \epsilon^{\nu\alpha\beta} f_{\alpha\beta} = 0 \,. \tag{1.11}$$

In 2+1 dimensions e^2 has a dimension of mass. This tells us that the gauge field A is no longer massless, i.e. the CS term gives a mass of $2\kappa e^2$ to the photon. One can see the origin of this mass by simply calculating the photon propagator. This can be done by adding a gauge fixing term to the Lagrangian $-\frac{1}{\zeta e^2}(\partial_\mu A^\mu)^2$, where *zeta* is the gauge parameter with zero value for the Landau gauge. The photon with momentum p has a propagator

$$D_{\mu\nu} = e^2 \left[\frac{p^2 g_{\mu\nu} - p_\mu p_\nu - 2i\kappa e^2 \epsilon_{\mu\nu\sigma} p^\sigma}{p^2 (p^2 - (2\kappa e^2)^2)} + \zeta \frac{p_\mu p_\nu}{(p^2)^2} \right] . \tag{1.12}$$

The propagator in equation (1.12) has a pole exactly at the photon mass-squared $p^2 = (2\kappa e^2)^2$. The photon becomes infinitely massive in the limit $e^2 \to \infty$ and the theory will not contain any physical excitations.

1.2.2 Non-Abelian Chern-Simons theory

Let us now consider a non-abelian CS gauge theory in 2+1 dimensions by writing the Lagrangian in the trace (Tr) form to be

$$\mathscr{L}_{CS}^{SU(N)} = \kappa\epsilon^{\mu\nu\sigma}\mathrm{Tr}\left(A_\mu\partial_\nu A_\sigma + \frac{2}{3}A_\mu A_\nu A_\sigma\right), \tag{1.13}$$

where $A_\mu = A_\mu^a T^a$, $a = 1, \ldots, N$ is the color index, and $T^a \in SU(N)$ are the generators of the $SU(N)$ gauge group with the following identities

$$\begin{aligned}\left[T^a, T^b\right] &= f^{abc}T^c\,,\\ \mathrm{Tr}\left(T^aT^b\right) &= -\frac{1}{2}\delta^{ab}\,,\\ \left(T^a\right)^\dagger &= -T^a\,.\end{aligned} \tag{1.14}$$

The equations of motion of this Lagrangian looks similar to the abelian case and can be found by applying an infinitesimal transformation to the gauge field. The equation of motion is then

$$\kappa\epsilon^{\mu\nu\sigma}\mathcal{F}_{\nu\sigma} = J^\mu\,, \tag{1.15}$$

where $\mathcal{F}_{\mu\nu} = \partial_\mu A_\nu - \partial_\nu A_\mu + [A_\mu,\, A_\nu]$ is the non-Abelian field strength, and J^μ is the non-Abelian current following the covariant current conservation $D_\mu J^\mu = 0$.

Let us now check the gauge invariance by applying a gauge transformation $g \in SU(N)$ such that $A_\mu \to A_\mu^g \equiv g^{-1}\left(A_\mu + \partial_\mu\right)g$, the change in the Lagrangian is then

$$\delta\mathscr{L}_{CS}^{SU(N)} = -\frac{\kappa}{4\pi}\epsilon_{\mu\nu\sigma}\partial_\mu\mathrm{Tr}\left(\partial_\nu g g^{-1}A_\sigma\right) - \frac{\kappa}{3}\epsilon^{\mu\nu\sigma}\mathrm{Tr}\left[\left(g^{-1}\partial_\mu g\right)\left(g^{-1}\partial_\nu g\right)\left(g^{-1}\partial_\sigma g\right)\right]. \tag{1.16}$$

The first term vanishes under some boundary conditions because it is a total derivative, while the second term is the winding number density $w(g)$ of the group

element $g \in G$, for a general gauge group G [32]

$$w(g) = \frac{1}{24\pi^2}\epsilon^{\mu\nu\sigma}\mathrm{Tr}\left[\left(g^{-1}\partial_\mu g\right)\left(g^{-1}\partial_\nu g\right)\left(g^{-1}\partial_\sigma g\right)\right] . \tag{1.17}$$

In the action form, the second term gives the winding number ν. The number of times the map image (g) wraps around the gauge group is described by the winding number. The change in the action becomes

$$\delta S_{CS} = -8\pi^2\kappa\nu\,. \tag{1.18}$$

In path integral formalism, one needs the measure $[\mathcal{D}A]\, e^{iS_{CS}[A]}$ to be invariant under gauge transformation, so we require δS_{CS} to be an integer multiplied by 2π. Hence, one must choose the coupling κ to be $integer/4\pi$. Then we rewrite $\kappa = k/4\pi$, where k is the famous Chern-Simons level. From now on, we label the CS gauge theory with a gauge group G and CS level k to be G_k.

It is worth emphasising that the CS action does not depend on the metric of the space-time manifold but rather on its topology. As a result, the theory has topological invariants that cannot be ignored in low-energy effective action, and it is thus called topological [30].

1.2.3 The topological aspect of Chern-Simons theories

To understand the topological nature of the Chern-Simons theory, we compare the kinetic term of the Maxwell theory to the Chern-Simons term when the theory is promoted to curved space-time (i.e. coupled to a background metric $g_{\mu\nu}$). The action term of the Maxwell theory in curved space-times is then

$$S_M = -\frac{1}{4e^2}\int \sqrt{-g}g^{\mu\rho}g^{\nu\sigma}f_{\mu\nu}f_{\rho\sigma} \tag{1.19}$$

while the action of the abelian Chern-Simons theory becomes

$$S_{CS} = \frac{k}{4\pi} \int A \wedge dA \tag{1.20}$$

where $A \wedge dA$ is a 3-form, and the integral is over any $2+1$-dimensional manifold. The difference between the two actions is easily noticeable; the Maxwell action is dependent on the metric g, which raises the indices of $f_{\mu\nu}$ for contraction, and it also provides the measure $\sqrt{-g}$ for respecting diffeomorphism while integrating. In the Chern-Simons term, however, the two preceding properties are not required. As a result, the Chern-Simons action remains independent of the metric in curved space-time, and the term is said to be topological. It is worth noting that the topology of the underlying manifold plays a crucial role in Chern-Simons theory, particularly in low-energy effective theories [30].

The Chern-simons term has an interesting property in that it preserves rotational invariance while breaking parity and time-reversal, as shown in section 1.1. Anomalies result from symmetry breaking at the quantum level, and matching these anomalies is essential in determining the consistency of any conjectured phases of a given three-dimensional theory.

1.3 level/rank dualities

Dualities between two pure Chern-Simons theories in which the CS level k and the gauge group rank are exchanged are known as level/rank dualities. We are interested in QCD-like theory in $2+1$ dimensions, hence we will concentrate on level/rank dualities, which encompass theories with gauge groups $U(N)$ and $SU(N)$. Before we start discussing the dual theories, let us introduce certain notations and norms. In the language of differential geometry, a non-abelian pure CS theory with gauge group $SU(N)$ and CS level k is denoted by $SU(N)_k$, with

a Lagrangian given by

$$\mathscr{L}_{SU(N)_k} = \frac{k}{4\pi}\mathrm{Tr}\left(A\wedge dA - \frac{2i}{3}A\wedge A\wedge A\right). \tag{1.21}$$

For the theories with $U(N)$ gauge group, the group $U(N)$ has an $SU(N)$ part and a $U(1)$ part with two independent CS levels, so we write the quotient

$$U(N)_{k,k'} \equiv \frac{SU(N)_k \times U(1)_{k'N}}{\mathbb{Z}_N}. \tag{1.22}$$

However, the gauge invariant form of this theory is $U(N)_{k,k+nN}$, for $n \in \mathbb{Z}$. The theory is then defined by a Lagrangian

$$\mathscr{L}_{U(N)_{k,k+nN}} = \frac{k}{4\pi}\mathrm{Tr}\left(A\wedge dA - \frac{2i}{3}A\wedge A\wedge A\right) + \frac{n}{4\pi}\mathrm{Tr}(A)d(\mathrm{Tr}A). \tag{1.23}$$

We also denote the theory with $n = 0$ by $U(N)_k \equiv U(N)_{k,k}$.

Chern-Simons theories become anomalous when defined on a manifold with a boundary. On such a manifold, the boundary term in equation (1.16) can not be ignored, an hence gauge invariance is lost. To address this issue and restore gauge invariance, one may add extra degrees of freedom to the boundary. The theory with these extra degrees of freedom is known as the Wess-Zumino-Witten (WZW) model [33, 34]. The extra degrees of freedom consist of a chiral boson for the Abelian case, whereas in the non-Abelian case they constitute a non-trivial $1+1$ dimensional conformal field theory for the non-Abelian case. One implication of these CFTs is the equivalence in a theory describing NK complex chiral fermions given by [35]

$$SU(N)_k \longleftrightarrow \frac{SU(Nk)_1}{SU(k)_N}. \tag{1.24}$$

The right-hand side of equation (1.24) is a GKO coset. The GKO coset construction is a method to establish the highest weight representations of the Virasoro algebra and was first introduced in [36]. This is to define a duality between theories

described by the following Lagrangians

$$\mathscr{L}_{SU(N)_k} \longleftrightarrow \mathscr{L}_{SU(NK)_1/SU(k)_N} \equiv \mathscr{L}_{(SU(NK)_1 \times SU(k)_{-N})/\mathbb{Z}_k} \,. \tag{1.25}$$

We can rewrite $SU(Nk)_1 = U(Nk)_1 \times U(1)$, where the $U(Nk)_1$ is a trivial theory. The second $U(1)$ kills the $U(1)$ part of the $U(Nk)_1$ theory leading to the following duality

$$SU(N)_k \longleftrightarrow \frac{U(1)_{-Nk} \times SU(k)_{-N}}{\mathbb{Z}_k} \equiv U(k)_{-N,-N} \,. \tag{1.26}$$

We saw that the WZW models are theories that exist on the boundary of Chern-Simons theories. Thus, this duality between boundary theories can be promoted to the $2+1$ dimension to represent a level/rank duality between Chern-Simons theories. As a result, we write the following set of level/rank dualities

$$SU(N)_{\pm k} \longleftrightarrow U(k)_{\mp N,\mp N} \,, \tag{1.27}$$

$$U(N)_{k,k\pm N} \longleftrightarrow U(k)_{-N,-N\mp k} \,. \tag{1.28}$$

The level/rank dualities have been rigorously demonstrated. However, Po-Shen Hsin and Seiberg have identified several complex challenges when dealing with these dualities [37]. The most confusing aspect is that some of these theories on one side of the dualities are dependent on the spin structure chosen, such as

$$\begin{aligned} &SU(N)_k;\ \text{for all values of k} \\ &U(N)_{k,k};\ \text{for odd values of k} \\ &U(N)_{k,k\pm N};\ \text{for even values of k}\,. \end{aligned}$$

None of the theories is a spin theory on the other side of the dualities. This raises an intriguing question: how can a spin theory be described as a dual description of a non-spin theory?

In summary, the solution to this problem is to convert all spin theories into non-spin theories in two steps: The first is to connect the spin theory to a background $spin^c$-connection, which defines the theory on a $spin^c$ manifold rather than the spin manifold. This makes the theory independent of the spin structure employed. The naive method of coupling a background field with a $spin^c$ connection does not necessarily produce the same contact terms as the dual theory [38, 39]. As a result, we proceed to the second step, coupling the non-spin theory to a background $U(1)$ field that adds a counterterm to ensure that the theories have the same contact terms.

An example of the process of the spin to non-spin conversion is the $U(N)_{k,k}$, which is only a spin theory for odd k. The Lagrangian of this theory is given by

$$\mathscr{L}_{U(N)_{k,k}}[A] = \frac{k}{4\pi}\mathrm{Tr}\left(A\wedge dA - \frac{2i}{3}A\wedge A\wedge A\right), \tag{1.29}$$

where A is a $U(N)$ gauge field. First, we couple the spin theory (with odd values of k) to a $spin^c$-connection C, we get

$$\mathscr{L}_{U(N)_{k,k}}[A;C] = \frac{k}{4\pi}\mathrm{Tr}\left(A\wedge dA - \frac{2i}{3}A\wedge A\wedge A\right) + \frac{1}{2\pi}\left(\mathrm{Tr}A\right)dC\,. \tag{1.30}$$

Then we couple the non-spin theory (even k) to a $U(1)$ background field B, we get

$$\mathscr{L}_{U(N)_{k,k}}[A;B] = \frac{k}{4\pi}\mathrm{Tr}\left(A\wedge dA - \frac{2i}{3}A\wedge A\wedge A\right) + \frac{1}{2\pi}\left(\mathrm{Tr}A\right)dB\,. \tag{1.31}$$

Combining equations (1.30) and (1.31), the resultant theory has a Lagrangian

$$\mathscr{L}_{U(N)_{k,k}}[A;B+kC] = \frac{k}{4\pi}\mathrm{Tr}\left(A\wedge dA - \frac{2i}{3}A\wedge A\wedge A\right) + \frac{1}{2\pi}\left(\mathrm{Tr}A\right)d\left(B+kC\right). \tag{1.32}$$

The second term of equation (1.32) ensures that the theory remains non-spin for all values of k; For even k, $(B+kC)$ becomes an ordinary $U(1)$ field, and

the theory is non-spin. For odd k, $(B + kC)$ becomes a $spin^c$-connection and the theory becomes non-spin. The conversion of the theories $SU(N)_k$ and $U(N)_{k,k\pm N}$ can be done in the same spirit.

1.4 Boson/fermion dualities in $2+1$ dimensions

One of the most common approaches to finding non-supersymmetric dualities is to begin with a duality between supersymmetric theories and then turn on some operators that violate supersymmetry. Then allow these theories to flow to the IR; if the flow is smooth, the non-supersymmetric counterparts of these dualities can be conjectured [4, 40, 41].

An alternate approach is to explore the provided Chern-Simons matter theory in the limit of large N and k with fixed N/k, which simplifies the calculations of several observables using large N techniques [42–53]. Large N calculations revealed the presence of non-supersymmetric dualities between Chern-simons theories coupled to scalars and other theories linked to fermions. The next logical step is to extend these large N dualities to finite N dualities. The validity of the potential finite N dualities may be determined by simply giving masses to matter and flowing to pure Chern-Simons theories that are linked to the well-established level/rank dualities.

With the above methodologies in hand, Ofer Aharony used the Chern-Simons theories' mapping between baryon operators and monopole operators to conjecture a complete and broad version of the level/rank dualities that includes matter to Chern-Simons theories' dualities at finite N [54].

Consider Chern-Simons theories coupled to F scalars ϕ or Dirac fermions ψ in the fundamental representation of the gauge group. The conjectured Chern-Simons-matter dualities are

$$SU(N)_k + F\phi \longleftrightarrow U(k)_{-N+F/2,-N+F/2} + F\psi\,, \tag{1.33}$$

$$U(N)_{k,k} + F\phi \longleftrightarrow SU(k)_{-N+F/2} + F\psi\,, \tag{1.34}$$

$$U(N)_{k,k\pm N} + F\phi \longleftrightarrow U(k)_{-N+F/2,-N\mp k+F/2} + F\psi\,. \tag{1.35}$$

The first three dualities were conjectured in [54], while the last one, with the minus sign in its level, was presented in [37]. The dualities of Aharony have been demonstrated to fit both the supersymmetric and large N pictures. They were also proven to be consistent with mass deformations and lead directly to level/rank dualities when we set $F = 0$. Above all, the baryon and monopole operators match appropriately [55]. Additional four dualities can be encountered by reversing the orientation of the theories in equations (1.33) to (1.35), resulting in a change of sign of all levels. The issue of coupling these theories to background fields, as well as the puzzle of introducing a duality between a fermionic theory (spin theory) and a bosonic theory (non-spin theory), has been discussed in [37].

The special case $N = k = F = 1$ has also been analyzed in [56–58], where it leads to the abelian 3d bosonization

$$\text{Free } \phi \qquad \longleftrightarrow U(1)_{-1/2} + \psi\,, \tag{1.36}$$

$$U(1)_1 + \phi \longleftrightarrow \text{Free } \psi\,, \tag{1.37}$$

$$U(1)_2 + \phi \longleftrightarrow U(1)_{-3/2} + \psi\,. \tag{1.38}$$

These dualities are interpreted to indicate that the fermions are coupled to gauge fields without any extra interactions. In particular, the fermion is free in the second duality. The scalar in the first duality, on the other hand, should be regarded as being in a Wilson–Fisher fixed point, and this Wilson–Fisher theory is gauged in the other dualities.

The theories on both sides of each of Aharony's dualities have a global $U(F)$ flavour symmetry that rotates the matter fields. We will see later that breaking this symmetry plays a crucial role in probing the phase diagram of a given Chern-Simons-matter theory. It is worth noting that there is a more general version of Chern-Simons-matter duality that includes bosons and fermions on both sides;

this duality is known as master duality, and it takes the form [59, 60]

$$SU(N)_{k-F/2} + S\phi + F\psi \longleftrightarrow U(k)_{-N+S/2} + F\psi + S\psi,$$
$$\text{with } S \leq N,\ F \leq k,\ \text{and } (S,F) \neq (N,k)\,. \quad (1.39)$$

The dualities of Aharony and the master duality are subject to a flavour bound set by k and F. To better understand this limitation and stay within the scope of this thesis, consider the example of $SU(N)_k$ gauge theory coupled to F fermions. A dual formulation of this theory is given by $U(k+F/2)_{-N}$ coupled to F scalars. Giving a negative mass squared for all scalars in the bosonic theory and the assumption that the theory is maximally higgsed, the scalars may have a vacuum expectation value (VEV) of the form

$$\langle\phi\rangle = v \begin{pmatrix} \mathbb{1}_{F\times F} \\ 0_{(k-F/2)\times F} \end{pmatrix}\,. \quad (1.40)$$

As a result, the gauge group is partially broken to $U(k-F/2)_{-N}$. The gauge group is now completely broken for $k < F/2$, implying that Aharony's unitary duality only holds for $k \geq F/2$.

Chapter 2

Fundamental QCD_3 with one and two sets of fermions

In this chapter, we review the results of [1, 2, 61]. We discuss the dualities and phases of a $SU(N)$ gauge theory coupled to F fermions in the fundamental representation, as well as a Chern-Simons term with level k. The first section delves into the theory where all fermions have the same mass, whereas the second section dives into the splitting of these fermions into two families with different masses. The Lagrangian of this theory is given by

$$\mathscr{L}_{SU(N)_k+F\psi} = -\frac{1}{4g^2}\mathrm{Tr}\mathcal{F}^2 + \frac{k_{bare}}{4\pi}\mathrm{Tr}\left(A\wedge dA - \frac{2i}{3}A\wedge A\wedge A\right) + \sum_{j=1}^{F}\left(i\bar{\psi}^j \not{D}\psi_j + \frac{m}{4\pi}\bar{\psi}^j\psi_j\right) \ , \quad (2.1)$$

where $k_{bare}\in\mathbb{Z}$ denotes the bare Chern-Simons level. We use the terminology and conventions specified in [1], which defined $k = k_{bare} - F/2$. This level shift guarantees that the Chern-Simons level is appropriately normalized, where k is a half-integer if and only if F is odd. This convention is made to the half-integer contribution to the CS level from the η-invariant [62]. Massive fermions can be integrated out, resulting in a change in the level of the low energy effective theory

given by

$$k_{IR} = k - \mathrm{sgn}(m)\frac{F}{2}\,. \tag{2.2}$$

The given theory has a dual bosonic description given by $U(k+F/2)_{-N+F}+\phi$, where ϕ is a scalar, based on Aharony's dualities. This duality, however, was predicted to hold for a limited number of flavours $k \geq F/2$ as discussed in section 1.4. One of the main implications of [1] is that Aharony's dualities hold not only for small values of F but also for a large number of flavours. This conjecture is constrained by the large F limits of the $2+1$ dimensional QCD [63]. The study of the domain walls in four dimensions, [64, 65], lends support to this conjecture as well as the proposed phase diagram. The fundamental QCD$_3$ has a $U(F)$ global symmetry that rotates the F flavours. We also consider that $k > 0$ and the negative k case can be easily found by applying time-reversal, which inverts the sign of the mass term.

2.1 Flavour symmetry breaking and the one-dimensional phase diagram

Komargodski and Seiberg [1] investigated the phase diagram of $SU(N)$ gauge theory in $2+1$ dimensions coupled to Chern-Simons term with level k and F fermions in the fundamental representation. The theory features a global flavour symmetry $U(F)$, which is spontaneously broken for small k values. Because of the spontaneous breaking of the flavour symmetry, the authors were able to divide the phase diagram into two cases:

2.1.1 No-symmetry breaking case: $k \geq F/2$

In this range of k, the theory in the IR is semiclassically accessible, and the phase diagram is described by the asymptotic theories obtained after integrating the fermions out when their mass m is positive or negative. The two phases are

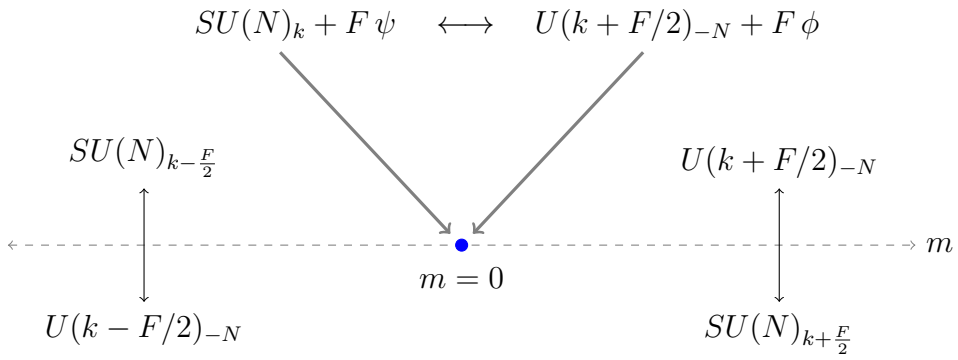

Figure 2.1: Phase diagram of $SU(N)_k + F\,\psi$ with $k \geq F/2$.

then $SU(N)_{k+F/2}$ for positive m, which has a level/rank dual $U(k+F/2)_{-N}$, and $SU(N)_{k-F/2}$ for negative m with a level/rank dual $U(k-F/2)_{-N}$. The two phases are separated by a phase transition described by the critical theory $SU(N)_k + F\,\psi^0$, where the superscript 0 refers to the fermions being massless. This phase transition could be of the first or second order, or it could be a series of phase transitions [66–70]. However, The entire description of the phase diagram is independent of the type of these phase transitions. The asymptotic phases are pure gapped topological quantum field theories (TQFT). The phase diagram is as in figure 2.1, where the transition between the two asymptotic phases occurs at the blue point ($m = 0$).

2.1.2 Broken-symmetry case: $k < F/2$

In this case, the theory is semiclassically accessible only for large mass ($m \to \pm\infty$). The asymptotic theories are $SU(N)_{k+F/2} \longleftrightarrow U(k+F/2)_{-N}$ for large positive m and $SU(N)_{k-F/2} \longleftrightarrow U(F/2-k)_N$ for large negative m. However, integrating out the scalars from the dual bosonic theory $U(k+F/2)_{-N} + F\,\phi$ for large negative mass squared leads to a sigma model phase which does not appear in the fermionic phase. In [1], the authors suggested that for the fermionic theory, there is some value of the number of flavours F^* at which the $U(F)$ symmetry is spontaneously broken into $U(F/2+k) \times U(F/2-k)$, leading to a sigma model σ in the IR that

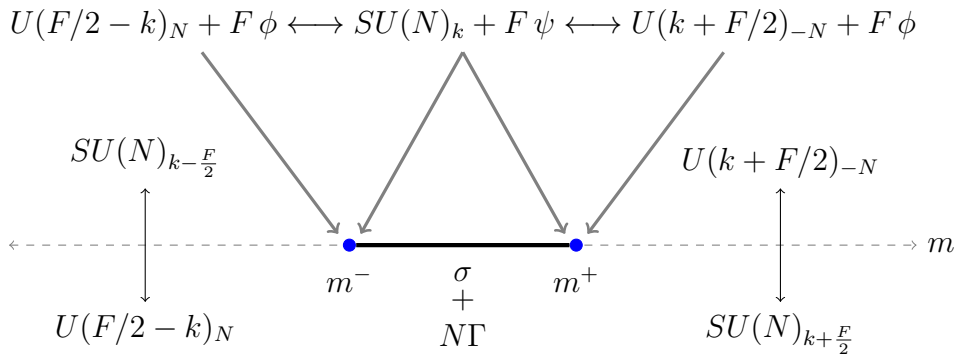

Figure 2.2: Phase diagram of $SU(N)_k + F\,\psi$ with $k < F/2$.

matches the bosonic phase and is given by the Grassmannian

$$Gr(F/2+k, F) = \frac{U(F)}{U(F/2+k) \times U(F/2-k)}\,. \tag{2.3}$$

The sigma model is a purely quantum gapless phase that does not appear semi-classically. This non-linear sigma model is accompanied by a Wess-Zumino term Γ whose coefficient is N, which is crucial in matching the anomalies for the sigma model phase. The phase diagram now consists of the two asymptotic topological phases separated by a new quantum region for small $|m|$. The quantum region is bounded by two transition points that are described by some positive mass m^+ and some negative mass m^-, as shown in figure 2.2. The authors also conjectured the existence of a new duality in the form $SU(N)_k + F\,\psi \longleftrightarrow U(F/2-k)_N + F\,\phi$ to cover the phase diagram for negative m.

2.1.3 Consistency checks: One-family case

It was shown that for $m = k = 0$ with even F, the theory breaks its global symmetry to $U(F/2) \times U(F/2)$ leading to a non-linear sigma model given by a Grassmannian with target space [71, 72]

$$Gr(F, k=0) = \frac{U(F)}{U(F/2) \times U(F/2)}\,. \tag{2.4}$$

This is a trivial consistency check for the presence of the quantum phase in the proposed phase diagram. It might also serve as a jumping-off point in building the entire phase diagram for finite k. A mass deformation of the sigma model presented in equation (2.4) reveals that the symmetry breaking scenario occurs throughout a region of the parameter space rather than at one point.

Another option to put the predicted phases to the test is to employ the dual bosonic description to identify the bosonic phases around the critical point(s) and compare them to fermionic theory phases. The authors of [2] suggested this consistency check for the two-family situation, but it may also be applied for the single flavour case.

Bosonic Phases

Consider a $U(n)_l$ gauge theory coupled to F scalars ϕ_i^α in the fundamental representation, with $n = F/2 \pm k$, $l = \mp N$, $i = 1, \ldots, f$, and $\alpha = 1, \ldots, n$. One can build a gauge invariant operator $X_i^j = \phi_i^\alpha \phi_\alpha^{*j}$, where X is an $F \times F$ matrix with rank r following the constraint $r \leq \min(n, F)$. $diag(x_1, x_2, \ldots, x_r, 0, \ldots, 0)$ is the diagonalized matrix, where x_i represent the eigenvalues of the matrix X. Because the theory includes a $U(F)$ global symmetry, one may derive a potential from this gauge invariant operator and preserve this symmetry such that

$$V = M^2 \mathrm{tr}(X) + \lambda(\mathrm{tr}X)^2 + \mu \mathrm{tr}X^2 \,. \tag{2.5}$$

where M^2 is the mass squared of the scalars, μ and λ are the coupling constants for the quartic term. To confine this potential from below, we pick $\mu > 0$, which necessitates $\mu + \min(n, F)\lambda > 0$. Now we seek for possible minimization, which is dependent on the value of M^2. If $M^2 \geq 0$, the potential is minimized by simply setting $X = 0$, and the IR effective theory is a pure $U(n)_l$. If $M^2 < 0$, the

minimum of the potential can be found by solving the vacuum equation

$$\frac{dV}{dX} = M^2 + 2\lambda \mathrm{tr}X + 2\mu X = 0\,. \tag{2.6}$$

Equation (2.6) provides a set of equivalent linear equations, implying that all eigenvalues are degenerate ($x_i = x$). Solving equation (2.6) gives the following eigenvalues

$$x = \frac{-M^2}{2\lambda + 2\mu}\,, \tag{2.7}$$

and the potential becomes

$$V(x) = \frac{-M^4 r}{4\lambda r + 4\mu}\,. \tag{2.8}$$

When r reaches its maximum value (i.e. $r = \min(n, F)$), the potential in equation (2.8) is minimized. The phase diagram of the bosonic theory is thus divided into two cases

1. $\underline{F < n}$: This implies $r = F$, the gauge group is broken in all F directions (i.e. maximally Higgsed), but the global $U(F)$ symmetry remains unbroken. Integrating the massive scalars out produces a pure $U(n-F)_l$ as a consequence. Thus the IR description for $(n, l) = (F/2 + k, -N)$ is pure $U(k - F/2)_{-N}$ for negative M^2 (i.e. on the left of the critical point of figure 2.1), which corresponds to the fermionic phase.

2. $\underline{F > n}$: We require $r = n$, so the gauge group is completely Higssed, and the global symmetry $U(F)$ spontaneously breaks to $U(F) \times U(F-n)$. As a result, the IR dynamics are characterized by a non-linear sigma model with a target space given by the Grassmannian

$$Gr(n, F) = \frac{U(F)}{U(n) \times U(F-n)}\,. \tag{2.9}$$

A Wess-Zumino term with the coefficient $|l|$ is also included. The theory has a sigma model with a Grassmannian that matches the sigma model of the fermionic phase for all (n, l) values.

The authors of [1] originally proposed the sigma model for the fermionic theory based on the symmetry breaking scenario. They predicted, from the start, that the sigma model from the fermionic and scalar theories are comparable, which we demonstrated in this section using mass deformation. The power of the mass deformation method as a testing tool will become more apparent for the two and three-family scenarios.

2.2 Two-dimensional phase diagram

We now move to the work in [2, 61] where the authors considered the case when the F fermions are split into two sets of fermions: $p\,\psi_1$ fermions with mass m_1 and $(F-p)\,\psi_2$ fermions with mass m_2. The flavour symmetry is now explicitly broken into $U(p) \times U(F-p)$ and the phase diagram looks different for three particular cases: $k \geq F/2$, $F/2 - p \leq k < F/2$, and $0 \leq k < F/2 - p$, where the range of p is such that $0 \leq p \leq F/2$. In analogy to the one-family case, there are two dual bosonic theories $U(k+F/2)_{-N}+p\,\phi_1+(F-p)\,\phi_2$ and $U(F/2-k)_N+p\,\phi_1+(F-p)\,\phi_2$ for small values of k to cover the full phase diagram.

2.2.1 Type I: $k \geq F/2$

There is no flavour symmetry breaking, and the four topological theories describe the phase diagram. Integrating out both ψ_1 and ψ_2 when their masses are both positive and negative, one obtains various topological phases $\mathrm{T}_a(m_1 > 0, m_2 > 0)$,

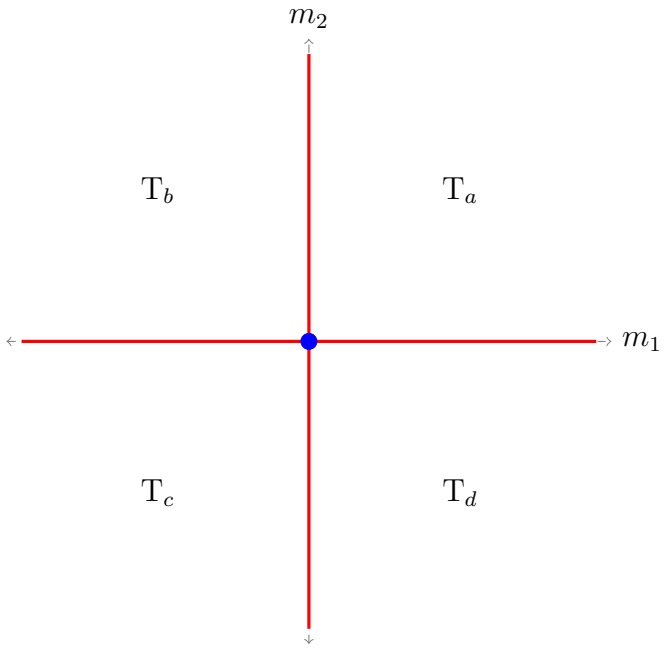

Figure 2.3: Phases of $SU(N)_k + p\,\psi_1 + (F-p)\,\psi_2$ with $k \geq F/2$: Type I.

$\mathrm{T}_b(m_1 < 0, m_2 > 0), \mathrm{T}_c(m_1 < 0, m_2 < 0), \mathrm{T}_d(m_1 > 0, m_2 < 0)$:

$$\begin{aligned}
&\mathrm{T}_a : SU(N)_{k+\frac{F}{2}} \quad \longleftrightarrow \; U(k+F/2)_{-N}\,, \\
&\mathrm{T}_b : SU(N)_{k+\frac{F}{2}-p} \longleftrightarrow U(k+F/2-p)_{-N}\,, \\
&\mathrm{T}_c : SU(N)_{k-\frac{F}{2}} \quad \longleftrightarrow U(k-F/2)_{-N}\,, \\
&\mathrm{T}_d : SU(N)_{k-\frac{F}{2}+p} \longleftrightarrow U(k-F/2+p)_{-N}\,.
\end{aligned} \tag{2.10}$$

These topological phases are separated by critical theories represented as red lines in figure 2.3. The critical theories are $SU(N)_{k\pm\frac{p}{2}} + (F-p)\,\psi_2^0$ on the horizontal red line and $SU(N)_{k\pm\frac{F-p}{2}} + p\,\psi_1^0$ on the vertical red line. The blue point is a transition point that separates the four different topological phases. We will use the term type I phase diagram to label this case.

2.2.2 Type II: $F/2 - p \leq k < F/2$

The asymptotic phases can be found similarly by sending both masses to $\pm\infty$. The topological phases T_a, T_b, and T_d remain as in equation (2.10) while T_c

becomes

$$\mathrm{T}_c \to \tilde{\mathrm{T}}_c : SU(N)_{k-\frac{F}{2}} \longleftrightarrow U(F/2-k)_N \,. \tag{2.11}$$

There are quantum regions in this case where the flavour symmetry is spontaneously broken. The strategy is to check the asymptotic phases where we send only one of the masses to $\pm\infty$, and the theory becomes one-family with a shifted level. The theory is strongly coupled and has sigma model descriptions σ_{bc} and σ_{cd} for small and/or negative m_1 and m_2, respectively. The sigma-models have target spaces with the following Grassmannians

$$\sigma_{bc} : Gr(F/2-k, F-p) = \frac{U(F-p)}{U(F/2-k)\times U(k+F/2-p)} \,, \tag{2.12}$$

$$\sigma_{cd} : Gr(F/2-k, p) \qquad = \frac{U(p)}{U(F/2-k)\times U(k-F/2+p)} \,. \tag{2.13}$$

The theory also includes a sigma model σ on the diagonal line $m_1 = m_2$, which reduces it to the one-family case. In this case, σ acts as a phase transition between σ_{bc} and σ_{cd}. The red line that separates T_a and T_d corresponds to the critical theory $SU(N)_{k+\frac{p}{2}} + (F-p)\,\psi_2^0$ while the red line separating T_a and T_b corresponds to the critical theory $SU(N)_{k+\frac{F-p}{2}} + p\,\psi_1^0$. The asymptotic theories and the quantum phases are separated by lines of critical theories, which are described via the dual bosonic theories. For example, the red line that separates T_b and σ_{bc} is given by the critical theory $U(F/2-k)_N + (F-p)\,\phi_2^0$, and this applies similarly for the remaining red lines. The full phase diagram for this case is shown in figure 2.4, and we label it as a type II phase diagram.

2.2.3 Type III: $0 \leq k < F/2 - p$

The phase diagram in this range is similar to the preceding case. It consists of topological theories that can be found semiclassically and quantum regions arising from the symmetry breaking scenario. The topological phases T_a, T_b, and $\tilde{\mathrm{T}}_c$

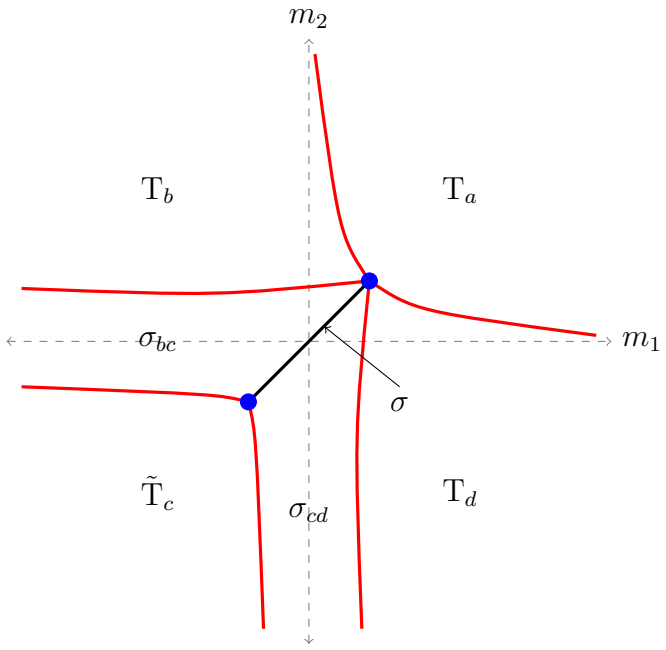

Figure 2.4: Phases of $SU(N)_k + p\,\psi_1 + (F-p)\,\psi_2$ with $F/2 - p \leq k < F/2$: Type II.

remain the same while T_d becomes

$$T_d \to \tilde{T}_d : SU(N)_{k-\frac{F}{2}+p} \longleftrightarrow U(F/2-p-k)_N \,. \tag{2.14}$$

In this case, the quantum phases are σ models on the diagonal line with a Grassmannian given by equation (2.3). They are σ_{bc} which is a plane describing the quantum region for small and negative m_2 with a Grassmannian given by equation (2.12) and σ_{ad} for small and positive m_2 with a Grassmannian

$$\sigma_{ad} : Gr(F/2+k, F-p) = \frac{U(F-p)}{U(F/2+k) \times U(F/2-p-k))} \,. \tag{2.15}$$

The phase diagram is shown in figure 2.5 which is a type III phase diagram. As in type II, the σ line acts as a transition between σ_{bc} and σ_{ad}. To summarize, the two-family theory has the following features:

- For $k \geq F/2$, the theory in the IR is described by the four topological field theories in equation (2.10).

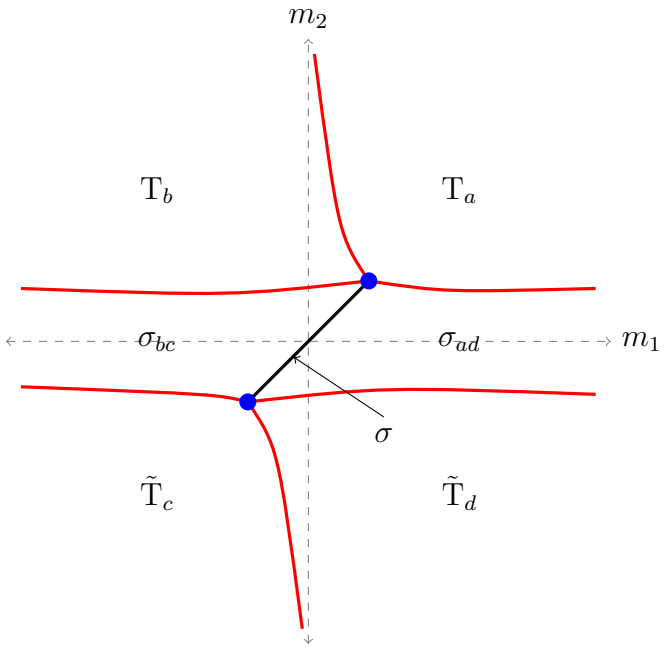

Figure 2.5: Phases of $SU(N)_k + p\,\psi_1 + (F-p)\,\psi_2$ with $0 \leq k < F/2 - p$: Type III.

- For small k, the IR description is given by four topological field theories and a line of sigma model σ separating two planes of sigma models (σ_{bc}, σ_{cd}) or (σ_{bc}, σ_{ad}).

2.2.4 Consistency checks: Two-family case

The two-dimensional phase diagram depiction passes various consistency checks. A very straightforward check is to match the phases of the one-dimensional phase diagram with the phases recovered on the diagonal line of the two-dimensional picture (i.e. $m_1 = m_2$). Other checks include matching the phases of the dual bosonic theory around the critical points and perturbing the sigma model σ on the diagonal to ensure that the description is valid when both masses are simultaneously small [2].

Phases of the bosonic theory

In this section, we perform the same procedure as in section 2.1.3, where we aim to deform the massless theories at the critical points via mass deformation. Here

we consider $U(n)_l$ gauge theory coupled to two sets of scalars $p\,\phi_1$ and $(F-p)\phi_2$. The gauge invariants operators formed from the combination of these scalars are given by

$$\begin{aligned} X &= \phi_1\phi_1^\dagger\,, \\ Y &= \phi_2\phi_2^\dagger\,, \\ Z &= \phi_1\phi_2^\dagger\,. \end{aligned} \tag{2.16}$$

X and Y are positive semidefinite Hermitian matrices of dimension p and $F-p$, while Z has a dimension $p\times(F-p)$. The deformation potential up to quartic terms is then

$$\begin{aligned} V = M_1^2\mathrm{Tr}X + M_2^2\mathrm{Tr}Y + \lambda\left(\mathrm{Tr}^2X + \mathrm{Tr}^2Y + 2\mathrm{Tr}X\mathrm{Tr}Y\right) \\ + \mu\left(\mathrm{Tr}X^2 + \mathrm{Tr}Y^2 + 2\mathrm{Tr}ZZ^\dagger\right)\,. \end{aligned} \tag{2.17}$$

We require $\mu + \min(n,F)\lambda > 0$ from the positivity of μ, just like in the one-flavour case. We also diagonalize the matrices X and Y to obtain

$$X = diag(x_1,\ldots,x_{r_1},0,\ldots,0)\,, \tag{2.18}$$

$$Y = diag(y_1,\ldots,y_{r_2},0,\ldots,0)\,, \tag{2.19}$$

where r_1 and r_2 are the ranks of X and Y respectively. For $(M_1^2,M_2^2)>0$, the gauge group is not Higgsed and the global $U(p)\times U(F-p)$ is preserved. Otherwise, we may have Higgsing (i.e. scalar condensation) or/and spontaneous symmetry breaking. The vacuum equations are then

$$\frac{\partial V}{\partial X} = M_1^2 + 2\lambda\mathrm{Tr}X + 2\lambda\mathrm{Tr}Y + 2\mu\mathrm{Tr}X = 0\,, \tag{2.20}$$

$$\frac{\partial V}{\partial Y} = M_2^2 + 2\lambda\mathrm{Tr}Y + 2\lambda\mathrm{Tr}X + 2\mu\mathrm{Tr}Y = 0\,. \tag{2.21}$$

Recall that X and Y are diagonal with r_1 and r_2 degenerate eigenvalues donated by x and y respectively. Thus solving the vacuum equations yields

$$x = \frac{-(\mu + \lambda r_2)M_1^2 + \lambda r_2 M_2^2}{2\mu^2 + 2\lambda\mu(r_1 + r_2)}\,, \tag{2.22}$$

$$y = \frac{-(\mu + \lambda r_1)M_2^2 + \lambda r_1 M_1^2}{2\mu^2 + 2\lambda\mu(r_1 + r_2)}\,. \tag{2.23}$$

The constraints on r_1 and r_2 are

$$\begin{aligned} r_1 &\leq \min(n, p)\,, \\ r_2 &\leq \min(n, F - p)\,, \\ r_1 + r_2 &\leq \min(n, F)\,. \end{aligned} \tag{2.24}$$

The positivity condition on x and y imply that a simultaneous condensation of ϕ_1 and ϕ_2 only occurs in a subregion ($\mathcal{R}$) of the third quadrant of (M_1^2, M_2^2) plane. Only x or y can be non-zero outside of this zone (i.e. we only have a single condensation). The minimization of V occurs at the boundary of each line of equation (2.24), as in the one-family case. The two-family scalar theory phase diagram is divided into four cases, each of which is explained by studying the four quadrants of the (M_1^2, M_2^2) plane.

1. $\underline{p \leq F - p \leq F \leq n}$:

   (i) For $M_1^2, M_2^2 > 0$, no scalar condensation nor spontaneous symmetry breaking for the global symmetry. Thus the theory in the IR is pure $U(n)_l$.

   (ii) For $M_1^2 < 0, M_2^2 > 0$, only ϕ_1 condenses leading to a partial Higssing of the gauge group to $U(n - r_1)_l$. When we apply the restriction on r_1 and take into consideration that $p < n$, we get $U(n - p)_l$.

   (iii) For $M_1^2 < 0, M_2^2 < 0$, both ϕ_1 and ϕ_2 condense, but only on a subregion $\mathcal{R}$ of this third quadrant, with the rest joining either the phases of the second or fourth quadrants. The rank constraints are thus $r_1 = p$ and

$r_2 = F - p$. The gauge group is broken down into $U(n-(r_1+r_2))_l = U(n-F)_l$ as a result of the double condensation.

(iv) For $M_1^2 > 0, M_2^2 < 0$, only ϕ_2 condenses where r_2 is saturated to $F-p$. Thus the IR description is $U(n-F+p)_l$.

The $U(n)_l$ gauge theory represents the whole first quadrant, which we identify as region $\mathcal{A}$. The area of the second quadrant, as well as what is left of the subregion $\mathcal{R}$ of the third quadrant, is denoted by $\mathcal{B}$. We also call the subregion of the third quadrant $\mathcal{C}$ since it has a double condensation as well as complete saturation of r_1 and r_2. Similarly, the last region is $\mathcal{D}$, which represents the fourth quadrant plus the region leftover from the third quadrant. Once we substitute $n = F/2 \pm k$, we get the phases of the bosonic theory. In this case, however, only $n = F/2 + k$ is allowed, and the phases are described in table 2.1.

Region	r_1	r_2	Phase	$n = F/2 + k$	$n = F/2 - k$
$\mathcal{A}$	0	0	$U(n)_l$	T_a	N/A
$\mathcal{B}$	p	0	$U(n-p)_l$	T_b	N/A
$\mathcal{C}$	p	$F-p$	$U(n-F)_l$	T_c	N/A
$\mathcal{D}$	0	$F-p$	$U(n-F+p)_l$	T_d	N/A

Table 2.1: Phases of the bosonic theory $U(n)_l + p\phi_1 + (F-p)\phi_2$ with $p \leq F-p \leq F \leq n$.

2. $\underline{p \leq F-p \leq n < F}$:

(i) For $M_1^2, M_2^2 > 0$, this is similar to the previous case with no scalar condensation leading to the same region $\mathcal{A}$ with $U(n)_l$ gauge theory.

(ii) For $M_1^2 < 0, M_2^2 > 0$, this is also similar to the previous case with region $\mathcal{B}$ represented by $U(n-p)_l$ gauge theory.

(iii) For $M_1^2 < 0, M_2^2 < 0$, we have Higgsing as well as spontaneous symmetry breaking to the global symmetry leading to a sigma model. We use the constraint on $r_1 + r_2$ to find the Grassmannians of the sigma model.

Because there are two ways to saturate the $r_1 + r_2$ constraint, the $\mathcal{C}$ region is divided into two subregions: $\mathcal{C}_1$ and $\mathcal{C}_2$. When r_1 is entirely saturated, r_2 takes the value $n - p$, and the subregion $\mathcal{C}_1$ appears, resulting in a Grassmannian $Gr(n - p, F - p)$. The subregion $\mathcal{C}_2$ can be found by saturating r_2 to $F - p$ while $r_1 = n - F + p$, as a result, the Grassmannian is given by $Gr(n - F + p, p)$.

(iv) For $M_1^2 > 0, M_2^2 < 0$, only a condensation of ϕ_2 occurs, as in the previous case, leading to $U(n - F + p)_l$.

Region	r_1	r_2	Phase	$n = F/2 + k$	$n = F/2 - k$
$\mathcal{A}$	0	0	$U(n)_l$	T_a	N/A
$\mathcal{B}$	p	0	$U(n-p)_l$	T_b	N/A
$\mathcal{C}_1$	p	$n-p$	$Gr(n-p, F-p)$	σ_{bc}	N/A
$\mathcal{C}_2$	$n-F+p$	$F-p$	$Gr(n-F+p, p)$	σ_{cd}	N/A
$\mathcal{D}$	0	$F-p$	$U(n-F+p)_l$	T_d	N/A

Table 2.2: Phases of the bosonic theory $U(n)_l + p\phi_1 + (F-p)\phi_2$ with $p \leq F - p \leq n < F$.

3. $\underline{p \leq n < F - p \leq F}$:

(i) For $M_1^2, M_2^2 > 0$, we have $U(n)_l$ theory describing region $\mathcal{A}$.

(ii) For $M_1^2 < 0, M_2^2 > 0$, the theory $U(n-p)_l$ describes region $\mathcal{B}$.

(iii) For $M_1^2 < 0, M_2^2 < 0$, we have Higgsing as well as spontaneous symmetry breaking. The (n, F) relationship requires the value of $r_1 + r_2$ to be n. As a result, we have two possibilities to achieve this condition: the first is to use $r_1 = p$ and $r_2 = n - p$, which leads to a Grassmannian $Gr(n-p, F-p)$ representing the subregion $\mathcal{C}_1$. The subregion $\mathcal{C}_2$ is now different, with $r_1 = 0$ and $r_2 = n$, so this region has a new Grassmnnian given by $Gr(n, F - p)$. We will see later that this region joins the region from the fourth quadrant to form a whole new region, so we will name it $\mathcal{D}_1$.

(iv) For $M_1^2 > 0, M_2^2 < 0$, we have Higgsing plus spontaneous symmetry breaking with $r_1 = 0$ and $r_2 = n$, which provides the Grassmannian $Gr(n, F-p)$ (i.e. the whole fourth quadrant is part of $\mathcal{D}_1$).

Region	r_1	r_2	Phase	$n = F/2 + k$	$n = F/2 - k$
$\mathcal{A}$	0	0	$U(n)_l$	T_a	$\tilde{\mathrm{T}}_c$
$\mathcal{B}$	p	0	$U(n-p)_l$	T_b	$\tilde{\mathrm{T}}_d$
$\mathcal{C}_1$	p	$n-p$	$Gr(n-p, F-p)$	σ_{bc}	σ_{ad}
$\mathcal{D}_1$	0	n	$Gr(n, F-p)$	σ_{ad}	σ_{bc}

Table 2.3: Phases of the bosonic theory $U(n)_l + p\phi_1 + (F-p)\phi_2$ with $p \leq n < F - p \leq F$.

4. $\underline{n < p \leq F - p \leq F}$:

(i) For $M_1^2, M_2^2 > 0$, region $\mathcal{A}$ exists with $U(n)_l$ gauge theory.

(ii) For $M_1^2 < 0, M_2^2 > 0$, we have only one possibility to satisfy the $r_1 + r_2$ condition where we choose $r_1 = n$ and $r_2 = 0$. This is exactly similar to what happens for the subregion $\mathcal{C}_1$ from the third quadrant ($M_1^2 < 0, M_2^2 < 0$). Thus, regions $\mathcal{B}$ joins the subregion $\mathcal{C}_1$ to form a whole new region $\mathcal{B}_1$ with sigma model described by $Gr(n, p)$.

(iii) The rest of the third quadrant joins region $\mathcal{D}$ to reproduce $\mathcal{D}_1$ with a Grassmannian $Gr(n, F-p)$.

Region	r_1	r_2	Phase	$n = F/2 + k$	$n = F/2 - k$
$\mathcal{A}$	0	0	$U(n)_l$	N/A	$\tilde{\mathrm{T}}_c$
$\mathcal{B}_1$	n	0	$Gr(n, p)$	N/A	σ_{cd}
$\mathcal{D}_1$	0	n	$Gr(n, F-p)$	N/A	σ_{bc}

Table 2.4: Phases of the bosonic theory $U(n)_l + p\phi_1 + (F-p)\phi_2$ with $n < p \leq F - p \leq F$.

It is straightforward to see that the phases of the bosonic theory in tables 2.1 to 2.4 match their correspondance from the fermionic theory. This is a powerful tool for testing conjectured phases in figures 2.3 to 2.5, particularly around the critical points.

σ perturbation: Matching theories off diagonal

Another non-trivial consistency check discussed in [2] is achieved via mass deformation of the sigma model σ on the diagonal line (i.e. $m_1 = m_2$). σ can be represented in terms of n with Grassmannian $Gr(n, p)$, so mass deformation modifies it accordingly. The perturbation is done by adding an infinitesimal mass squared to either ϕ_1 or ϕ_2. The sign of the additional mass, as well as the relationship between n, p, and F, determine the shape of such modification (i.e. theories above or below σ). It is worth noting that the outcome is independent of the choice of whether we deform ϕ_1 or ϕ_2.

Now, let us add δM_1^2 to ϕ_1 and check the effect of such deformation. If $\delta M_1^2 > 0$ (i.e. below the diagonal line), the family ϕ_1 condenses first causing either partial or complete Higgsing to the gauge group depending on the $(n, F-p)$ relationship. For $F - p > n$, the gauge group is completly Higgsed, so one may integrate ϕ_1 out resulting in a sigma model with grassmannian $Gr(n, F-p)$. For $F - p < n$, ϕ_2 partially Higgs the gauge group down to $U(n - F + p)$, then ϕ_1 condenses leading to a sigma model with Grassmannian $Gr(F-n, p)$.

On the other hand, For $\delta M_1^2 < 0$, the set ϕ_2 condenses first, and the result describes the theory above the diagonal line. Since we only have $p\phi_1$ to integrate, the theory now relies on the (n, p) relationship. For $p > n$, the condensation of ϕ_2 completely Higgs the gauge group, so we integrate ϕ_2 out without compromising the remaining theory. As a result, the theory is described via a sigma model with Grassmannian $Gr(n, p)$. For $p < n$, ϕ_1 partially Higgs the gauge group down to $U(n-p)$, then ϕ_2 condenses leading to a sigma model with Grassmannian $Gr(F-n, F-p)$.

We summarize the phases due to mass perturbation of σ in table 2.5. The results show clearly that these phases match exactly the ones in figures 2.4 and 2.5 when we make the substitution $n = F/2 \pm k$.

	Phase	$n = F/2 + k$	$n = F/2 - k$
$\delta M_1^2 > 0$			
$F - p > n$	$Gr(n, F-p)$	σ_{ad}	N/A
$F - p < n$	$Gr(F-n, p)$	σ_{cd}	N/A
$\delta M_1^2 < 0$			
$p > n$	$Gr(n, p)$	N/A	σ_{cd}
$p < n$	$Gr(F-n, F-p)$	N/A	σ_{bc}

Table 2.5: Phases around σ due to mass perturbation.

Chapter 3

Three-dimensional phase diagrams of fundamental QCD_3

We now proceed to build on the prior work by integrating a third flavour family into the theory. The discussion of this chapter is based on a published work [3]. We split the F fermions into three sets: $p\,\psi_1$ fermions with mass m_1, $q\,\psi_2$ fermions with mass m_2, and $(F-p-q)\,\psi_3$ fermions with mass m_3. The global flavour symmetry $U(F)$ is explicitly broken into $U(p)\times U(q)\times U(F-p-q)$. There are two possible scenarios to cover the entire phase diagram of the three-family situation. The two scenarios are determined by the number of flavours for the additional family; the first is for $F-p-q \leq F/2$, and the second is for $F-p-q > F/2$; each scenario is divided into five different cases depending on the value of k. However, the majority of these cases are the same in both scenarios, with the difference appearing when we examine the phases of k with a boundary of $|F/2-p-q|$ flavours.

3.1 $F-p-q \leq F/2$ Scenario

In order to keep the analysis under control, we propose setting p and q such that $0 < q \leq p \leq F-(p+q) \leq F/2$. The range of k diagram is divided into five cases:

$k \geq F/2$, $F/2-q \leq k < F/2$, $F/2-p \leq k < F/2-q$, $(p+q)-F/2 \leq k < F/2-p$, and $0 \leq k < (p+q)-F/2$, each with its own phase diagram.

Our technique for identifying the topological phases is to send the three masses to $\pm\infty$. For small values of k, we look for the quantum regions in two steps: first, we identify the asymptotic limits when two of the masses are sent to $\pm\infty$, and then we find the asymptotic limit when just one of the three masses is sent to $\pm\infty$. The theory on the three-dimensional diagonal line $m_1 = m_2 = m_3$ is simplified to the one-family case with the phase diagrams shown in figures 2.1 and 2.2, which indicates that we always anticipate σ to emerge as a phase for all ranges of $k < F/2$.

3.1.1 Case 1: $k \geq F/2$

The theory in the IR is weakly-coupled in this case, with no symmetry breaking scenario. The phase diagram is defined by eight topological field theories and associated level/rank dual descriptions; six critical lines separate these phases. The topological phases are derived by finding the asymptotic limits of the three masses, and they appear in the mass ranges m_1, m_2, and m_3 as $\mathrm{T}_1(m_1 > 0, m_2 > 0, m_3 > 0), \mathrm{T}_2(m_1 > 0, m_2 > 0, m_3 < 0), \mathrm{T}_3(m_1 > 0, m_2 < 0, m_3 > 0)\mathrm{T}_4(m_1 < 0, m_2 > 0, m_3 > 0), \mathrm{T}_5(m_1 < 0, m_2 < 0, m_3 > 0), \mathrm{T}_6(m_1 < 0, m_2 > 0, m_3 < 0)$, $\mathrm{T}_7(m_1 < 0, m_2 < 0, m_3 > 0), \mathrm{T}_8(m_1 < 0, m_2 < 0, m_3 < 0)$. They are

$$
\begin{aligned}
\mathrm{T}_1 &: SU(N)_{k+\frac{F}{2}} &&\longleftrightarrow\ U(k+F/2)_{-N} \\
\mathrm{T}_2 &: SU(N)_{k+p+q-\frac{F}{2}} &&\longleftrightarrow\ U(k+p+q-F/2)_{-N} \\
\mathrm{T}_3 &: SU(N)_{k+\frac{F}{2}-q} &&\longleftrightarrow\ U(k+F/2-q)_{-N} \\
\mathrm{T}_4 &: SU(N)_{k+\frac{F}{2}-p} &&\longleftrightarrow\ U(k+F/2-p)_{-N} \\
\mathrm{T}_5 &: SU(N)_{k+p-\frac{F}{2}} &&\longleftrightarrow\ U(k+p-F/2)_{-N} \\
\mathrm{T}_6 &: SU(N)_{k+q-\frac{F}{2}} &&\longleftrightarrow\ U(k+q-F/2)_{-N} \\
\mathrm{T}_7 &: SU(N)_{k+\frac{F}{2}-p-q} &&\longleftrightarrow\ U(k+F/2-p-q)_{-N}
\end{aligned}
\tag{3.1}
$$

$$\mathrm{T}_8 : SU(N)_{k-\frac{F}{2}} \qquad \longleftrightarrow \; U(k - F/2)_{-N}$$

The phase diagram is three-dimensional in the space (m_1, m_2, m_3) as shown in figure 3.2 and the six different projections are shown in figure 3.1. The separation between the eight topological theories occurs via points, lines, and planes of critical theories. The blue point is described by a critical theory given by $SU(N)_k + p\,\psi_1^0 + q\,\psi_2^0 + (F - p - q)\,\psi_3^0$. Each point on the critical lines belong to one of the following critical theories

$$\begin{aligned} C_1^{\pm} &: SU(N)_{k\pm\frac{p}{2}} + q\,\psi_2^0 + (F - p - q)\,\psi_3^0 \;, \\ C_2^{\pm} &: SU(N)_{k\pm\frac{q}{2}} + p\,\psi_1^0 + (F - p - q)\,\psi_3^0 \;, \\ C_3^{\pm} &: SU(N)_{k\pm\frac{F-p-q}{2}} + p\,\psi_1^0 + q\,\psi_2^0 \,. \end{aligned} \tag{3.2}$$

$C_1^{\pm}$, $C_2^{\pm}$, and $C_3^{\pm}$ describe the lines on the mass axes m_1, m_2, and m_3, respectively. The plus or minus sign indicates whether the theory is along the positive or negative axes. The critical planes are given by any of the following theories:

$$\begin{aligned} C_{12}^{\pm} &: SU(N)_{k\pm\frac{p+q}{2}} + (F - p - q)\,\psi_3^0 \;, \\ C_{21}^{\pm} &: SU(N)_{k\pm\frac{p-q}{2}} + (F - p - q)\,\psi_3^0 \;, \\ C_{13}^{\pm} &: SU(N)_{k\pm\frac{F-q}{2}} + q\,\psi_2^0 \;, \\ C_{31}^{\pm} &: SU(N)_{k\pm\left(\frac{F-q}{2}-p\right)} + q\,\psi_2^0 \;, \\ C_{23}^{\pm} &: SU(N)_{k\pm\frac{F-p}{2}} + p\,\psi_1^0, \\ C_{32}^{\pm} &: SU(N)_{k\pm(\frac{F-p}{2}-q)} + p\,\psi_1^0 \,. \end{aligned} \tag{3.3}$$

$C_{ij}^{\pm}$ describes the theories on the planes (m_i, m_j) with both of the masses being positive or negative, while $C_{ji}^{\pm}$ for the planes when one of the masses is positive and the other is negative.

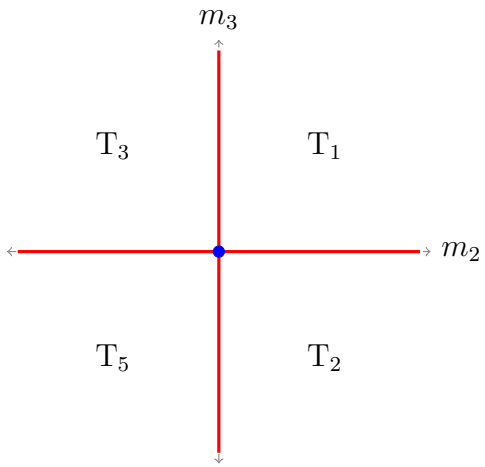

(a) (m_2, m_3), $m_1 > 0$

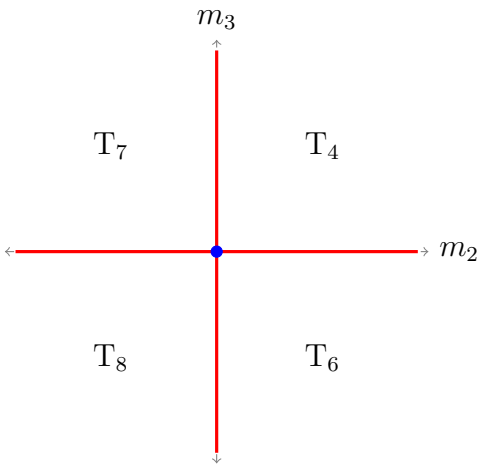

(b) (m_2, m_3), $m_1 < 0$

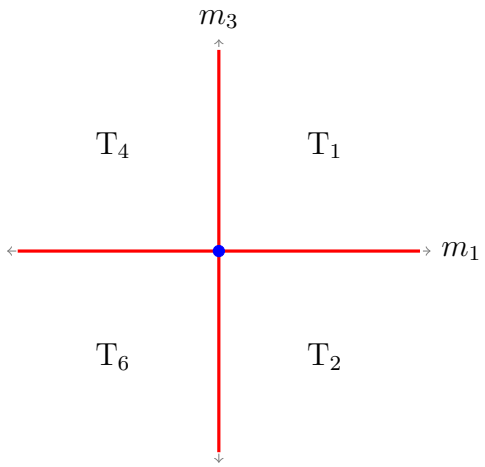

(c) (m_1, m_3), $m_2 > 0$

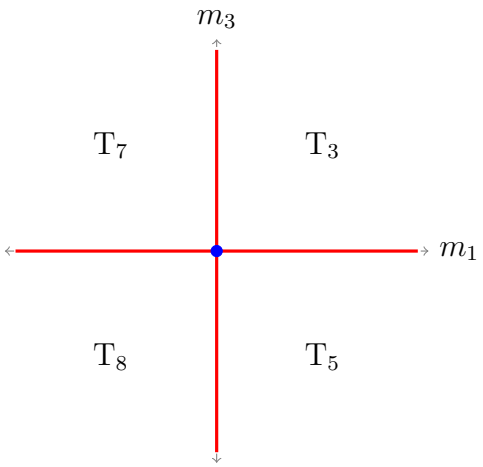

(d) (m_1, m_3), $m_2 < 0$

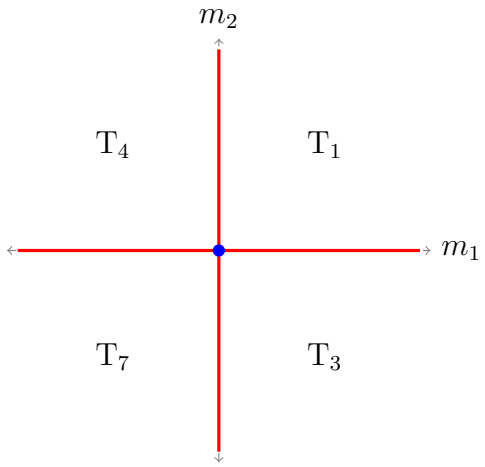

(e) (m_1, m_2), $m_3 > 0$

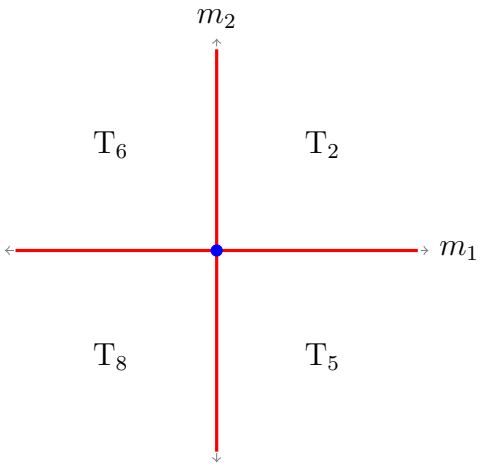

(f) (m_1, m_2), $m_3 < 0$

Figure 3.1: Phases of $SU(N)_k + p\,\psi_1 + q\,\psi_2 + (F - p - q)\,\psi_3$ with $k \geq F/2$.

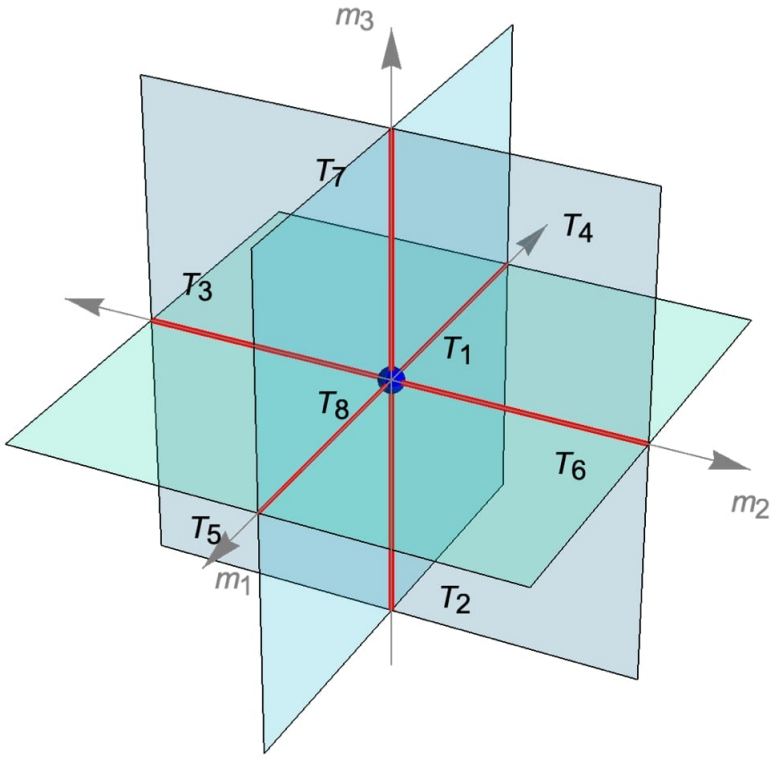

Figure 3.2: The three-dimensional phase diagram of $SU(N)_k + p\,\psi_1 + q\,\psi_2 + (F - p - q)\,\psi_3$ with $k \geq F/2$. The blue ball represents the critical point, the red lines are the critical lines given by equation (3.2) while the planes in cyan are the critical planes, each plane is described by one of the critical theories in equation (3.3).

3.1.2 Case 2: $F/2 - q \leq k < F/2$

In this range of k and all the remaining cases, we need two bosonic dual descriptions to fill in the full phase diagram as conjectured in [1]. These bosonic theories are $U(F/2+k)_{-N}+p\,\phi_1+q\,\phi_2+(F-p-q)\,\phi_3$ and $U(F/2-k)_N+p\,\phi_1+q\,\phi_2+(F-p-q)\,\phi_3$, where ϕ_1, ϕ_2, and ϕ_1 are scalars in the fundamental representation of $SU(N)$. The three masses asymptotic limits yield the same topological theories as in **??** except for T_8, which becomes

$$\mathrm{T}_8 \to \tilde{\mathrm{T}}_8 : SU(N)_{k-\frac{F}{2}} \longleftrightarrow U(F/2-k)_N\,. \tag{3.4}$$

The two mass asymptotic limits produce a one-family theory with a shifted level. In some limits, the shifted level becomes less than the remaining number of flavours divided by two, and the theory becomes strongly-coupled. The three-

dimensional phase diagram includes quantum regions described by sigma models, but this time they appear as cuboids in the three-dimensional picture. The cuboid quantum phases are the signature of the three-family theory as the planes of sigma-models were signatures of the two-family case. The theory that has a level within this range experience a cuboid sigma model in its phase diagram in the following cases:

- $m_2,\, m_3 \to -\infty$: the theory becomes $SU(N)_{k-F/2+p/2} + p\,\psi_1$. The cuboid quantum region is described by a sigma model σ_1^c. From now on, we shorthand the cuboid Grassmannains by their corresponding sigma models, the Grassmannian for this region is

$$\sigma_1^c = \frac{U(p)}{U(F/2-k)\times U(k-F/2+p)}\,. \tag{3.5}$$

- $m_1,\, m_3 \to -\infty$: the theory becomes $SU(N)_{k-F/2+q/2} + q\,\psi_2$ which has a sigma model σ_2^c given by

$$\sigma_2^c = \frac{U(q)}{U(F/2-k)\times U(k-F/2+q)}\,. \tag{3.6}$$

- $m_1,\, m_2 \to -\infty$: the theory is $SU(N)_{k-p/2-q/2} + (F-p-q)\,\psi_3$ with a sigma model σ_3^c given by

$$\sigma_3^c = \frac{U(F-p-q)}{U(F/2-k)\times U(F/2-p-q+k)}\,. \tag{3.7}$$

Now let us perform a consistency check by sending one mass to infinity where the theory with the remaining flavours is reduced to a two-family case with shifted level. In each limit, we check the relation between the remaining number of flavours and the shifted level, which determines whether the phase diagram is type I, II, or III. We summarize the check as follows:

(i) $m_1 \to +\infty$: we integrate ψ_1 out, and the theory is reduced to

$$SU(N)_{k+\frac{p}{2}} + q\,\psi_2 + (F-p-q)\,\psi_3 \equiv SU(N)_{k_1^+} + q\,\psi_2 + (F_1-q)\,\psi_3\ , \tag{3.8}$$

where $k_1^+ = k + p/2$ and $F_1 = F - p$ with $k_1^+ > F_1/2$. Due to the range of k_1^+, this region of the three-dimensional phase diagram has a type I phase diagram with the topological theories T_1, T_2, T_3, and T_5.

(ii) $m_1 \to -\infty$: integrating ψ_1 out leads to

$$SU(N)_{k-\frac{p}{2}} + q\,\psi_2 + (F-p-q)\,\psi_3 \equiv SU(N)_{k_1^-} + q\,\psi_2 + (F_1-q)\,\psi_3\ , \tag{3.9}$$

where $k_1^- = k - p/2$ and $F_1/2 - q < k_1^- < F_1$. Due to the range of k_1^-, the phase diagram is then of type II with the topological theories T_4, T_6, T_7, and $\tilde{\mathrm{T}}_8$. Alongside these topological phases, we have a sigma model on the diagonal given by

$$\sigma_{23}^d : Gr(F_1/2 + k_1^-, F_1) = \frac{U(F-p)}{U(F/2-k)\times U(F/2-p+k)}\,. \tag{3.10}$$

This diagonal sigma model is not a line but rather a plane region in the three-dimensional picture. Only one side appears here, which will become clear in section 3.3. The horizontal and vertical sigma models are σ_{78} which separates T_7 and $\tilde{\mathrm{T}}_8$ as well as σ_{68} separating T_6 and $\tilde{\mathrm{T}}_8$. They are given by

$$\sigma_{78} : Gr(F_1/2 - k_1^-, F_1 - q) = \frac{U(F-p-q)}{U(F/2-k)\times U(F/2-p-q+k)} \equiv \sigma_3^c\ , \tag{3.11}$$

$$\sigma_{68} : Gr(F_1/2 - k_1^-, q) = \frac{U(q)}{U(F/2-k)\times U(k-F/2+q)} \equiv \sigma_2^c\,. \tag{3.12}$$

We notice that $\sigma_{78} \equiv \sigma_3^c$ which means that σ_{78} is just one side of the three-dimensional quantum region σ_3^c, the same thing applies for σ_{68} which is equivalent to σ_2^c.

(iii) $m_2 \to +\infty$: we integrate ψ_2 out, and the theory becomes

$$SU(N)_{k+\frac{q}{2}} + p\,\psi_1 + (F-p-q)\,\psi_3 \equiv SU(N)_{k_2^+} + p\,\psi_1 + (F_1-p)\,\psi_3 \ , \tag{3.13}$$

where $k_2^+ = k + p/2$ and $F_2 = F - q$ with $k_2^+ > F_2/2$ and the phase diagram is of type I with the topological phases T_1, T_2, T_4, and T_6.

(iv) $m_2 \to -\infty$: integrating ψ_2 gives

$$SU(N)_{k-\frac{q}{2}} + p\,\psi_1 + (F-p-q)\,\psi_3 \equiv SU(N)_{k_2^-} + p\,\psi_1 + (F_1-p)\,\psi_3 \ , \tag{3.14}$$

where $k_2^- = k - p/2$ and $F_2/2 - q < k_2^- < F_2$. The phase diagram is then of type II with the topological theories T_3, T_5, T_7, and $\tilde{\mathrm{T}}_8$. The diagonal sigma model is

$$\sigma_{13}^d : Gr(F_2/2 + k_2^-, F_2) = \frac{U(F-q)}{U(F/2-k) \times U(F/2-q+k)} \ , \tag{3.15}$$

the quantum phase σ_{78} also exists in this side as in equation (3.11) alongside the phase σ_{58} that separates T_5 and $\tilde{\mathrm{T}}_8$ which is given by

$$\sigma_{58} : Gr(F_2/2 - k_2^-, p) = \frac{U(p)}{U(F/2-k) \times U(k-F/2+p)} \equiv \sigma_1^c \, . \tag{3.16}$$

We should emphasize here that the equivalence between these phases and the cuboid sigma models is itself a consistency check of our analysis.

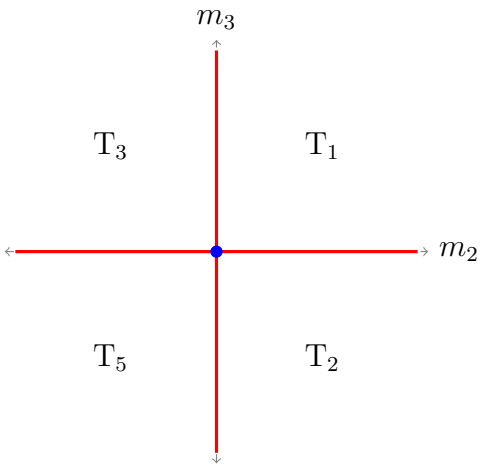

(a) (m_2, m_3), $m_1 > 0$

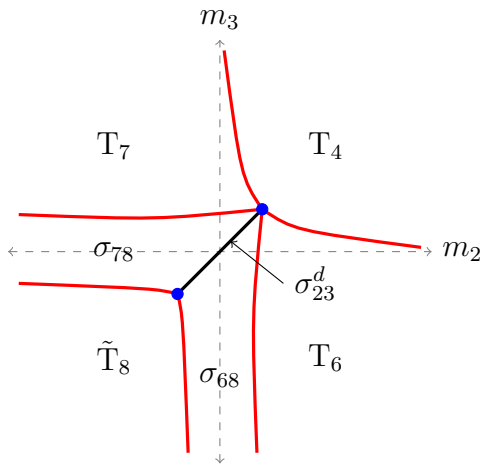

(b) (m_2, m_3), $m_1 < 0$

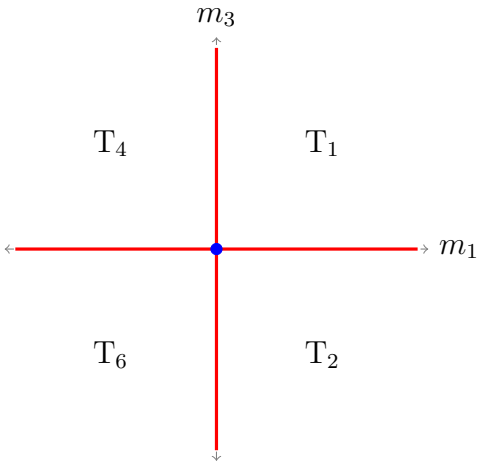

(c) (m_1, m_3), $m_2 > 0$

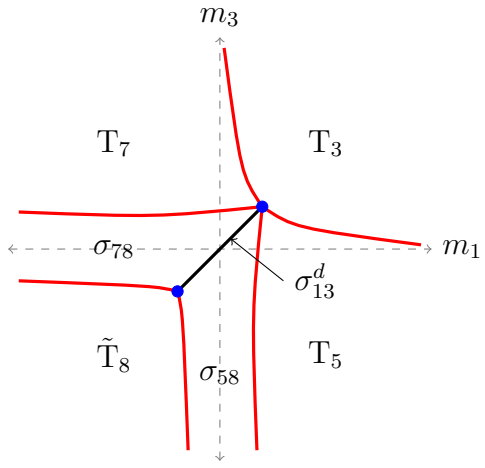

(d) (m_1, m_3), $m_2 < 0$

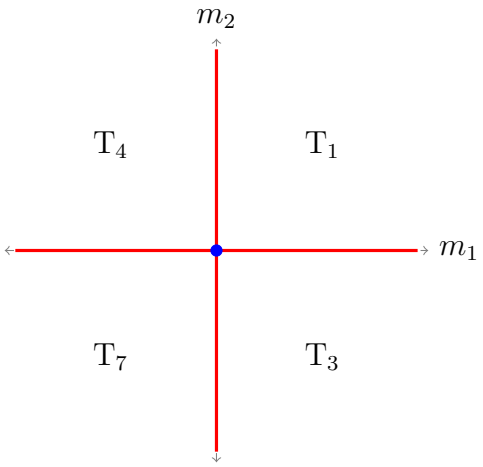

(e) (m_1, m_2), $m_3 > 0$

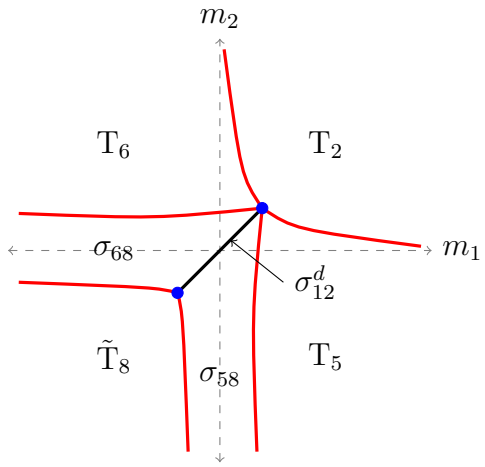

(f) (m_1, m_2), $m_3 < 0$

Figure 3.3: Phases of $SU(N)_k + p\,\psi_1 + q\,\psi_2 + (F-p-q)\,\psi_3$ with $F/2 - q \leq k < F/2$.

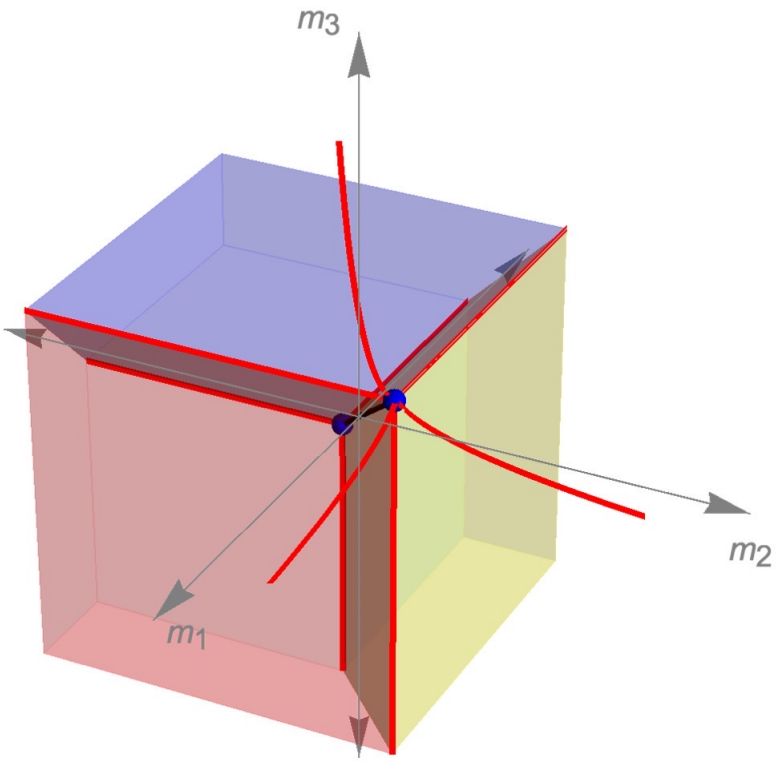

Figure 3.4: The three-dimensional phase diagram of $SU(N)_k + p\,\psi_1 + q\,\psi_2 + (F - p - q)\,\psi_3$ with $F/2 - q \leq k < F/2$. σ is represented by the thick black line between the two critical points. σ_1^c, σ_2^c, and σ_3^c are represented by the red, yellow, and blue regions, respectively. The diagonal sigma models are the dark brown planes separating the cuboid quantum regions.

(v) $m_3 \to +\infty$: after integrating ψ_3 out the theory is

$$SU(N)_{k+\frac{F-p-q}{2}} + p\,\psi_1 + q\,\psi_2 \equiv SU(N)_{k_3^+} + p\,\psi_1 + (F_3 - p)\,\psi_2 \ , \qquad (3.17)$$

where $k_3^+ = k + (F - p - q)/2$ and $F_3 = p + q$, the relation $k_3^+ > F_3/2$ holds, and we have a type I phase diagram with the topological phases T_1, T_3, T_4, and T_7.

(vi) $m_3 \to -\infty$: integrating ψ_3 gives

$$SU(N)_{k-\frac{F-p-q}{2}} + p\,\psi_1 + q\,\psi_2 \equiv SU(N)_{k_3^-} + p\,\psi_1 + (F_3 - p)\,\psi_3 \ , \qquad (3.18)$$

where $k_3^- = k - (F - p - q)/2$ and $F_3/2 - q < k_3^- < F_3$, but $p > q$ which makes this case cover the range of type II phase diagram. The phase diagram

has the topological phases T_2, T_5, T_6, and $\tilde{\mathrm{T}}_8$. The diagonal sigma model of this side is

$$\sigma_{12}^d : Gr(F_3/2 + k_3^-, F_3) = \frac{U(p+q)}{U(F/2-k) \times U(k - F/2 + p + q)} \,, \tag{3.19}$$

while the horizontal and vertical quantum regions are σ_{68} and σ_{58} respectively and given by equations (3.12) and (3.16).

In this range of k, we summarize the phase diagram in figures 3.3 and 3.4 where the IR theory has the following phases; eight topological phases ($\mathrm{T}_{1-7}, \tilde{\mathrm{T}}_8$), three cuboid sigma models ($\sigma_1^c, \sigma_2^c, \sigma_3^c$), three planes of sigma models ($\sigma_{12}^d, \sigma_{13}^d, \sigma_{23}^d$), as well as a line of sigma model σ that appears on the diagonal line $m_1 = m_2 = m_3$. In the limiting case $q = 0$, the phase diagram becomes equivalent to the $k = F/2$ case where all the sigma models, as well as the topological theories T_6 and T_8 trivialize. The phase diagram is then reduced to a two-dimensional phase diagram with three topological theories T_a, T_b, and T_d, as well as a trivial theory $SU(N)_0$.

3.1.3 Case 3: $F/2 - p \leq k < F/2 - q$

As in the previous case, the theory has two bosonic dual descriptions. The topological phases are given by **??** and equation (3.4) except for T_6, which becomes

$$\mathrm{T}_6 \to \tilde{\mathrm{T}}_6 : SU(N)_{k-\frac{F}{2}+q} \longleftrightarrow U(F/2 - q - k)_N \,. \tag{3.20}$$

T_8 is also replaced by $\tilde{\mathrm{T}}_8$ as before.

The cuboid quantum regions exist in the following cases:

- $m_2 \to +\infty$ and $m_3 \to -\infty$: the theory is reduced to $SU(N)_{k-F/2+p/2+q} + p\,\psi_1$ which has a sigma model phase given by

$$\bar{\sigma}_1^c = \frac{U(p)}{U(F/2 - q - k) \times U(k - F/2 + p + q)} \,. \tag{3.21}$$

- $m_2,\, m_3 \to -\infty$: the theory has the same cuboid sigma model as in equation (3.5).

- $m_2 \to +\infty$ and $m_1 \to -\infty$: the theory is reduced to $SU(N)_{k-p/2+q/2} + (F - p - q)\,\psi_3$ with a sigma model given by

$$\hat{\sigma}_3^c = \frac{U(F-p-q)}{U(F/2-p+k) \times U(F/2-q-k)}\,. \tag{3.22}$$

- $m_1,\, m_2 \to -\infty$: the theory has the same cuboid sigma model σ_3^c as in equation (3.7).

The phases that appear when we take one of the masses to $\pm\infty$ are as follows:

(i) $m_1 \to +\infty$: this is similar to case 2, where we have a type I phase diagram with only topological phases.

(ii) $m_1 \to -\infty$: this limit is different from the previous case, as in this range of k the value of k_1^- lies between $F_1/2 - p$ and $F_1/2 - q$, which gives a type III phase diagram. The sigma models σ_{23}^d and σ_{78} remain the same, while a new phase σ_{46} appears between T_4 and $\tilde{\mathrm{T}}_6$ and is given by

$$\sigma_{46} : Gr(F_1/2 + k_1^-, F_1 - q) = \frac{U(F-p-q)}{U(F/2-p+k) \times U(F/2-q-k)} \equiv \hat{\sigma}_3^c\,. \tag{3.23}$$

(iii) $m_2 \to +\infty$: the range of k_2^+ within this range of k is $F_2/2 - p \leq k_2^+ < F_2/2$ and the phase diagram is of type II with a new diagonal sigma model $\bar{\sigma}_{13}^d$ given by

$$\bar{\sigma}_{13}^d : Gr(F_2/2 + k_2^+, F_2) = \frac{U(F-q)}{U(F/2+k) \times U(F/2-q-k)}\,. \tag{3.24}$$

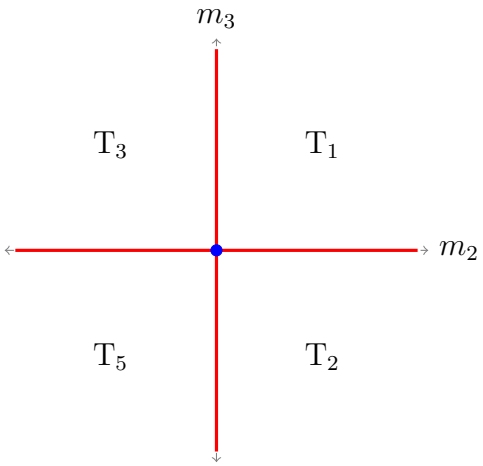

(a) (m_2, m_3), $m_1 > 0$

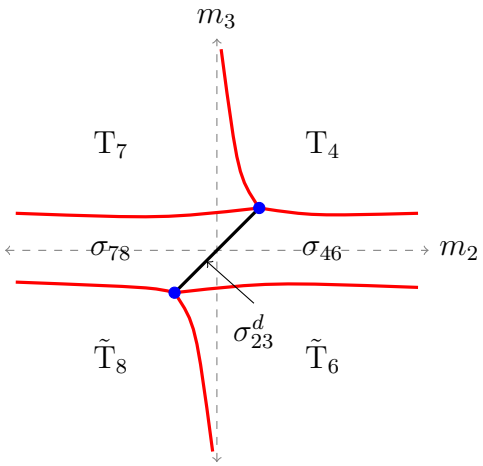

(b) (m_2, m_3), $m_1 < 0$

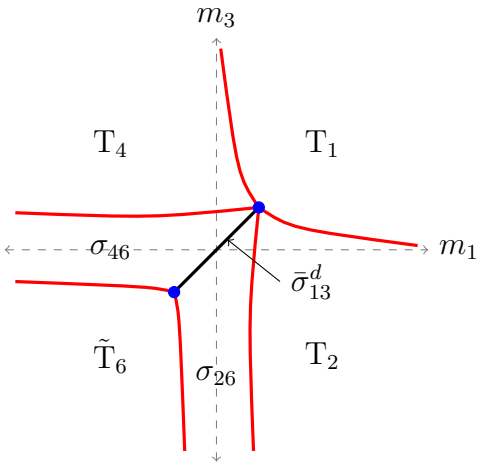

(c) (m_1, m_3), $m_2 > 0$

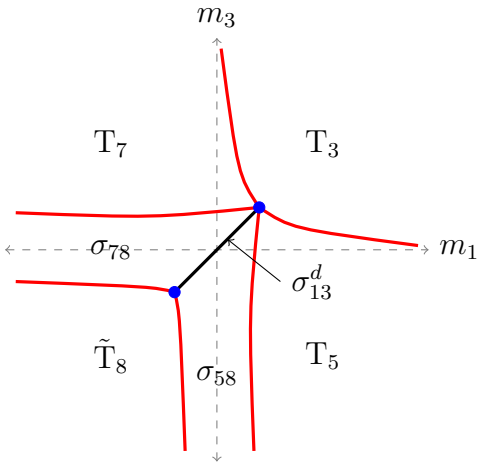

(d) (m_1, m_3), $m_2 < 0$

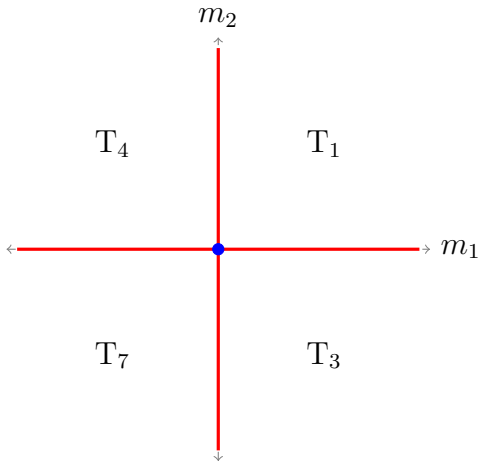

(e) (m_1, m_2), $m_3 > 0$

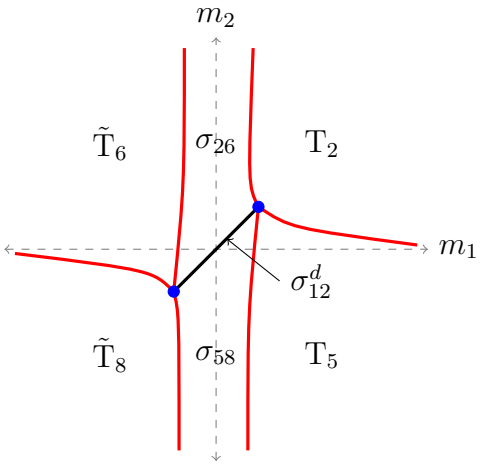

(f) (m_1, m_2), $m_3 < 0$

Figure 3.5: Phases of $SU(N)_k + p\,\psi_1 + q\,\psi_2 + (F - p - q)\,\psi_3$ with $F/2 - p \leq k < F/2 - q$.

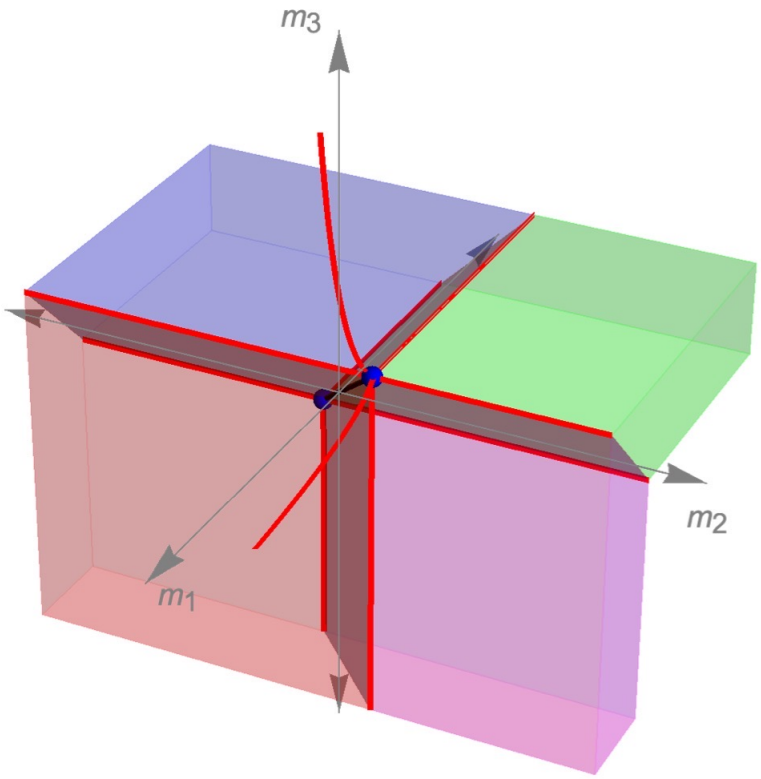

Figure 3.6: The three-dimensional phase diagram of $SU(N)_k + p\,\psi_1 + q\,\psi_2 + (F - p - q)\,\psi_3$ with $F/2 - p \leq k < F/2 - q$. $\bar{\sigma}_1^c$ is given by the region in magenta color and $\hat{\sigma}_3^c$ is represented by the green region.

The other two sigma models are σ_{46} as in equation (3.23) and a new σ_{26} that separates T_2 and $\tilde{\mathrm{T}}_6$ with a Grassmannian given by

$$\sigma_{26} : Gr(F_2/2 - k_2^+, p) = \frac{U(p)}{U(F/2 - q - k) \times U(k - F/2 + p + q)} \equiv \bar{\sigma}_1^c \,. \tag{3.25}$$

(iv) $m_2 \to -\infty$: in this case, k_2^- is within $F_2/2 - p \leq k_2^- < F_2/2$, which is just similar to case 2 with the same quantum phases σ_{13}^d, σ_{78}, and σ_{58}.

(v) $m_3 \to +\infty$: $k_3^+ > F_3/2$ giving a type I phase diagram just like in case 2.

(vi) $m_3 \to -\infty$: it is not clear whether this case is of type II or III because k_3^- takes some negative values in this range of k. The theory is better understood by rewriting its reduction in the form $SU(N)_{k_3^-} + q\,\psi_2 + (F_3 - q)\,\psi_1$. Hence it becomes clear that $|k_3^-| < F_3/2 - q$ and the theory is type III with sigma

models appearing only for small m_1 both negative and positive sides which are σ_{58} and σ_{26} respectively, as shown in figure 3.5f.

The phases of case 3 are summarized in figures 3.5 and 3.6. These phases are eight topological field theories ($\mathrm{T}_{1-5}, \tilde{\mathrm{T}}_6, \mathrm{T}_7, \tilde{\mathrm{T}}_8$), four cuboid sigma models ($\sigma_1^c, \bar{\sigma}_1^c, \hat{\sigma}_3^c, \sigma_3^c$), four planes of sigma models ($\sigma_{12}^d, \sigma_{13}^d, \bar{\sigma}_{13}^d, \sigma_{23}^d$), as well as the one-dimensional sigma model σ. In the limiting case $q = 0$, the Chern-Simons level range becomes $F/2 - p \leq k < F/2$ and the phase diagram is reduced to figure 2.4.

3.1.4 Case 4: $(p + q) - F/2 \leq k < F/2 - p$

Following the same procedure, we found that this case has the same topological phases as in case 3 with an extra change being that T_5 is replaced by $\tilde{\mathrm{T}}_5$ as

$$\mathrm{T}_5 \to \tilde{\mathrm{T}}_5 : SU(N)_{k-\frac{F}{2}+p} \longleftrightarrow U(F/2 - p - k)_N \,. \tag{3.26}$$

The two masses asymptotic limits show that the theory has the following cuboid sigma models

- $m_1 \to +\infty$ and $m_3 \to -\infty$:

$$\bar{\sigma}_2^c = \frac{U(q)}{U(F/2 - p - k) \times U(k - F/2 + p + q)} \,. \tag{3.27}$$

- $m_1 \to +\infty$ and $m_2 \to -\infty$:

$$\bar{\sigma}_3^c = \frac{U(F - p - q)}{U(F/2 - p - k) \times U(F/2 - q + k)} \,, \tag{3.28}$$

  along with $\bar{\sigma}_1^c$, $\hat{\sigma}_3^c$, and σ_3^c.

The six sides of the three-dimensional picture have the following phases:

(i) $m_1 \to +\infty$: $F_1/2 - q \leq k_1^+ < F_1/2$ and the theory has a type II phase diagram with a diagonal sigma model $\bar{\sigma}_{23}^d$ given by

$$\bar{\sigma}_{23}^d : Gr(F_1/2 + k_1^+, F_1) = \frac{U(F-p)}{U(F/2+k) \times U(F/2-p-k)} \,. \tag{3.29}$$

This diagonal sigma model separates two other sigma models given by

$$\sigma_{35} : Gr(F_1/2 - k_1^+, F_1 - q) = \frac{U(F-p-q)}{U(F/2-p-k) \times U(F/2-q+k)} \equiv \bar{\sigma}_3^c \,, \tag{3.30}$$

$$\sigma_{25} : Gr(F_1/2 - k_1^+, q) = \frac{U(q)}{U(F/2-p-k) \times U(k-F/2+p+q)} \equiv \bar{\sigma}_2^c \,. \tag{3.31}$$

(ii) $m_1 \to -\infty$: this limit is similar to case 3 with σ_{23}^d, σ_{78}, and σ_{46} appear as quantum phases.

(iii) $m_2 \to +\infty$: this is also similar to case 3 with $\bar{\sigma}_{13}^d$, σ_{46}, and σ_{26}.

(iv) $m_2 \to -\infty$: we have $k_2^- < F_2/2 - p$ within this range of k, which makes this limit to be of type III with σ_{13}^d, σ_{78}, and σ_{35}.

(v) $m_3 \to +\infty$: this remains of type I phase diagram just like in cases 2 and 3.

(vi) $m_3 \to -\infty$: this limit gives a shifted level within the range $F_3/2 - p < k_3^- < F_3/2$, which makes this case of type II phase diagram. However, k_3^- is always negative in this range of k, which requires a flip of the masses signs to get the right phase diagram. This allows sigma models to appear for small m_2 but positive m_1 (σ_{25}) and small m_1 with positive m_2 (σ_{26}) instead of σ_{68} and σ_{58}, as shown in figure 3.7f. σ_{25} and σ_{26} are the correct phases to appear in this limit as they are part of $\bar{\sigma}_1^c$ and $\bar{\sigma}_2^c$ while σ_{68} and σ_{58} are part of σ_1^c and σ_2^c which do not appear in this range of k.

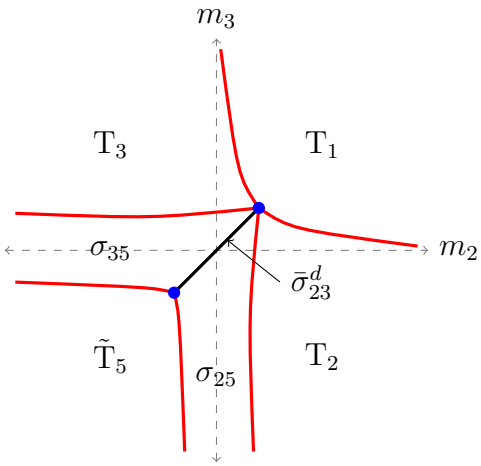

(a) (m_2, m_3), $m_1 > 0$

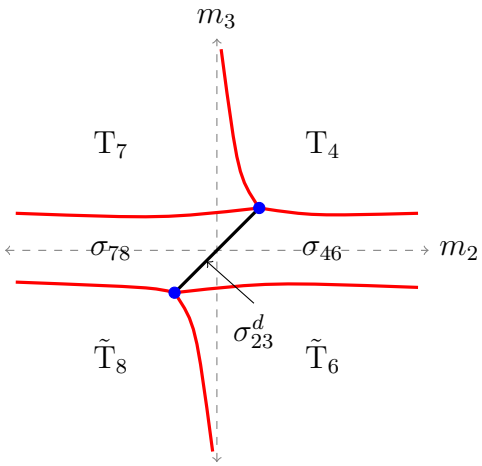

(b) (m_2, m_3), $m_1 < 0$

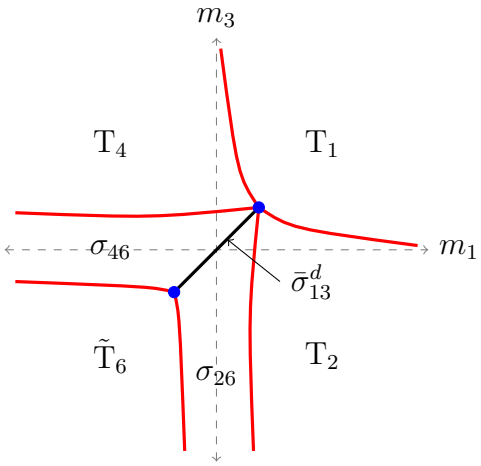

(c) (m_1, m_3), $m_2 > 0$

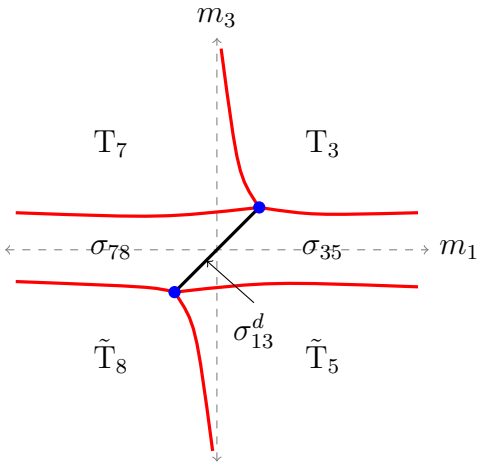

(d) (m_1, m_3), $m_2 < 0$

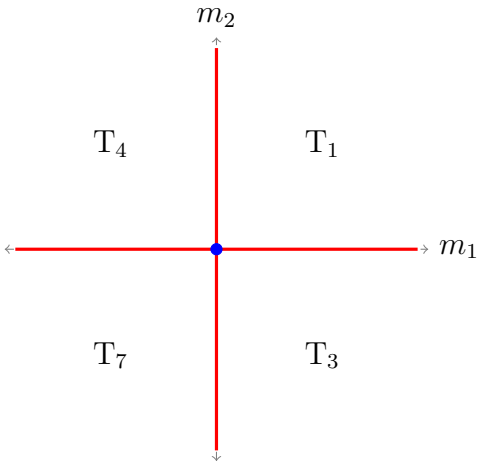

(e) (m_1, m_2), $m_3 > 0$

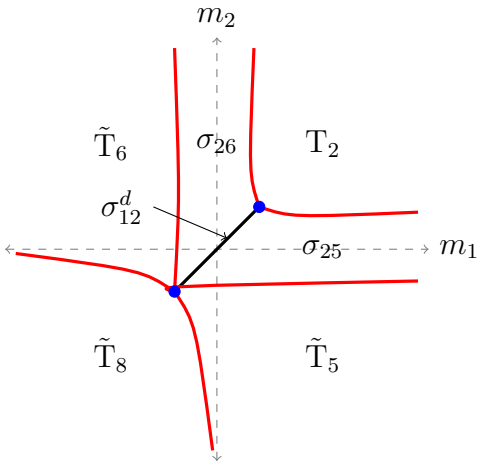

(f) (m_1, m_2), $m_3 < 0$

Figure 3.7: Phases of $SU(N)_k + p\,\psi_1 + q\,\psi_2 + (F - p - q)\,\psi_3$ with $(p+q) - F/2 \leq k < F/2 - p$.

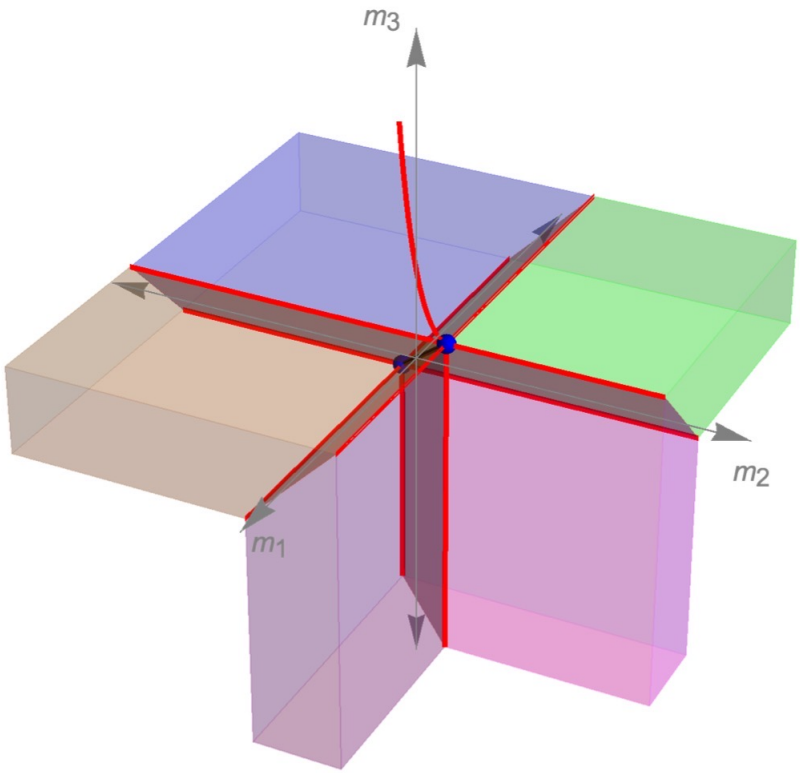

Figure 3.8: The three-dimensional phase diagram of $SU(N)_k + p\,\psi_1 + q\,\psi_2 + (F - p - q)\,\psi_3$ with $(p+q) - F/2 \leq k < F/2 - p$. $\bar{\sigma}_2^c$ is the region in purple and $\bar{\sigma}_3^c$ is represented by the light brown region.

Figures 3.7 and 3.8 summarize the phases of case 4, which include the following; the eight topological phases (T_{1-4}, $\tilde{\mathrm{T}}_5, \tilde{\mathrm{T}}_6, \mathrm{T}_7, \tilde{\mathrm{T}}_8$), five cuboid sigma models ($\bar{\sigma}_1^c, \bar{\sigma}_2^c, \bar{\sigma}_3^c, \hat{\sigma}_3^c, \sigma_3^c$), five planes of sigma models ($\sigma_{12}^d, \sigma_{13}^d, \bar{\sigma}_{13}^d, \sigma_{23}^d, \bar{\sigma}_{23}^d$) together with the sigma model line σ. In the limiting case $q = 0$, the phase diagram becomes equivalent to a theory with level $k = F/2 - p$ where all the sigma models and the topological theories T_2 and T_5, trivialize. The phase diagram is then reduced to a two-dimensional phase diagram with three topological theories T_a, T_b, and T_c, as well as a trivial theory $SU(N)_0$.

3.1.5 Case 5: $0 \leq k < (p+q) - F/2$

This is the last possible range of k has a three-dimensional phase diagram with the same topological phases as in case 4 except that T_7 is now

$$\mathrm{T}_7 \to \tilde{\mathrm{T}}_7 : SU(N)_{k+\frac{F}{2}-p-q} \longleftrightarrow U(p+q-F/2-k)_N\,. \tag{3.32}$$

The topological theories come along with $\bar{\sigma}_1^c$, $\bar{\sigma}_2^c$, $\bar{\sigma}_3^c$, $\hat{\sigma}_3^c$, and the following new cuboid quantum regions

- $m_2 \to -\infty$, $m_3 \to +\infty$:

$$\hat{\sigma}_1^c = \frac{U(p)}{U(F/2+k-q) \times U(p+q-F/2-k)} \,. \tag{3.33}$$

- $m_1 \to -\infty$, $m_3 \to +\infty$:

$$\hat{\sigma}_2^c = \frac{U(q)}{U(F/2+k-p) \times U(p+q-F/2-k)} \,. \tag{3.34}$$

The one mass asymptotic limits are now

(i) $m_1 \to +\infty$: $F_1/2 - q \leq k_1^+ < F_1/2$ which gives a type II phase diagram with the quantum regions $\bar{\sigma}_{23}^d$, σ_{35}, and σ_{25}

(ii) $m_1 \to -\infty$: $F_1/2 - q \leq |k_1^-| < F_1/2$ with negative k_1^- which leads to a time-reversed type II phase diagram as shown in figure 3.9b with the phases σ_{23}^d, σ_{46}, and σ_{47}, where

$$\sigma_{47} : Gr(F_1/2 + k_1^-, q) = \frac{U(q)}{U(F/2+k-p) \times U(p+q-F/2-k)} \equiv \hat{\sigma}_2^c \,. \tag{3.35}$$

(iii) $m_2 \to +\infty$: $F_2/2 - p < k_2^+ < F_2/2$ and the phase diagram is of type II with the phases $\bar{\sigma}_{13}^d$, σ_{46}, and σ_{26}.

(iv) $m_2 \to -\infty$: $F_2/2 - p < |k_2^-| < F_2/2$, with $k_2^- < 0$, hence we have a time-reversed type II phase diagram with σ_{13}^d, σ_{35}, and σ_{37}, where

$$\sigma_{37} : Gr(F_2/2 + k_2^-, p) = \frac{U(p)}{U(F/2+k-q) \times U(p+q-F/2-k)} \equiv \hat{\sigma}_1^c \,. \tag{3.36}$$

(v) $m_3 \to +\infty$: $F_3/2 - p \leq |k_3^+| < F_3/2$ which gives a type II phase diagram with σ_{37}, σ_{47}, and a new diagonal sigma model $\bar{\sigma}_{12}^d$ given by

$$\bar{\sigma}_{12}^d : Gr(F_3/2 + k_3^+, F_3) = \frac{U(p+q)}{U(F/2+k) \times U(p+q-F/2-k)} \ , \qquad (3.37)$$

(vi) $m_3 \to -\infty$: $F_3/2 - p \leq |k_3^-| < F_3/2$ this limit has a time-reversed type II phase diagram with σ_{12}^d, σ_{25}, and σ_{26}.

We summarize the phases of case 5 infigures 3.9 and 3.10 where these are: eight topological field theories ($\mathrm{T}_1, \mathrm{T}_2, \mathrm{T}_3, \mathrm{T}_4, \tilde{\mathrm{T}}_5, \tilde{\mathrm{T}}_6, \tilde{\mathrm{T}}_7, \tilde{\mathrm{T}}_8$), six cuboid sigma models ($\bar{\sigma}_1^c, \hat{\sigma}_1^c, \bar{\sigma}_2^c, \hat{\sigma}_2^c, \bar{\sigma}_3^c, \hat{\sigma}_3^c$), six planes of sigma models ($\sigma_{12}^d, \bar{\sigma}_{12}^d, \sigma_{13}^d, \bar{\sigma}_{13}^d, \sigma_{23}^d, \bar{\sigma}_{23}^d$), as well as σ. The limiting case $q = 0$ reproduces the phase diagram in figure 2.5.

3.2 $F - p - q > F/2$ Scenario

In this scenario we consider the choice of p and q such that $0 < q \leq p \leq p+q \leq F/2$. The range of k diagram is divided into: $k \geq F/2$, $F/2 - q \leq k < F/2$, $F/2 - p \leq k < F/2 - q$, $F/2 - (p+q) \leq k < F/2 - p$, and $0 \leq k < F/2 - (p+q)$, we label these cases by $\bar{1}$, $\bar{2}$, $\bar{3}$, $\bar{4}$, and $\bar{5}$, respectively. We notice that the cases $\bar{1}$ to $\bar{3}$ are precisely similar to cases 1 to 3 of the first scenario, and the phase diagrams of these cases are equivalent. Case $\bar{4}$ is identical to case 4 in the first scenario since we have $k > |F/2 - (p+q)|$ in both scenarios. The only difference then would be in the $0 \leq k < F/2 - (p+q)$ case.

3.2.1 Case $\bar{5}$: $0 \leq k < F/2 - (p+q)$

This range of k under the constraint of this scenario has a three-dimensional phase diagram with the same topological phases as in case 4 of the first scenario except that T_2 is now

$$\mathrm{T}_2 \to \tilde{\mathrm{T}}_2 : SU(N)_{k-\frac{F}{2}+p+q} \longleftrightarrow U(F/2-p-q-k)_N \, . \qquad (3.38)$$

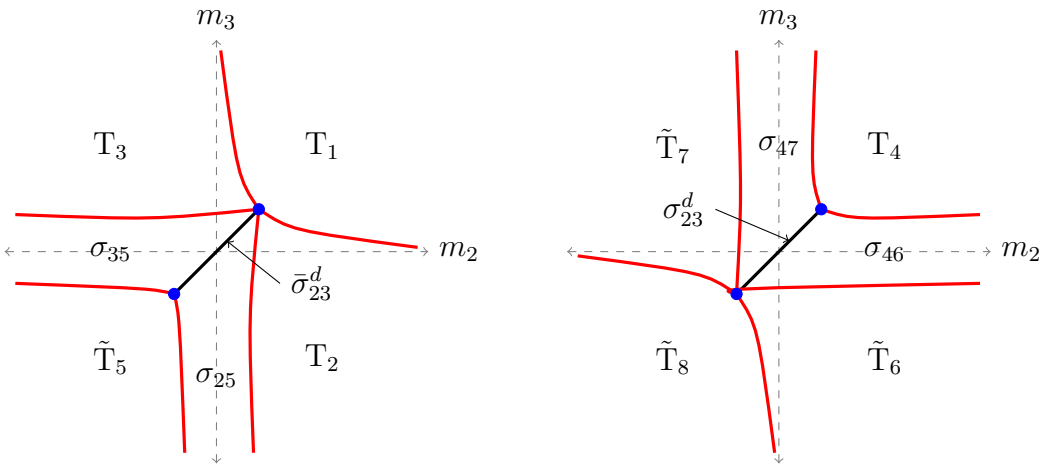

(a) (m_2, m_3), $m_1 > 0$ (b) (m_2, m_3), $m_1 < 0$

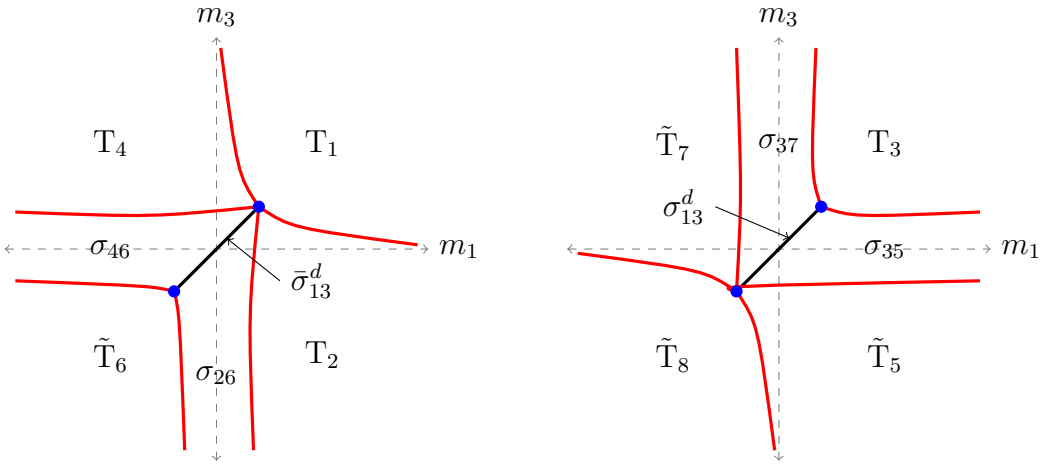

(c) (m_1, m_3), $m_2 > 0$ (d) (m_1, m_3), $m_2 < 0$

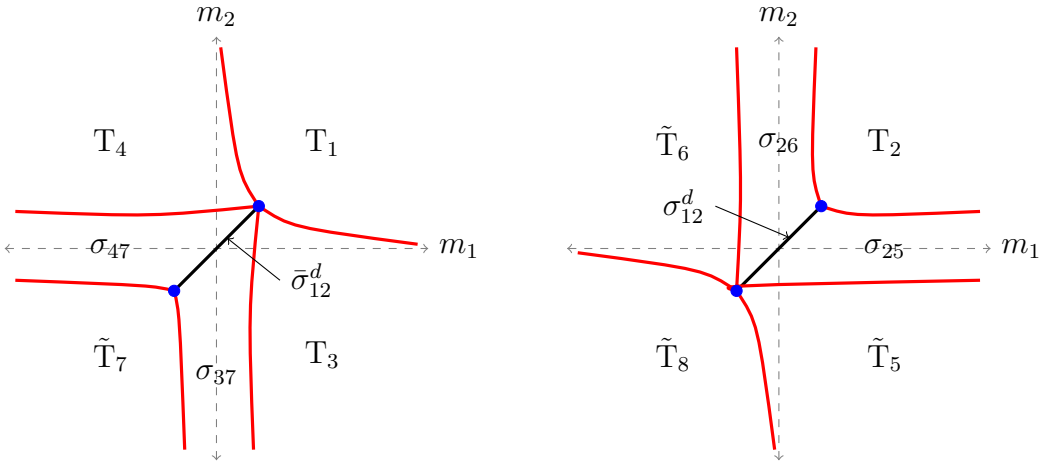

(e) (m_1, m_2), $m_3 > 0$ (f) (m_1, m_2), $m_3 < 0$

Figure 3.9: Phases of $SU(N)_k + p\,\psi_1 + q\,\psi_2 + (F-p-q)\,\psi_3$ with $0 \leq k < (p+q) - F/2$.

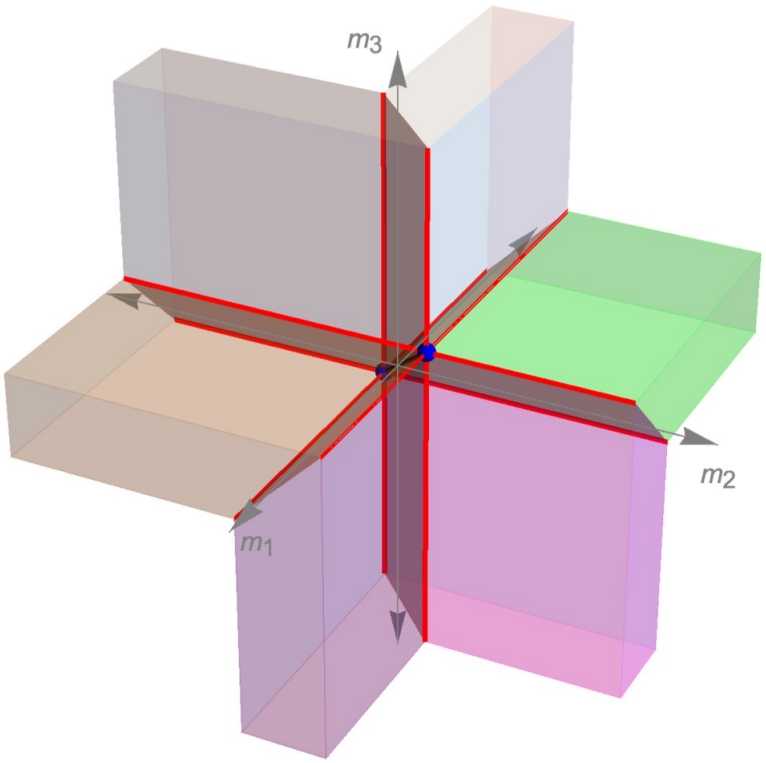

Figure 3.10: The three-dimensional phase diagram of $SU(N)_k + p\,\psi_1 + q\,\psi_2 + (F - p - q)\,\psi_3$ with $0 \leq k < (p+q) - F/2$. $\hat{\sigma}_1^c$ is represented by the region in gray, while $\hat{\sigma}_2^c$ is the white region.

The topological theories come along with σ_3^c, $\bar{\sigma}_3^c$, $\hat{\sigma}_3^c$, and a new cuboid region when we send m_1, $m_2 \to +\infty$ given by

$$\tilde{\sigma}_3^c = \frac{U(F-p-q)}{U(F/2+k) \times U(F/2-p-q-k)}\,. \tag{3.39}$$

The one mass asymptotic limits are now

(i) $m_1 \to +\infty$: $p/2 \leq k_1^+ < F_1/2 - q$ which gives a type III phase diagram with the quantum regions $\bar{\sigma}_{23}^d$, σ_{35} as well as a new region for small m_3 but positive m_2:

$$\sigma_{12} : Gr(F_1/2 + k_1^+, F_1 - q) = \frac{U(F-p-q)}{U(F/2+k) \times U(F/2-p-q-k)} \equiv \tilde{\sigma}_3^c\,. \tag{3.40}$$

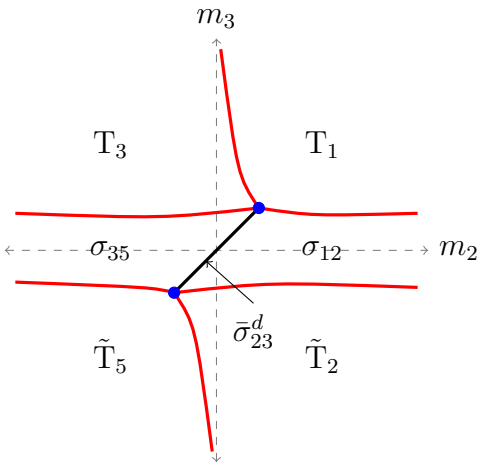

(a) (m_2, m_3), $m_1 > 0$

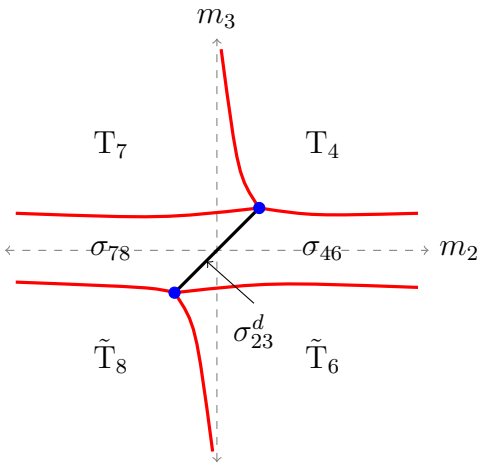

(b) (m_2, m_3), $m_1 < 0$

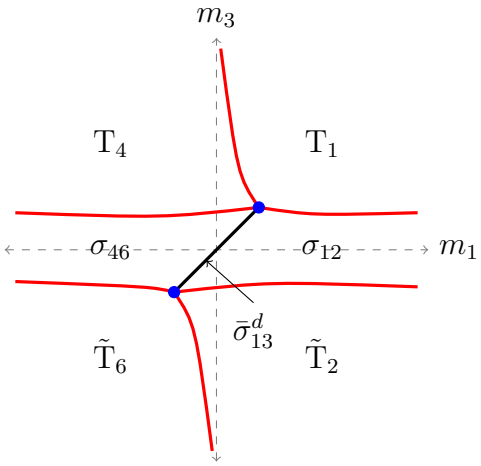

(c) (m_1, m_3), $m_2 > 0$

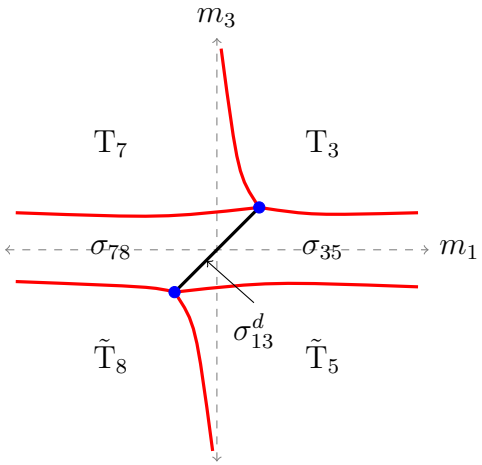

(d) (m_1, m_3), $m_2 < 0$

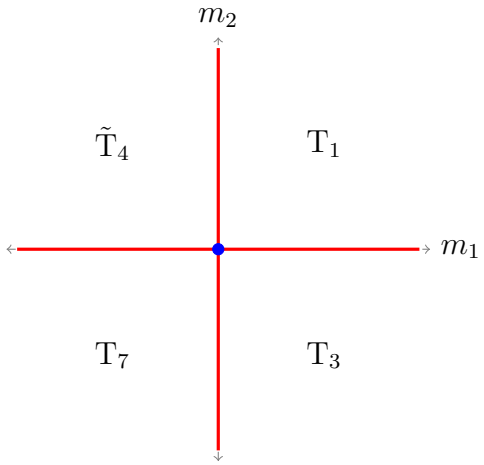

(e) (m_1, m_2), $m_3 > 0$

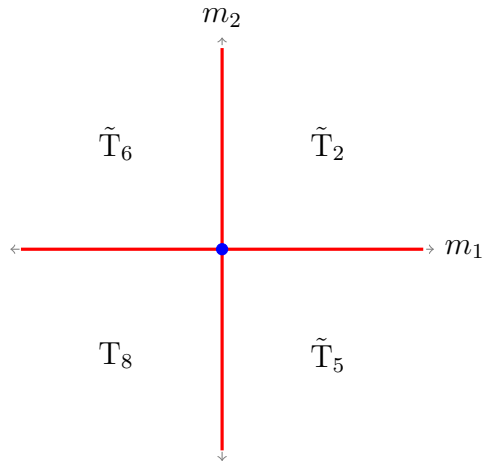

(f) (m_1, m_2), $m_3 < 0$

Figure 3.11: Phases of $SU(N)_k + p\,\psi_1 + q\,\psi_2 + (F - p - q)\,\psi_3$ with $0 \leq k < F/2 - (p + q)$.

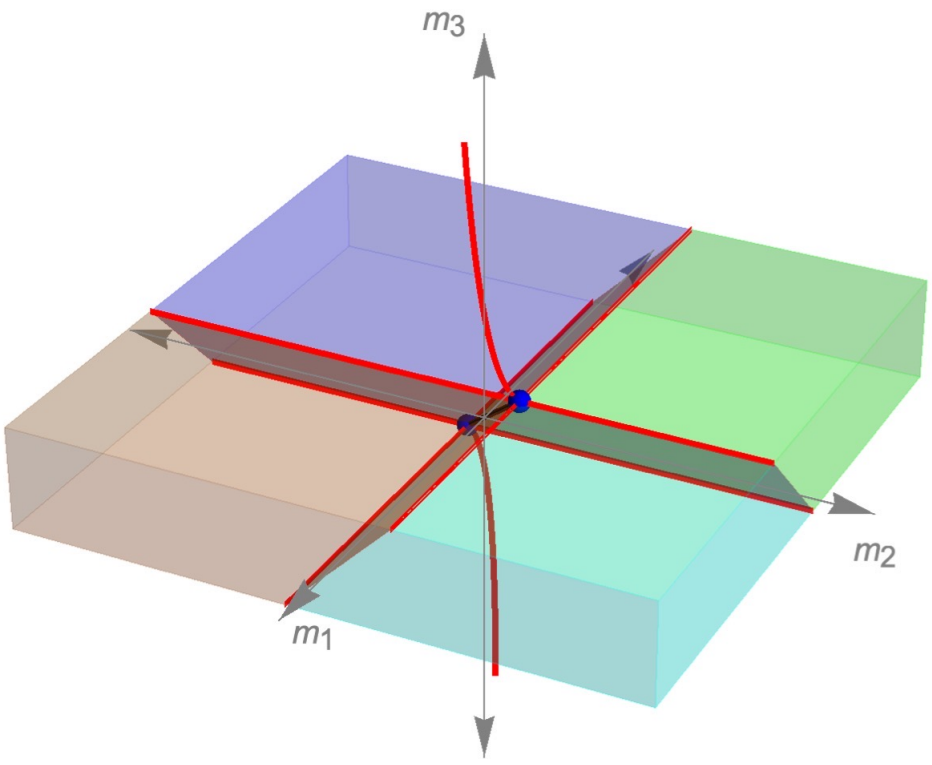

Figure 3.12: The three-dimensional phase diagram of $SU(N)_k + p\,\psi_1 + q\,\psi_2 + (F - p - q)\,\psi_3$ with $0 \leq k < F/2 - (p+q)$. $\tilde{\sigma}_3^c$ is represented by the region in cyan.

(ii) $m_1 \to -\infty$: $|k_1^-| < F_1/2 - q$ giving a type III phase diagram as in case 4 with the phases σ_{23}^d, σ_{78}, and σ_{46}.

(iii) $m_2 \to +\infty$: $q/2 < k_2^+ < F_2/2 - p$ and the phase diagram is of type III with the phases $\bar{\sigma}_{13}^d$, σ_{46}, and σ_{12}.

(iv) $m_2 \to -\infty$: this is a type III phase diagram with σ_{13}^d, σ_{78}, and σ_{35}.

(v) $m_3 \to +\infty$: type I phase diagram.

(vi) $m_3 \to -\infty$: this limit has a type I phase diagram with no quantum regions as it satisfies $|k_3^-| > F_3/2$.

We summarize the phases of case $\bar{5}$ in figures 3.11 and 3.12 where these are: eight topological field theories ($\mathrm{T}_1, \tilde{\mathrm{T}}_2, \mathrm{T}_3, \mathrm{T}_4, \tilde{\mathrm{T}}_5, \tilde{\mathrm{T}}_6, \mathrm{T}_7, \tilde{\mathrm{T}}_8$), four cuboid sigma models ($\tilde{\sigma}_3^c$, $\bar{\sigma}_3^c$, $\hat{\sigma}_3^c, \sigma_3^c$), four planes of sigma models ($\sigma_{13}^d, \bar{\sigma}_{13}^d, \sigma_{23}^d, \bar{\sigma}_{23}^d$), and the one-dimensional sigma model σ. The limiting case $q = 0$ reproduces the phase diagram in figure 2.5.

We see that this scenario does not include $\bar{\sigma}^d_{12}$, $\hat{\sigma}^c_1$, and $\hat{\sigma}^c_2$ as in the first scenario. However, this scenario includes $\tilde{\sigma}^c_3$, which was missing in the first scenario. Hence there is no single analysis that discusses the full phases of the three-family case; one should choose a scenario for the analysis based on the number $F - p - q$. The difference appears in some new and other missing quantum phases for each scenario.

3.3 Consistency checks: Three-family case

In this section, we discuss a few ways to check our analysis for the three-family case. We mostly zoom on the region around the blue critical points on our figures, when we use the boson/fermion duality adapted to our three-family situation. We generalize the procedure used in [2] to our model of the three-family theory. The discussion for this section is mainly for the first scenario discussed in section 3.2, and we will mention the possible changes to the analysis when we use the second scenario accordingly.

3.3.1 Planar sigma models

Before we start looking at the bosonic phases, we give an alternative way of the reduction to the two-family case by looking at the planes where two of the masses are equal. This reduction gives more insights into the nature of the diagonal sigma models that appear in the three-family theory.

$(\mathbf{m_1 = m_2}, \mathbf{m_3})$ plane

The theory is reduced to $SU(N)_k + \bar{p}\,\psi_1 + (F - \bar{p})\,\psi_3$ with $\bar{p} = p + q$ fermions of mass $m_1 = m_2$ and $F - \bar{p}$ of mass m_3. However, in this case the choice of $\bar{p}$ is such that $0 \leq F - \bar{p} \leq F/2$, which makes the quantum regions appear for small $m_1 = m_2$ in the type III phase diagram. The phase diagram is then of type I in case 1, type II in cases 2, 3, and 4, and type III in case 5 of section 3.1. The

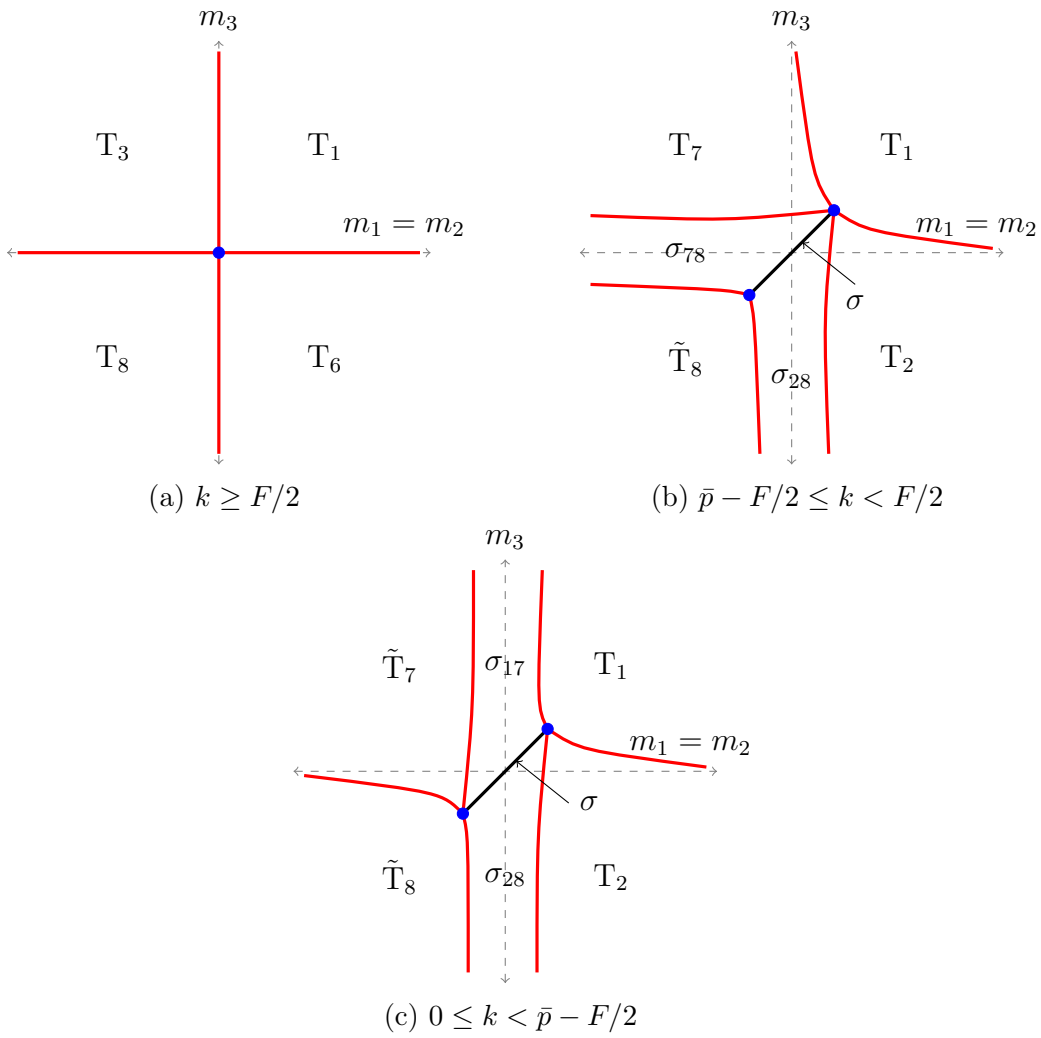

(a) $k \geq F/2$ (b) $\bar{p} - F/2 \leq k < F/2$

(c) $0 \leq k < \bar{p} - F/2$

Figure 3.13: Phase diagrams in the limiting case $m_1 = m_2$.

phase diagrams are now reduced to the phases in figure 3.13. In figure 3.13b, the quantum phases are σ_{17} and σ_{28} where

$$\sigma_{17} : Gr(F/2 + k, \bar{p}) = \frac{U(p+q)}{U(F/2+k) \times U(p+q-F/2-k)} \equiv \bar{\sigma}^d_{12}\,, \tag{3.41}$$

$$\sigma_{28} : Gr(F/2 - k, \bar{p}) = \frac{U(p+q)}{U(F/2-k) \times U(k-F/2+p+q)} \equiv \sigma^d_{12}\,. \tag{3.42}$$

We note that σ_{28} is equivalent to σ^d_{12}, which clearly shows that σ^d_{12} is not a line of quantum phase but rather a plane, and it appears in cases 2, 3, and 4. The quantum regions in figure 3.13c are σ_{78} and σ_{17}, which are given by equations (3.11) and (3.41).

The only difference between the first and second scenarios is that the phase diagram in figure 3.13c becomes a type III with quantum regions for small m_3 instead of small $m_1 = m_2$. This makes the diagonal sigma model $\bar{\sigma}^d_{12}$ disappear as we expected from the discussion of case $\bar{5}$.

$(\mathbf{m_1} = \mathbf{m_3}, \mathbf{m_2})$ plane

The theory is reduced to $SU(N)_k + q\,\psi_2 + (F-q)\,\psi_3$ with q fermions of mass $m_1 = m_3$ and $F - q$ fermions of mass m_2. The phase diagram is now of type I in case 1, type II in case 2, and type III in cases 3, 4, and 5. The phase diagram is summarized in figure 3.14 with the following quantum regions: in figure 3.14b we have σ_{68} and σ_{38} where

$$\sigma_{38} : Gr(F/2-k, F-q) = \frac{U(F-q)}{U(F/2-k) \times U(F/2-q+k)} \equiv \sigma^d_{13}\,. \tag{3.43}$$

In figure 3.14c the quantum phases are σ_{38} and σ_{16} where

$$\sigma_{16} : Gr(F/2+k, F-q) = \frac{U(F-q)}{U(F/2+k) \times U(F/2-q-k)} \equiv \bar{\sigma}^d_{13}\,. \tag{3.44}$$

We conclude that the diagonal sigma model σ^d_{13} appears in all the cases except case 1 while $\bar{\sigma}^d_{13}$ appears only in cases 3, 4, and 5 of section 3.1. The analysis is the same for the second scenario.

$(\mathbf{m_1}, \mathbf{m_2} = \mathbf{m_3})$ plane

The theory is reduced to $SU(N)_k + p\,\psi_1 + (F-p)\,\psi_3$ where $\psi_2 = \psi_3$. The phase diagram is of type I in case 1, type II only in cases 2 and 3, and type III in cases 4 and 5. The phase diagram is summarized in figure 3.15, wherein figure 3.15b, the quantum regions are σ_{58} and σ_{48} with

$$\sigma_{48} : Gr(F/2-k, F-p) = \frac{U(F-p)}{U(F/2-k) \times U(F/2-p+k)} \equiv \sigma^d_{23}\,. \tag{3.45}$$

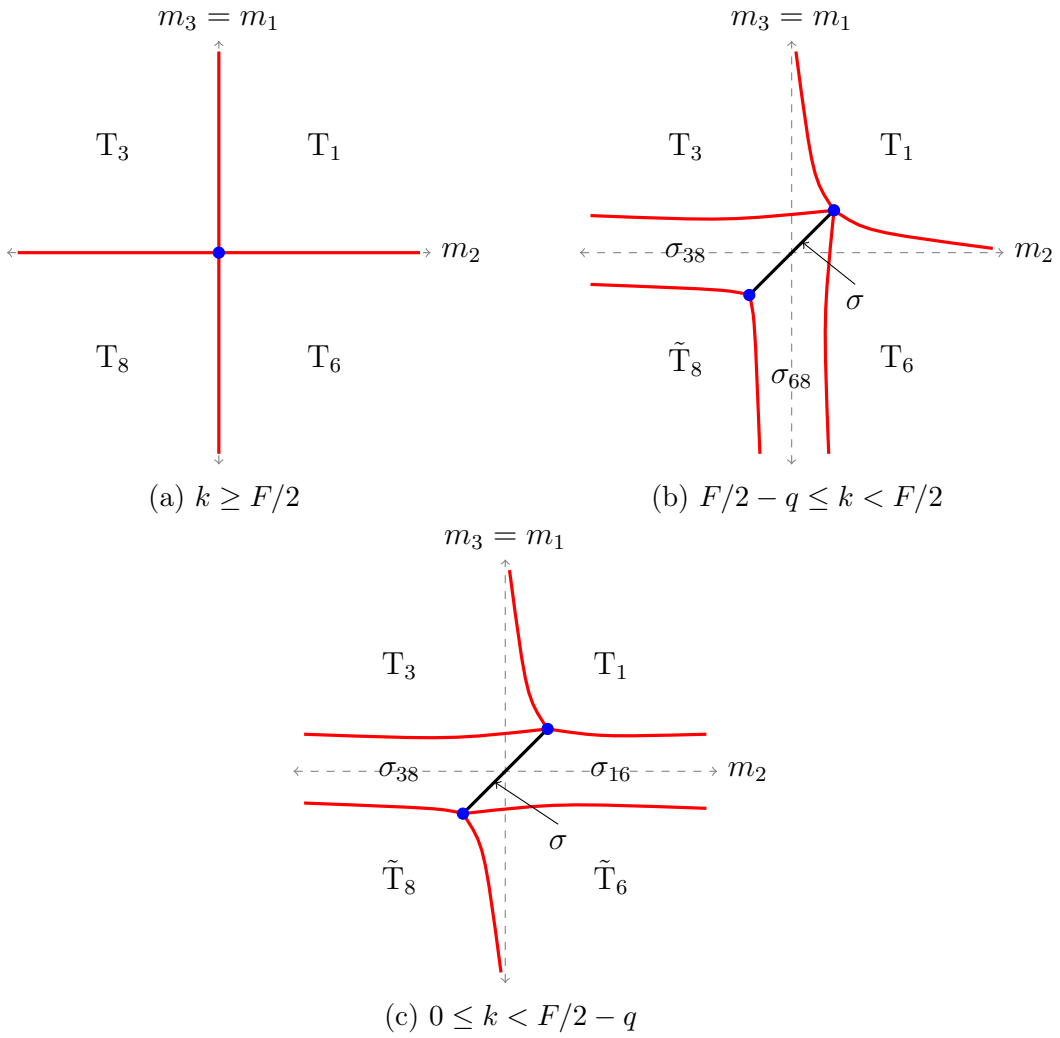

(a) $k \geq F/2$ (b) $F/2 - q \leq k < F/2$

(c) $0 \leq k < F/2 - q$

Figure 3.14: Phase diagrams in the limiting case $m_1 = m_3$

In figure 3.15c the quantum phases are σ_{48} and σ_{15} where

$$\sigma_{15} : Gr(F/2+k, F-p) = \frac{U(F-p)}{U(F/2+k) \times U(F/2-p-k)} \equiv \bar{\sigma}^d_{23}\,, \qquad (3.46)$$

which shows that the diagonal sigma model σ^d_{23} appears in cases 2 and 3 while $\bar{\sigma}^d_{23}$ appears in cases 4 and 5. The analysis is also the same for the second scenario in this limiting case.

3.3.2 Matching the bosonic phases

We employ the bosonic dual description to match the phases around the critical points, just as we did for the two-family example. We begin with a theory

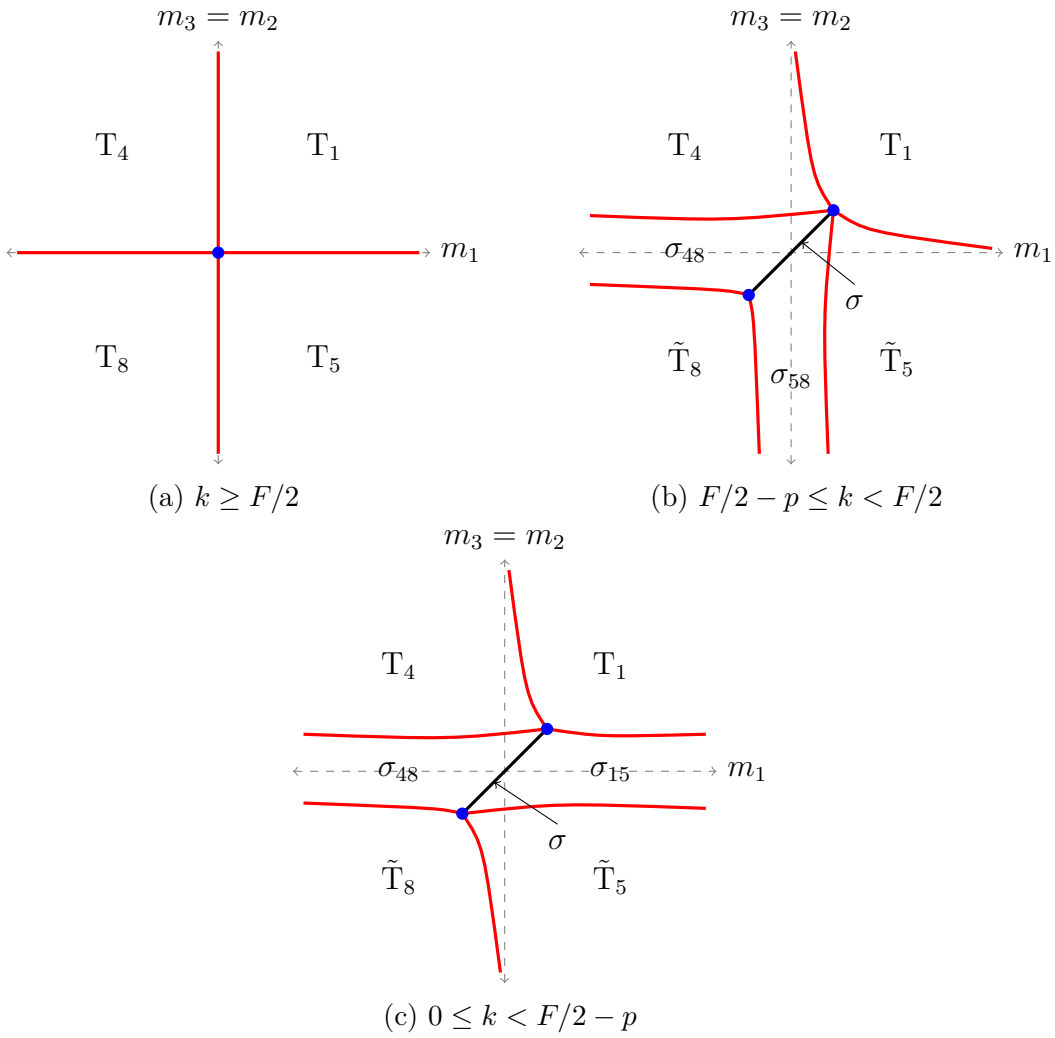

(a) $k \geq F/2$ (b) $F/2 - p \leq k < F/2$

(c) $0 \leq k < F/2 - p$

Figure 3.15: Phase diagrams in the limiting case $m_2 = m_3$

formed of a gauge group $U(n)_l$ and three sets of scalar fields in the fundamental representation: $p\,\phi_1$, $q\,\phi_2$, and $(F-p-q)\,\phi_3$. We divided the F scalars into three groups that can acquire distinct mass deformations, denoted by M_i^2, $i = 1, 2, 3$.

This bosonic theory has six gauge invariant operators which can be written in terms of the three scalars as

$$\begin{aligned} X &= \phi_1\,\phi_1^\dagger,\ Y = \phi_2\,\phi_2^\dagger,\ Z = \phi_3\,\phi_3^\dagger \\ U &= \phi_1\,\phi_2^\dagger,\ W = \phi_1\,\phi_3^\dagger,\ T = \phi_2\,\phi_3^\dagger\,, \end{aligned} \tag{3.47}$$

where X, Y, and Z are positive semidefinite diagonal Hermitian matrices of dimensions p, q, and $F-p-q$, respectively. We consider a scalar potential for the critical theory up to quartic order in the scalar field, which is further deformed by

symmetry breaking mass operators. Written in terms of the six gauge invariant operators, this is

$$\begin{aligned} V = M_1^2 \mathrm{Tr}X + M_2^2 \mathrm{Tr}Y + M_3^2 \mathrm{Tr}Z + \lambda(\mathrm{Tr}^2 X + \mathrm{Tr}^2 Y \\ + \mathrm{Tr}^2 Z + 2\mathrm{Tr}X\mathrm{Tr}Y + 2\mathrm{Tr}X\mathrm{Tr}Z + 2\mathrm{Tr}Y\mathrm{Tr}Z) + \\ \mu(\mathrm{Tr}X^2 + \mathrm{Tr}Y^2 + \mathrm{Tr}Z^2 + 2\mathrm{Tr}UU^\dagger + 2\mathrm{Tr}WW^\dagger + 2\mathrm{Tr}TT^\dagger)\,, \end{aligned} \tag{3.48}$$

where λ and μ are the coupling constants for the quartic terms. The quartic couplings are chosen such that the full $U(F)$ flavour symmetry is preserved. We choose $\mu \geq 0$, which requires $\mu + \min(n, F)\lambda > 0$ for the potential to be bounded from below.

Consider that X, Y, and Z have r_1, r_2, and r_3 degenerate eigenvalues x, y, and z respectively such that

$$\mathrm{Tr}X = r_1 x,\ \mathrm{Tr}Y = r_2 y,\ \mathrm{Tr}Z = r_3 z,\ . \tag{3.49}$$

The gauge group $U(n)$ is never Higgsed if the squared mass of X, Y, and Z are non-negative. In this case, all the six gauge invariant operators vanish on-shell, so there is no scalar condensation, all matter fields are integrated out due to being massive, and one obtains a topological $U(n)_l$ theory in the infrared.

On the other hand, if at least one of the scalars has a negative mass squared, the minimum of the potential can be found by solving the equations of motion

$$M_1^2 + 2\lambda(\mathrm{Tr}X + \mathrm{Tr}Y + \mathrm{Tr}Z) + 2\mu X = 0\,, \tag{3.50}$$

$$M_2^2 + 2\lambda(\mathrm{Tr}X + \mathrm{Tr}Y + \mathrm{Tr}Z) + 2\mu Y = 0\,, \tag{3.51}$$

$$M_3^2 + 2\lambda(\mathrm{Tr}X + \mathrm{Tr}Y + \mathrm{Tr}Z) + 2\mu Z = 0\,. \tag{3.52}$$

It also implies that $U = W = T = 0$. Solving the equations of motion gives the following eigenvalues

$$x = \frac{\lambda(M_2^2 r_2 + M_3^2 r_3) - M_1^2[\mu + \lambda(r_2 + r_3)]}{2\mu[\mu + \lambda(r_1 + r_2 + r_3)]}\,, \tag{3.53}$$

$$y = \frac{\lambda(M_1^2 r_1 + M_3^2 r_3) - M_2^2[\mu + \lambda(r_1 + r_3)]}{2\mu[\mu + \lambda(r_1 + r_2 + r_3)]}\,, \tag{3.54}$$

$$z = \frac{\lambda(M_1^2 r_1 + M_2^2 r_2) - M_3^2[\mu + \lambda(r_1 + r_2)]}{2\mu[\mu + \lambda(r_1 + r_2 + r_3)]}\,. \tag{3.55}$$

It can be easily seen that minimizing the potential always requires maximization of $r_1 + r_2 + r_3$. The ranks r_1, r_2, and r_3 are non-negative integers satisfying the following conditions

$$\begin{aligned} r_1 &\leq \min(n, p)\,, \\ r_2 &\leq \min(n, q)\,, \\ r_3 &\leq \min(n, F - p - q)\,, \\ r_1 + r_2 + r_3 &\leq \min(n, F)\,. \end{aligned} \tag{3.56}$$

The constraints in **??** and the sign of the mass squared of each gauge invariant operator defines the phases that appear in the bosonic theory. The bosonic theory experiences Higgsing of the gauge group or Higgsing plus spontaneous symmetry breaking except when M_1^2, M_2^2, and M_3^2 are all non-negative, as discussed above.

The phase diagram of the bosonic theory can be divided into five cases:

1. $\underline{q \leq p \leq F - p - q \leq F < n}$:

   $F < n$ does not allow any spontaneous symmetry breaking for the flavour symmetry $U(F)$. We expect to have eight different regions to describe the phase diagram in this range. Region $\mathbb{A}$ describes the theory when all the masses squared are non-negative with no scalar condensation. The regions $\mathbb{B}$, $\mathbb{C}$, and $\mathbb{D}$ are reached when only one scalar mass squared is negative, allowing a condensation for ϕ_1, ϕ_2, or ϕ_3, respectively. There are also three regions $\mathbb{E}$, $\mathbb{F}$, and $\mathbb{G}$ where two of the scalars condense before integrating

them out. The last region, $\mathbb{H}$, describes a phase when the three scalars condense simultaneously.

Region	r_1	r_2	r_3	Phase	Scenario 1		Scenario 2	
					$n = F/2 + k$	$n = F/2 - k$	$n = F/2 + k$	$n = F/2 - k$
$\mathbb{A}$	0	0	0	$U(n)_l$	T_1	$\tilde{T}_8$	T_1	$\tilde{T}_8$
$\mathbb{B}$	p	0	0	$U(n-p)_l$	T_4	$\tilde{T}_5$	T_4	$\tilde{T}_5$
$\mathbb{C}$	0	q	0	$U(n-q)$	T_3	$\tilde{T}_6$	T_3	$\tilde{T}_6$
$\mathbb{D}$	0	0	$F-p-q$	$U(n-F+p+q)_l$	T_2	$\tilde{T}_7$	T_2	N/A
$\mathbb{E}$	p	q	0	$U(n-p-q)_l$	T_7	N/A	T_7	$\tilde{T}_2$
$\mathbb{F}$	p	0	$F-p-q$	$U(n-F+q)_l$	T_6	N/A	T_6	N/A
$\mathbb{G}$	0	q	$F-p-q$	$U(n-F+p)_l$	T_5	N/A	T_5	N/A
$\mathbb{H}$	p	q	$F-p-q$	$U(n-F)_l$	T_8	N/A	T_8	N/A

Table 3.1: Phases of the bosonic theory $U(n)_l + p\phi_1 + q\phi_2 + (F-p-q)\phi_3$ with $q \leq p \leq F-p-q \leq F < n$.

The phases of the bosonic theory in this range are summarized in table 3.1. For $n = F/2 + k$, the phases reproduce the topological theories of **??**, which match the phases of case 1 in the fermionic description. For $n = F/2 - k$, the remaining topological phases from cases 2 to 5 appear.

For the second scenario, the bosonic phases are similar except that, for $n = F/2 - k$, region $\mathbb{D}$ will not be allowed, and region $\mathbb{E}$ will be described by $\tilde{T}_2$. The bosonic phases then match the topological phases of the fermionic theory for cases $\bar{1}$ to $\bar{5}$.

2. $\underline{q \leq p \leq F-p-q \leq n < F}$:

In this range, there is a possibility of spontaneous symmetry breaking, which allows sigma models to appear in the bosonic phases. The sigma models appear when there is a condensation of more than one scalar. The region $\mathbb{E}$, where ϕ_1 and ϕ_2 condense, splits into two regions: $\mathbb{E}_1$ where only the constraint on r_1 is saturated and $\mathbb{E}_2$ where the constraint on r_2 is saturated. The same scenario occurs for regions $\mathbb{F}$ and $\mathbb{G}$, while region $\mathbb{H}$ splits into three subregions, each of them is described when one of the constraints on r_1, r_2, or r_3 is saturated.

The phases of the bosonic theory in this range are summarized in table 3.2. For $n = F/2+k$, the quantum phases are (σ_1^c, $\bar{\sigma}_1^c$, $\hat{\sigma}_1^c$, σ_2^c, $\bar{\sigma}_2^c$, $\hat{\sigma}_2^c$, σ_3^c, $\bar{\sigma}_3^c$, $\hat{\sigma}_3^c$), which are equivalent to all the cuboid quantum phases of the fermionic theory in cases 2, 3, 4, and 5 of section 3.1. For $n = F/2-k$, the quantum phases are ($\bar{\sigma}_1^c$, $\hat{\sigma}_1^c$, $\bar{\sigma}_2^c$, $\hat{\sigma}_2^c$, $\bar{\sigma}_3^c$, $\hat{\sigma}_3^c$), which match the fermionic phases from case 5.

For the second scenario, the only allowed substitution is $n = F/2+k$ with slightly changed phases where the regions $\mathbb{E}_1$ and $\mathbb{E}_2$ will not be allowed under the constraint $F-p-q > F/2$. This makes the quantum phases $\hat{\sigma}_1^c$ and $\hat{\sigma}_2^c$ disappear, and the bosonic phases match correctly the fermionic phases in cases $\bar{2}$, $\bar{3}$, and $\bar{4}$.

Region	r_1	r_2	r_3	Phase	Scenario 1		Scenario 2
					$n = F/2+k$	$n = F/2-k$	$n = F/2+k$
$\mathbb{A}$	0	0	0	$U(n)_l$	T_1	$\tilde{\mathrm{T}}_8$	T_1
$\mathbb{B}$	p	0	0	$U(n-p)_l$	T_4	$\tilde{\mathrm{T}}_5$	T_4
$\mathbb{C}$	0	q	0	$U(n-q)$	T_3	$\tilde{\mathrm{T}}_6$	T_3
$\mathbb{D}$	0	0	$F-p-q$	$U(n-F+p+q)_l$	T_2	$\tilde{\mathrm{T}}_7$	T_2
$\mathbb{E}_1$	p	$n-p$	0	$Gr(n-p,q)$	$\hat{\sigma}_2$	$\bar{\sigma}_2^c$	N/A
$\mathbb{E}_2$	$n-q$	q	0	$Gr(n-q,p)$	$\hat{\sigma}_1$	$\bar{\sigma}_1^c$	N/A
$\mathbb{F}_1$	p	0	$n-p$	$Gr(n-p,F-p-q)$	$\hat{\sigma}_3^c$	$\bar{\sigma}_3^c$	$\hat{\sigma}_3^c$
$\mathbb{F}_2$	$n-F+p+q$	0	$F-p-q$	$Gr(n-F+p+q,p)$	$\bar{\sigma}_1^c$	$\hat{\sigma}_1^c$	$\bar{\sigma}_1^c$
$\mathbb{G}_1$	0	q	$n-q$	$Gr(n-q,F-p-q)$	$\bar{\sigma}_3^c$	$\hat{\sigma}_3^c$	$\bar{\sigma}_3^c$
$\mathbb{G}_2$	0	$n-F+p+q$	$F-p-q$	$Gr(n-F+p+q,q)$	$\bar{\sigma}_2^c$	$\hat{\sigma}_2^c$	$\bar{\sigma}_2^c$
$\mathbb{H}_1$	p	q	$n-p-q$	$Gr(n-p-q,F-p-q)$	σ_3^c	N/A	σ_3^c
$\mathbb{H}_2$	p	$n-F+q$	$F-p-q$	$Gr(n-F+q,q)$	σ_2^c	N/A	σ_2^c
$\mathbb{H}_3$	$n-F+p$	q	$F-p-q$	$Gr(n-F+p,p)$	σ_1^c	N/A	σ_1^c

Table 3.2: Phases of the bosonic theory $U(n)_l + p\phi_1 + q\phi_2 + (F-p-q)\phi_3$ with $q \le p \le F-p-q \le n < F$.

3. $\underline{q \le p \le n < F-p-q \le F}$:

   In this range, regions $\mathbb{A}$, $\mathbb{B}$, and $\mathbb{C}$ are similar to the previous cases. Since $n < F-p-q$, r_1 is saturated to n and region $\mathbb{D}$ now shrinks to a smaller region $\mathbb{D}_1$ with a sigma model phase. The regions $\mathbb{E}_1$ and $\mathbb{E}_2$ remain the same as in the previous case while only $\mathbb{F}_1$, $\mathbb{G}_1$, and $\mathbb{H}_1$ subregions appear in this case. Each of the remaining subregions shares the same phase as in one of the other regions (e. g. the subregion $\mathbb{F}_2$ has the same sigma model as in $\mathbb{D}_1$).

The phases of this case are summarized in table 3.3. Only $n = F/2 - k$ is allowed for the first scenario which gives the phases $(\bar{\sigma}_1^c,\ \bar{\sigma}_2^c,\ \sigma_3^c,\ \hat{\sigma}_3^c,\ \bar{\sigma}_3^c)$. These quantum phases are equivalent to the phases of the fermionic theory in case 4 of section 3.1.

For the second scenario, when $n = F/2 + k$, the phases are $(\bar{\sigma}_1^c,\ \bar{\sigma}_2^c,\ \bar{\sigma}_3^c,\ \hat{\sigma}_3^c,\ \tilde{\sigma}_3^c,\ \sigma_3^c)$, which are equivalent to the phases of the fermionic theory in cases $\bar{4}$ and $\bar{5}$. For $n = F/2 - k$, the bosonic phases are $(\sigma_3^c,\ \bar{\sigma}_3^c,\ \hat{\sigma}_3^c,\ \tilde{\sigma}_3^c)$ which match the fermionic phases in case $\bar{5}$ of section 3.2.

Region	r_1	r_2	r_3	Phase	Scenario 1	Scenario 2	
					$n = F/2 - k$	$n = F/2 + k$	$n = F/2 - k$
$\mathbb{A}$	0	0	0	$U(n)_l$	$\tilde{\mathrm{T}}_8$	T_1	$\tilde{\mathrm{T}}_8$
$\mathbb{B}$	p	0	0	$U(n-p)_l$	$\tilde{\mathrm{T}}_5$	T_4	$\tilde{\mathrm{T}}_5$
$\mathbb{C}$	0	q	0	$U(n-q)$	$\tilde{\mathrm{T}}_6$	T_3	$\tilde{\mathrm{T}}_6$
$\mathbb{D}_1$	0	0	n	$Gr(n, F-p-q)$	σ_3^c	$\tilde{\sigma}_3^c$	σ_3^c
$\mathbb{E}_1$	p	$n-p$	0	$Gr(n-p, q)$	$\bar{\sigma}_2^c$	N/A	$\bar{\sigma}_2^c$
$\mathbb{E}_2$	$n-q$	q	0	$Gr(n-q, p)$	$\bar{\sigma}_1^c$	N/A	$\bar{\sigma}_1^c$
$\mathbb{F}_1$	p	0	$n-p$	$Gr(n-p, F-p-q)$	$\bar{\sigma}_3^c$	$\hat{\sigma}_3^c$	$\bar{\sigma}_3^c$
$\mathbb{G}_1$	0	q	$n-q$	$Gr(n-q, F-p-q)$	$\hat{\sigma}_3^c$	$\bar{\sigma}_3^c$	$\hat{\sigma}_3^c$
$\mathbb{H}_1$	p	q	$n-p-q$	$Gr(n-p-q, F-p-q)$	N/A	σ_3^c	$\tilde{\sigma}_3^c$

Table 3.3: Phases of the bosonic theory $U(n)_l + p\phi_1 + q\phi_2 + (F-p-q)\phi_3$ with $q \leq p \leq n < F-p-q \leq F$.

4. $\underline{q \leq n < p \leq F-p-q \leq F}$:

In this case, the regions $\mathbb{A}$ and $\mathbb{C}$ do not experience any spontaneous symmetry breaking. Since $n < (p, F-p-q)$, both r_1 and r_3 are saturated to n in regions $\mathbb{B}$ and $\mathbb{D}$, which shrink to smaller regions $\mathbb{B}_1$ and $\mathbb{D}_1$ with sigma model phases. The subregions $\mathbb{F}_1$ and $\mathbb{H}_1$ now join the subregion $\mathbb{B}_1$ to form a broader region sharing the same sigma model, and the same happens for $\mathbb{F}_2$ and $\mathbb{H}_2$ which join the subregion $\mathbb{D}_1$.

The phases of this case are summarized in table 3.4. Only $n = F/2 - k$ is allowed in this case which gives $(\sigma_1^c,\ \bar{\sigma}_1^c,\ \sigma_3^c,\ \hat{\sigma}_3^c)$, which match the phases of the fermionic theory in case 3 of section 3.1. The analysis is precisely the same for the second scenario, where case 3 and case $\bar{3}$ are identical.

Region	r_1	r_2	r_3	Phase	$n = F/2 - k$
$\mathbb{A}$	0	0	0	$U(n)_l$	$\tilde{\mathrm{T}}_8$
$\mathbb{B}_1$	n	0	0	$Gr(n,p)$	σ_1^c
$\mathbb{C}$	0	q	0	$U(n-q)_l$	$\tilde{\mathrm{T}}_6$
$\mathbb{D}_1$	0	0	n	$Gr(n,F-p-q)$	σ_3^c
$\mathbb{E}_2$	$n-q$	q	0	$Gr(n-q,p)$	$\bar{\sigma}_1^c$
$\mathbb{G}_1$	0	q	$n-q$	$Gr(n-q,F-p-q)$	$\hat{\sigma}_3^c$

Table 3.4: Phases of the bosonic theory $U(n)_l + p\phi_1 + q\phi_2 + (F-p-q)\phi_3$ with $q \leq n < p \leq F-p-q \leq F$.

5. $n < q \leq p \leq F-p-q \leq F$:

   In this range, all the single condensation cases experience spontaneous symmetry breaking scenario where each of the corresponding ranks is saturated to n producing a sigma model. The double and triple condensation cases share the same sigma model as in the single condensation case.

   The phases are now reduced to include only regions $\mathbb{A}$, $\mathbb{B}_1$, $\mathbb{C}_1$, and $\mathbb{D}_1$, as shown in table 3.5. For $n = F/2 - k$, the phases are $(\sigma_1^c, \sigma_2^c, \sigma_3^c)$, matching the fermionic phases in case 2 of section 3.1. The analysis is also the same for the second scenario, where cases 2 and $\bar{2}$ are identical.

Region	r_1	r_2	r_3	Phase	$n = F/2 - k$
$\mathbb{A}$	0	0	0	$U(n)_l$	$\tilde{\mathrm{T}}_8$
$\mathbb{B}_1$	n	0	0	$Gr(n,p)$	σ_1^c
$\mathbb{C}_1$	0	n	0	$Gr(n,q)$	σ_2^c
$\mathbb{D}_1$	0	0	n	$Gr(n,F-p-q)$	σ_3^c

Table 3.5: Phases of the bosonic theory $U(n)_l + p\phi_1 + q\phi_2 + (F-p-q)\phi_3$ with $n < q \leq p \leq F-p-q \leq F$.

An additional and straightforward consistency check is to reduce the bosonic theory to the two-family case by putting $q = 0$ where the tables 3.1 to 3.5 reduce to the tables in [2].

3.3.3 Perturbing the lower dimension sigma models

We saw in the previous subsection how to match the phases of the bosonic and the fermionic theories around the critical points by considering perturbations in the bosonic dual descriptions. We now want to perturb the diagonal sigma models in both two-dimensional and three-dimensional pictures. We do this by adding a mass term which explicitly breaks the flavour symmetry $U(F)$, as considered in [2] for the two-family case. The target space of the sigma model σ is

$$\sigma : Gr(n, F) = \frac{U(F)}{U(n) \times U(F-n)} , \tag{3.57}$$

where again n can be either $F/2+k$ or $F/2-k$. σ appears on the diagonal line of the three different limiting cases discussed in the previous subsection, which show that there exist three different possibilities of the mass deformation corresponding to deforming the mass of each of the scalars independently.

Perturbing σ

For $(m_1, m_2 = m_3)$ plane, the theory has $p\,\phi_1 + (F-p)\,\phi_2$ scalars. This allows us to perturb σ by deforming ϕ_1 or ϕ_2 where the result is independent of the choice of the scalar set that we deform so let us say that we deform ϕ_1 by adding an infinitesimal mass squared δM_1^2 to M_1^2. Hence we have four possibilities:

- If $\delta M_1^2 > 0$ and $F - p > n$, ϕ_3 condenses first Higgsing the gauge group $U(n)$, then one can integrate ϕ_1 out and the resulting sigma model has a Grassmannian $Gr(n, F-p)$.

- If $\delta M_1^2 > 0$ but $F - p < n$ the condensation of ϕ_3 partially Higgs the gauge group down to $U(n-F+p)$ and then can be integrated out followed by integrating out ϕ_1. This gives a sigma model with a Grassmannian $Gr(F-n, p)$.

- For $\delta M_1^2 < 0$ and $p > n$, ϕ_1 condenses first with a complete Higgsing of the gauge group which leads to a sigma model with a Grassmannian $Gr(n, p)$.

- For $\delta M_1^2 < 0$ and $p < n$, the theory has a sigma model with a Grassmannian $Gr(F - n, F - p)$.

Substituting $n = F/2 \pm k$ gives Grassmannians describing the sigma models σ_{23}^d, σ_1^c, and $\bar{\sigma}_{23}^d$, which match the theories around σ in figure 3.15c.

Similarly for the $(m_2, m_1 = m_3)$ plane, where we deform the mass of ϕ_1 to perturb sigma leading to the Grassmannians $Gr(n, F-q)$, $Gr(F-n, q)$, $Gr(n, q)$, and $Gr(F-n, F-q)$. These Grassmanians correspond to the sigma models σ_{13}^d, σ_2^c, and $\bar{\sigma}_{13}^d$ matching the phases around σ in figure 3.14c. Lastly, the mass deformation of ϕ_3 in the $(m_1 = m_2, m_3)$ plane leads to the Grassmannians $Gr(n, F-p-q)$, $Gr(F-n, p+q)$, $Gr(n, p+q)$, and $Gr(F-n, F-p-q)$ describing the target space of the sigma models σ_3^c, σ_{12}^d, and $\tilde{\sigma}_3^c$ which match the phases around σ in the fermionic theory, as shown in figure 3.13c.

We now move to perturb the other diagonal sigma models when we simultaneously deform the mass of two scalars. We consider the perturbation of pairs of diagonal sigma models as follows:

Perturbing σ_{23}^d and $\bar{\sigma}_{23}^d$

We rewrite both theories in the general form $Gr(n, F-p)$ where σ_{23}^d can be found by substituting $n = F/2 - k$ while $\bar{\sigma}_{23}^d$ is found by substituting $n = F/2 + k$. This can be obtained by deforming the mass of ϕ_1 with $\delta M_1^2 > 0$ and $F - p > n$ on the $(m_1, m_2 = m_3)$ plane. In addition, we deform the mass of ϕ_2 and check the four possibilities.

Now we have a perturbation of $Gr(n, F_1)$ with $\delta M_2^2 > 0$ or $\delta M_2^2 < 0$. As in the previous discussion, this gives sigma models with the following Grassmannians: $Gr(n, F-p-q)$, for $\delta M_2^2 > 0$ and $F-p-q > n$, $Gr(F-p-n, q)$, for $\delta M_2^2 > 0$ and $F-p-q < n$, $Gr(n, q)$, for $\delta M_2^2 < 0$ and $q > n$, and $Gr(F-p-n, F-p-q)$, for $\delta M_2^2 < 0$ and $q < n$. For $n = F/2 - k$, these Grassmannians correspond to σ_3^c,

$\hat{\sigma}_3^c$, σ_2^c, and $\hat{\sigma}_2^c$ matching the fermionic phases around σ_{23}^d, as shown in figures 3.3b, 3.5b, 3.7b and 3.9b. For $n = F/2 + k$, these Grassmannians correspond to $\bar{\sigma}_3^c$ and $\bar{\sigma}_2^c$ matching the fermionic phases around $\bar{\sigma}_{23}^d$, as shown in figures 3.7a and 3.9a.

We should clarify that not all the Grassmannians are allowed when we make the substitution $n = F/2 \pm k$ where they are subject to k being non-negative and the constraint of the first deformation, which is $F - p > n$ in this case.

In the second scenario, $Gr(F-p-n, F-p-q)$ is not allowed for $n = F/2-k$ and $Gr(n, F-p-q)$ provides $\tilde{\sigma}_3^c$ for $n = F/2 + k$. Then we have only σ_3^c, $\hat{\sigma}_3^c$, and σ_2^c that surround σ_{23}^d, as shown in figures 3.3b, 3.5b, 3.7b and 3.11b. $\tilde{\sigma}_3^c$, $\bar{\sigma}_3^c$ and $\bar{\sigma}_2^c$ are the phases around $\bar{\sigma}_{23}^d$ matching the fermionic description, as shown in figures 3.7a, 3.9a and 3.11a.

Perturbing σ_{13}^d and $\bar{\sigma}_{13}^d$

These two sigma models have Grassmannians written in a single form $Gr(n, F-q)$ which is obtained by deforming the mass of ϕ_2 with $\delta M_2^2 > 0$ and $F - q > n$ on the $(m_2, m_1 = m_3)$ plane. By adding a deformation to the mass of ϕ_1, the resulting sigma models have Grassmannians $Gr(n, F-p-q)$, $Gr(F-q-n, p)$, $Gr(n, p)$, and $Gr(F-q-n, F-p-q)$.

For $n = F/2 - k$, these Grassmannians correspond to σ_3^c, σ_1^c, $\bar{\sigma}_3^c$, and $\hat{\sigma}_1^c$ which match the phases around σ_{13}^d. For $n = F/2+k$, the Grassmanians correspond to $\bar{\sigma}_1^c$ and $\hat{\sigma}_3^c$, which match the phases around $\bar{\sigma}_{13}^d$ in the fermionic picture. The analysis is similar for the second scenario except that the Grassmannian $Gr(F-q-n, F-p-q)$ is no longer allowed for $n = F/2 - k$.

Perturbing σ_{12}^d and $\bar{\sigma}_{12}^d$

We start from $Gr(n, p+q)$ which can be read from deforming the mass of ϕ_3 with $\delta M_3^2 < 0$ and $p + q > n$ on the $(m_1 = m_2, m_3)$ plane. An extra deformation of the mass of ϕ_1 gives sigma models. For $n = F/2 - k$, the only allowed sigma models have Grassmannians $Gr(F/2-k, p)$, $Gr(p+q-F/2+k, p)$, and

$Gr(p+q-F/2+k, q)$. These Grassmannians correspond to σ_1^c, $\bar{\sigma}_1^c$, and $\bar{\sigma}_2^c$, which are the phases that appear around σ_{12}^d.

For $n = F/2 + k$, the allowed sigma models are $\hat{\sigma}_1^c$ and $\hat{\sigma}_2^c$, which are the only quantum phases that appear around $\bar{\sigma}_{12}^d$. The substitution $n = F/2 + k$ is not allowed for the second scenario; the analysis remains the same elsewhere.

Chapter 4

Phases of QCD_3 with adjoint matter

In chapters 2 and 3, we analyzed the phase diagrams of a Chern-Simons theory coupled to a number of fermions in the fundamental representation. The next logical question is what happens for theories with matter in other gauge group representations. Right after conjecturing the phases of the fundamental theory, the theory with fermions in the adjoint representation received much attention [4, 6, 66].

This chapter starts with the case of a single Majorana fermion in the adjoint representation of an $SU(N)$ gauge group coupled to a Chern-Simons term of level k. We also discuss the extension of adding another adjoint fermion of the same mass, where the phase diagram remains one-dimensional in the mass axis. Lastly, we examine the possibility of having a two-dimensional phase diagram with adjoint matter (i.e. two adjoints with arbitrary distinct masses), which is part of an ongoing work that is expected to be published later [5].

4.1 Phases of adjoint QCD$_3$ via SUSY breaking

In this section, we review the work of Gomis, Komargodski, and Seiberg (GKS) on the phases of QCD-like theory in $2+1$ dimensions with a single adjoint fermion [4]. Consider an $SU(N)$ gauge theory coupled to a Chern-Simons term of level k and a Majorana fermion λ in the adjoint representation with mass m_λ. We choose, without loss of generality, $k \geq 0$ throughout this chapter, and the negative k analysis can be easily found by applying time-reversal ($k \to -k$). The Lagrangian density is then

$$\mathscr{L} = -\frac{1}{4g^2}\mathrm{Tr}\mathcal{F}^2 + \frac{k_{bare}}{4\pi}\mathrm{Tr}\left(AdA - \frac{2i}{3}A^3\right) + i\mathrm{Tr}\lambda D\lambda + M_\lambda \mathrm{Tr}(\lambda\lambda)\,, \tag{4.1}$$

where g is the $SU(N)$ coupling and k_{bare} is the bare level, which is normalized to $k = k_{bare} - N/2$, such that k becomes an integer for even N and half-integer for odd N [73]. The theory has no zero-form global symmetry but rather a one-form $\mathbb{Z}_N$ symmetry. It also exhibits $\mathcal{N} = 1$ supersymmetry for the special choice $m_\lambda = -kg^2/2\pi$.

The IR dynamics of this theory is well described semiclassically for large values of M_λ and/or k. For large mass limits $|m_\lambda| \gg g^2$, λ can be safely integrated out, causing a shift in k given by [74]

$$k_{IR} = k + sgn(m_\lambda)\frac{N}{2}\,. \tag{4.2}$$

Because the Yang-Mills term has greater derivatives than the CS term, it becomes irrelevant in the large mass limit. As a result, the IR description is a pure TQFT, with $SU(N)_{k+N/2}$ for large positive m_λ and $SU(N)_{k-N/2}$ for large negative m_λ. On the other hand, for a large k limit, the gauge field A has a mass of order kg^2 and may thus be integrated out, leaving a pure TQFT. As we adjust m_λ, the remaining light fields weakly interact, resulting in a weakly coupled CFT.

When m_λ and k are relatively small, the dynamics is obscure. However, GKS provides a comprehensive picture of the phase diagram, which may be understood as follows: Take the specific choice of $m_\lambda = m_{SUSY} = -kg^2/2\pi$, and the theory becomes an $\mathcal{N} = 1$ supersymmetric gauge theory, with λ being the gaugino. Moving away from the m_{SUSY} point explicitly breaks supersymmetry. Then, we integrate the heavy matter out, starting with the gaugino, which shifts k to $k - N/2$. Because the gauge fields are heavy ($\sim kg^2$) and can be integrated out, we end up with a pure topological $SU(N)_{k-N/2}$ theory.

Apart from explicitly breaking supersymmetry, there are some limitations on k where supersymmetry is spontaneously broken. We investigate the Witten (supersymmetric) index I_W for various k limits, as provided by [73]

$$I_W = \frac{(k + N/2 - 1)!}{(N-1)!(k - N/2)!}\,. \tag{4.3}$$

which can be rewritten as

$$I_W = \frac{1}{(N-1)!}\prod_{j=-N/2+1}^{N/2-1}(k-j) = \begin{cases} \neq 0, & \text{if } k \geq N/2. \\ = 0, & \text{if } 0 \leq k < N/2. \end{cases} \tag{4.4}$$

We notice that the supersymmetric index vanishes for $k < N/2$ (i.e supersymmetry is broken in this limit). As a result, the phase diagram is divided into two cases: $k \geq N/2$ and $k < N/2$.

Semiclassical limit: $k \geq N/2$

In this limit, supersymmetry is preserved at $m_\lambda = m_{SUSY}$. The theory is weakly-coupled, and the two asymptotic phases are pure $SU(N)_{k+N/2}$ TQFT for large positive mass and $SU(N)_{k-N/2}$ for large negative mass. The supersymmetric point is part of the negative mass phase $SU(N)_{k-N/2}$. The two asymptotic phases are separated by a phase transition, which is described by a CFT. The proposed phase diagram is depicted in figure 4.1 in terms of m_λ. The phase transition between

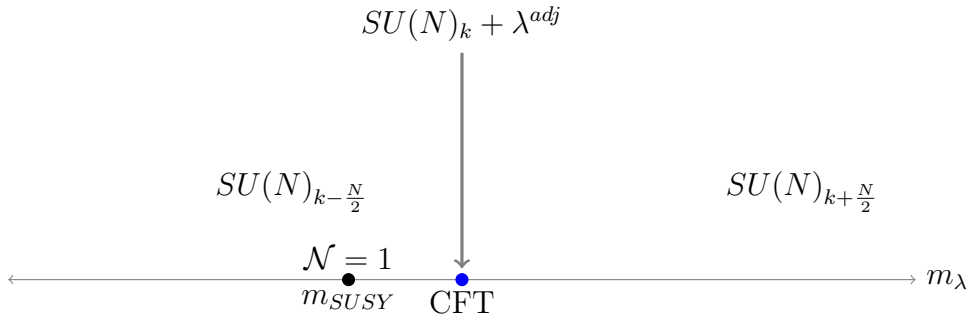

Figure 4.1: Phase diagram of $SU(N)_k + \lambda^{adj}$ for the range $k \geq \frac{N}{2}$. The solid line represents the flow to the IR fixed point at which the phase transition occurs. The blue bullet represents the transition point, while the black bullet depicts the supersymmetric point.

$SU(N)_{k-N/2}$ and $SU(N)_{k+N/2}$ is second-order, and the CFT point reflects a theory with $\dim[SU(N)] = N^2 - 1$ free fermions [4].

Quantum phase: $k < N/2$

In this range of k, supersymmetry is broken at $m_\lambda = m_{SUSY}$. The supersymmetry breaking scenario implies that there is a massless Goldstino (G_α) at this point. The first possibility is that the phase diagram is similar to the $k \geq N/2$ case, except at the supersymmetric point, where the $SU(N)_{k-N/2}$ is accompanied by the massless Goldstino. GKS argued that this scenario is only true for the special case $k = N/2 - 1$ and fails for the lower values of k. This is demonstrated by considering the special case of $k = 0$, where the two asymptotics are $SU(N)_{N/2}$ for large positive mass and $SU(N)_{-N/2}$ for large negative mass. In this scenario, the phase transition occurs at the supersymmetric point (i.e. $M_\lambda = m_\lambda = 0$), therefore the theory must be time-reversal invariant. The two asymptotic phases should then represent the theory in the IR at this point, which cannot be true unless there is a duality between the two asymptotic theories. However, even in our specific case with $SU(N)$, this is not the case for a generic gauge group.

Another possible scenario is that the phase at the supersymmetric point contains only the massless Goldstino. However, as previously stated, the original theory has a one-form symmetry that should be captured in the IR due to the

't Hooft anomalies. A single Goldstino can not match the one-form symmetry. The exclusion of this possibility becomes clearer if we take the special case $k = 0$, where we have time-reversal anomaly given by an integer ν modulo 16 [62, 75–79]. However, a phase with a single Goldstino does not match this anomaly. As a result, there must be a topological theory in the IR in addition to G_α, and this theory can not be $SU(N)_{k-N/2}$, except for $k = N/2 - 1$.

In the spirit of the fundamental QCD$_3$ discussion, GKS proposed the existence of a quantum phase for small mass. The quantum phase splits the transition point into two points at m_λ^-, m_λ^+. The quantum phase separates the two asymptotic phases $SU(N)_{k\pm N/2} \leftrightarrow U(N/2 \pm k)_{\mp N,\mp N}$ (by level/rank duality). As a result, there must be a dual theory $\mathcal{D}_A$ that flows to the m_λ^- point as well as a dual theory $\mathcal{D}_B$ that flows to the m_λ^+ point. These two theories are dual to the UV theory near each critical point but not necessarily dual to each other. The dual theories $\mathcal{D}_A$ and $\mathcal{D}_B$ contain dual adjoint fermions $\hat{\lambda}$ and $\tilde{\lambda}$ respectively. Each dual theory flows to an IR fixed point where the corresponding fermion is massless. The two dual theories are conjectured to be

$$\mathcal{D}_A : SU(N)_k + \lambda^{adj} \longleftrightarrow U\left(\frac{N}{2} - k\right)_{\frac{3}{4}N+\frac{k}{2},N} + \hat{\lambda}^{adj}\,, \text{near } m_\lambda^- \,. \tag{4.5}$$

$$\mathcal{D}_B : SU(N)_k + \lambda^{adj} \longleftrightarrow U\left(\frac{N}{2} + k\right)_{-\frac{3}{4}N+\frac{k}{2},-N} + \tilde{\lambda}^{adj}\,, \text{near } m_\lambda^+ \,. \tag{4.6}$$

The second duality is obtained from the first one by applying $k \to -k$ combined with orientation reversal. Hence, one may consider that $m_\lambda = 0$ point acts as a mirror between the two dual theories (i.e. the mass deformations are related by $\delta m_\lambda = -\delta m_{\hat{\lambda}}$ and $\delta m_\lambda = -\delta m_{\tilde{\lambda}}$).

Let us now understand how these dual theories are conjectured starting from the asymptotic phases and their level/rank dual descriptions. For $m_\lambda \to -\infty$, the phase is $SU(N)_{k-N/2} \leftrightarrow U(N/2 - k)_{N,N}$, where the theory in the right hand side must define one of the asymptotic phases of the dual theory $\mathcal{D}_A$ in the IR. Thus, the dual theory $\mathcal{D}_A$ is $U\left(N/2 - k\right)_{3N/4+k/2,N} + \hat{\lambda}$. Remarkably, we find that $\mathcal{D}_A$ is

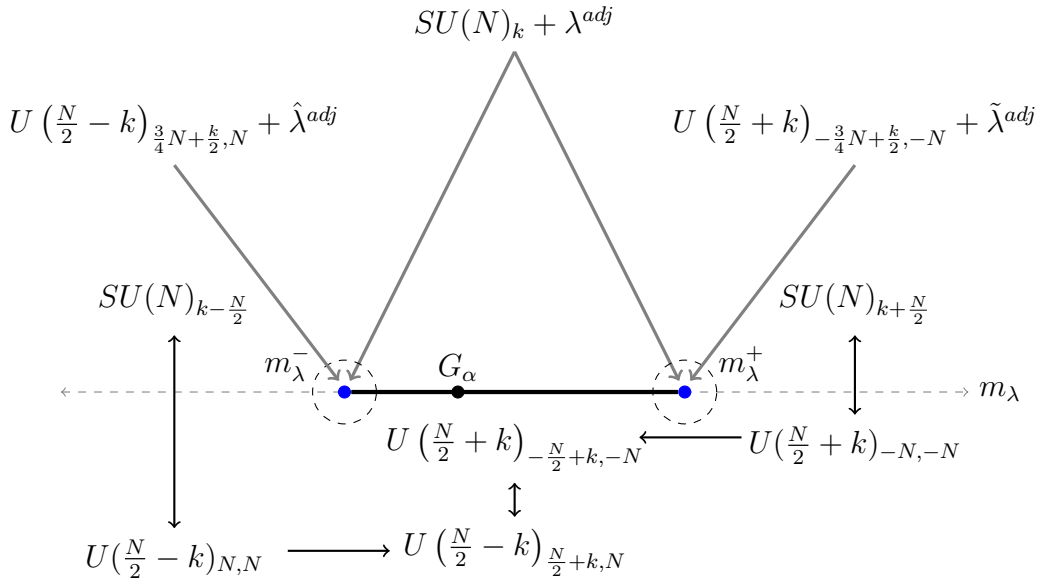

Figure 4.2: Phase diagram of $SU(N)_k + \lambda^{adj}$ for $k < \frac{N}{2}$. The thick black line represents the quantum region. The dashed circles show that the fermion-fermion dualities only hold near the critical points.

weakly-coupled, where $|\hat{k}| > \hat{N}/2$ ($\hat{k}$ and $\hat{N}$ are the level and rank of $\mathcal{D}_A$). This means that the theory has a single phase transition specified by the m_λ^- point, and only two phases one of them is the $U(N/2-k)_{N,N}$ phase and the other is $U(N/2-k)_{N/2+k,N}$. The later describes the intermediate region of the original theory. Similarly for the $m_\lambda \to \infty$ phase, we find that the dual theory $\mathcal{D}_B$ is $U(N/2+k)_{-3N/4+k/2,N} + \tilde{\lambda}$. $\mathcal{D}_B$ is also weakly-coupled, thus the intermediate phase is $U(N/2+k)_{N/2+k,N}$ after integrating $\tilde{\lambda}$ out. Surprisingly, the topological theories that describe the intermediate quantum phase, $U(N+N/2)_{-N/2+k,-N}$ and $U(N/2+k)_{N/2+k,N}$, are level/rank dual to each other.

It is worth mentioning that the phase transition does not cause a shift in the level of the $U(1)$ part of the level/rank dual descriptions because there is no particle charged under the $U(1)$. The phase diagram for this range of k is then summarized in figure 4.2. For the special case $k = N/2-1$, we see that the asymptotic phases are $SU(N)_{-1} \leftrightarrow U(1)_{N,N}$ for large negative mass and $SU(N)_{N-1} \leftrightarrow U(N-1)_{-N,-N}$ for large positive mass. The quantum phase is now $U(1)_{N,N}$, implying that the large negative mass phase and the quantum phase coincide, and the transition point to the left of figure 4.2 disappears. As a result,

the phase diagram looks similar to the $k \geq N/2$ case with a single phase transition separating the two asymptotic phases.

Consistency checks

A highly non-trivial test for the $k \geq N/2$ case is to consider the special case where $N = 2$ and k is odd ($SU(2)_{k_{odd}}$). The theory has an anomaly-free $\mathbb{Z}_2$ one-form symmetry. It was shown that this theory is dual to $O\left(\frac{K+1}{2}\right)^0_{-3,-3} + \phi^{vec}$, where ϕ^{vec} is a scalar in the vector representation [80] [1]. The dual bosonic theory has two phases in the IR described by two TQFTs: If $m^2_{\phi^{vec}} > 0$, the phase in the IR is level/rank dual to the $SU(2)_{k+1}$ TQFT, which matches the phase of the $SU(2)_1 + \lambda$ for $m_\lambda > 0$. If $m^2_{\phi^{vec}} < 0$, where the scalar condenses, the IR phase is level/rank dual to the $SU(2)_{k-1}$ matching the negative mass phase of the $SU(2)_1 + \lambda$ theory [80].

The description of the phase diagram for the $k < N/2$ case was conjectured by using the following methods: integrating the fermion out for large $|m_\lambda|$, using level/rank dualities, and a phase transition between weakly-coupled theories. The level/rank dualities are rigorously proven, and the transition between the weakly-coupled theories is smooth. This ensures that the phases of this range of k have the same global symmetry and their 't Hooft anomalies match. The anomaly matching is only questioned for the special case $k = 0$, at which we expect time-reversal anomaly. The above argument works well when we integrate λ out (i.e. $|m_\lambda| > 0$), but it is not necessarily true for the $m_\lambda = 0$ situation. For $k = 0$ case, the supersymmetric point coincides with the $m_\lambda = 0$ point at which the phase in the IR is a massless Majorana fermion and a $U(N/2)_{N/2,N}$ TQFT.

[1] We follow the notation and convention of [13, 80]. The first subscript is the CS level of the continuous group, while the second subscript describes the topological term in the $\mathbb{Z}_2$ sector. The superscript 0 indicates that there is no coupling between the continuous group and the $\mathbb{Z}_2$ symmetry

Matching time-reversal anomaly: $k = 0$

Let us now look at how the time-reversal anomalies match at $k = m_\lambda = 0$. As we mentioned earlier, the time-reversal anomaly is defined by an integer ν modulo 16. In the UV, the theory decouple to free gauge fields and dim $[SU(N)] = N^2 - 1$ free fermions; only the latter contributes to the anomaly with a value of ± 1. The time-reversal anomaly in the UV (ν_{UV}) is then $(N^2 - 1)$ mod $16 = \left(1 - 2(-1)^{N/2}\right)$ mod 16. In the IR, the theory is described by a $U(N/2)_{N/2,N}$ TQFT and a Goldstino. The Goldstino contributes with 1 to the anomaly while the TQFT part was calculated to contribute with ± 2, which is in total $-2(-1)^{N/2}$ [76, 77]. As a result, the total time-reversal anomaly in the IR (ν_{IR}) is $1 - 2(-1)^{N/2}$ matching the value of ν_{UV}.

4.2 QCD$_3$ with two degenerate adjoint fermions

In this section, we review the analysis of QCD$_3$ with two Majorana fermions in the adjoint representation [6]. The two adjoint fermions have the same mass m_λ, and the theory is coupled to a Chern-simons term with level k (i.e. we start from $SU(N)_k + 2\lambda^{adj}$). The proposal is to follow the work of [4] and analyse the asymptotic phases first, then look for possible quantum phases for sufficiently small k values. In this case, the phase diagram is split into three cases: $k \geq N$, $N/2 \leq k < N$, and $0 < k < N/2$. We expect quantum phases only for the last two cases where the theory is strongly-coupled in the UV.

4.2.1 Semiclassical limit: $k \geq N$

In this case, k is large enough for the theory to be expressed semiclassically, and the two fermions for large $|m_\lambda|$ can be integrated out. As a result, for large positive m_λ, the theory in the IR is described via a pure $SU(N)_{k+N} \leftrightarrow U(k+N)_{-N,-N}$ TQFT, whereas for large negative mass, the theory is $SU(N)_{k-N} \leftrightarrow U(k-N)_{-N,-N}$ TQFT. These two asymptotic phases also describe the small mass region, and the

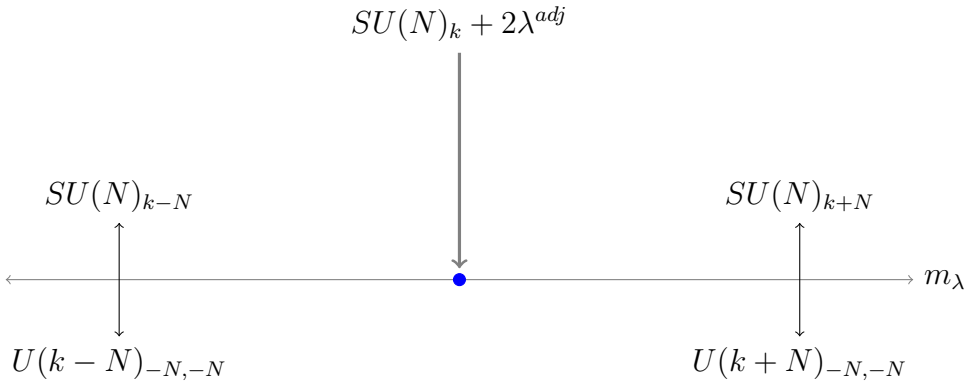

Figure 4.3: Phase diagram of $SU(N)_k + 2\lambda^{adj}$ for $k \geq N$.

theory has a single phase transition separating the two topological phases. The phase diagram is simple, as shown in figure 4.3.

4.2.2 Quantum phase I: $N/2 \leq k < N$

The theory is strongly-coupled for the range $k < N$, demanding a quantum region to fill the phase diagram. Let us now follow the lead of [1, 6] by finding the asymptotic phases first. The asymptotic phases are now $SU(N)_{k+N} \leftrightarrow U(k+N)_{-N,-N}$ for large positive mass and $SU(N)_{k-N} \leftrightarrow U(N-k)_{N,N}$ for large negative mass. The level/rank dual description of the negative mass asymptotic theory differs from the preceding case. Now it is time to propose fermion-fermion dualities near the transitions points, which can be written as follows

$$\mathcal{D}_A : SU(N)_k + 2\lambda^{adj} \longleftrightarrow U\left(N-k\right)_{k,N} + 2\hat{\lambda}^{adj}\,, \text{near } m_\lambda^- \,. \tag{4.7}$$

$$\mathcal{D}_B : SU(N)_k + 2\lambda^{adj} \longleftrightarrow U\left(N+k\right)_{k,-N} + 2\tilde{\lambda}^{adj}\,, \text{near } m_\lambda^+ \,. \tag{4.8}$$

We notice that the dual theory $\mathcal{D}_B$ is strongly-coupled for all values of $k < N$. However, the dual theory $\mathcal{D}_A$ is weakly-coupled for the range $N/2 < k < N$ ($\hat{k}_A = k > |N-k|$), and strongly-coupled otherwise. For this reason, we split the phase diagram for $k < N$ into two distinct cases: $N/2 \leq k < N$ and $0 < k < N/2$.

Since $\mathcal{D}_A$ is weakly-coupled in this range of k, we are allowed to use it to conjecture the quantum region. Integrating out the dual adjoint fermions $\hat{\lambda}$ for

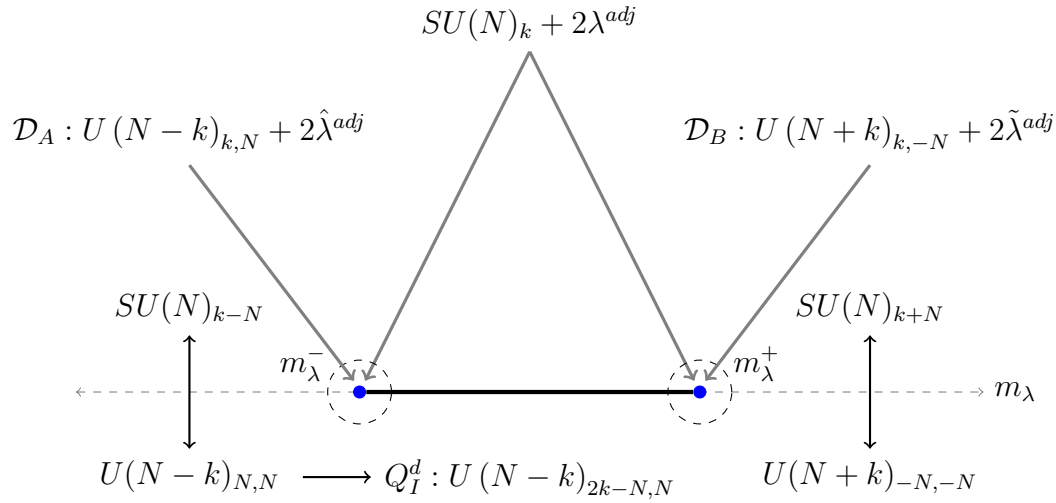

Figure 4.4: Phase diagram of $SU(N)_k + 2\lambda^{adj}$ for $\frac{N}{2} \leq k < N$.

negative mass gives

$$Q_I^d : U(N-k)_{2k-N,N} \,. \tag{4.9}$$

The phase diagram is depicted in figure 4.4.

4.2.3 Quantum phase II: $0 < k < N/2$

In this range of k, both $\mathcal{D}_A$ and $\mathcal{D}_B$ are strongly coupled, which make it difficult to conjecture the quantum phase. The author of [6] resolved this issue by introducing the concept of "Duality Chain". Duality chain is simply introducing a set of successive dual descriptions $\mathcal{D}_A^{(n)}$ near the left critical point. This is inspired by the observation that the rank of the dual theory $\mathcal{D}_A$ decreases each time a new fermion-fermion duality is defined. Hence, there must be n times after which we reach a weakly coupled theory (i.e. $\left|\hat{k}_A^{(n)}\right| > \hat{N}_A^{(n)}$).

Before delving into the specifics of chain duality, we address another remarkable idea defined in [6]: generalised level/rank duality which provides a modified version of equation (1.28).

Generalized level/rank dualities

The main objective is to find the level/rank dual description of a theory in the form of $U(N)_{k,k\pm pN}$, where p is an integer, using the effect of the transformations of the

$SL(2,\mathbb{Z})$ group. Consider a gauge theory in $2+1$ dimensions whose Lagrangian is $\mathscr{L}[a]$ where a is the gauge field. One may couple this theory to a $U(1)$ background field B which takes $\mathscr{L}[a] \to \mathscr{L}[a,B]$.

The $SL(2,\mathbb{Z})$ group has two relevant elements defined via the following operations: The S-operation, which promotes the background field B to a dynamical field b. The other element is the T-operation, which shifts the Chern-Simons coupling of the background field. The two operations are then defined as follows [37, 81]

$$S : \mathscr{L}[a,B] \to \mathscr{L}[a,b] - \frac{1}{2\pi} b dB \,, \tag{4.10}$$

$$T : \mathscr{L}[a,B] \to \mathscr{L}[a,B] + \frac{1}{4\pi} B dB \,. \tag{4.11}$$

The S and T-operations satisfy the identity $S^2 = (ST)^3 = C$, where C is the charge conjugation (i.e. $B \to -B$). Now let us start from the level rank dualities in equation (1.27) and make use of the ST operations. First, we identify the theories on both sides of $SU(N)_k \leftrightarrow U(k)_{-N,-N}$ in terms of the background field B by writing

$$SU(N)_k : \mathscr{L}[u,B] = \frac{k}{4\pi} \mathrm{Tr}_N \left(u du - \frac{2i}{3} u^3 \right) + \frac{1}{2\pi} c d(\mathrm{Tr} u + B) \,, \tag{4.12}$$

$$U(k)_{-N,-N} : \mathscr{L}[v,B] = \frac{-N}{4\pi} \mathrm{Tr}_k \left(v dv - \frac{2i}{3} v^3 \right) + \frac{1}{2\pi} (\mathrm{Tr} v) dB \,. \tag{4.13}$$

Now let us apply the operation T first followed by S. The two Lagrangians become

$$ST\, SU(N)_k : \mathscr{L}[u,B] = \frac{k}{4\pi} \mathrm{Tr}_N \left(u du - \frac{2i}{3} u^3 \right) + \frac{1}{2\pi} c d(\mathrm{Tr} u + b) + \frac{1}{4\pi} b db - \frac{1}{2\pi} b dB \,, \tag{4.14}$$

$$ST\, U(k)_{-N,-N} : \mathscr{L}[v,B] = \frac{-N}{4\pi} \mathrm{Tr}_k \left(v dv - \frac{2i}{3} v^3 \right) + \frac{1}{2\pi} (\mathrm{Tr} v) db$$

$$+\frac{1}{4\pi}bdb-\frac{1}{2\pi}edB\,. \quad (4.15)$$

One may now safely integrate c and b out, leading to the Lagrangian of the theories: $ST\,SU(N)_k = U(N)_{k,k+N}$ and $ST\,U(k)_{-N,-N} = U(k)_{-N,-k-N} \leftrightarrow U(N)_{k,k+N} + U(1)_1$. As a result, we get the duality $U(k)_{-N,-N} \leftrightarrow U(k)_{-N,-k-N}$ agreeing with equation (1.28). The other duality, with a negative sign in its level, can be obtained similarly by applying ST^{-1} operations.

Let us take it a step further and apply the T- operation p times followed by the S-operation to equations (4.12) and (4.13):

$$ST^p\,SU(N)_k : \mathscr{L}[u,B] = \frac{k}{4\pi}\mathrm{Tr}_N\left(udu-\frac{2i}{3}u^3\right)+\frac{1}{2\pi}cd(\mathrm{Tr}u+b) + \frac{p}{4\pi}bdb-\frac{1}{2\pi}bdB\,, \quad (4.16)$$

$$ST^p\,U(k)_{-N,-N} : \mathscr{L}[v,B] = \frac{-N}{4\pi}\mathrm{Tr}_k\left(vdv-\frac{2i}{3}v^3\right)+\frac{1}{2\pi}(\mathrm{Tr}v)db + \frac{p}{4\pi}bdb-\frac{1}{2\pi}edB\,. \quad (4.17)$$

We obtain $U(N)_{k,k+pN}$ from equation (4.16) by integrating out c and b. Applying the same procedure to the theory with negative level, we arrive at the following generalized level/rank dualities

$$U(N)_{\pm k,\pm k+pN} \longleftrightarrow ST^pU(k)_{\mp N,\mp N}\,. \quad (4.18)$$

The author of [6] made perfect use of the generalized level/rank dualities, as well as the duality chain, to determine the quantum region of the phase diagram when $k < N/2$. The implementation of the duality chain technique is depicted in figure 4.5, where each graph represents a step in a n-step chain of dualities.

In the first step, we define the first fermion-fermion dual descriptions near each critical point of the phase diagram of the original theory: $\mathcal{D}_A^{(1)} = U(N-k)_{k,N}+2\hat{\lambda}^{(1)}$

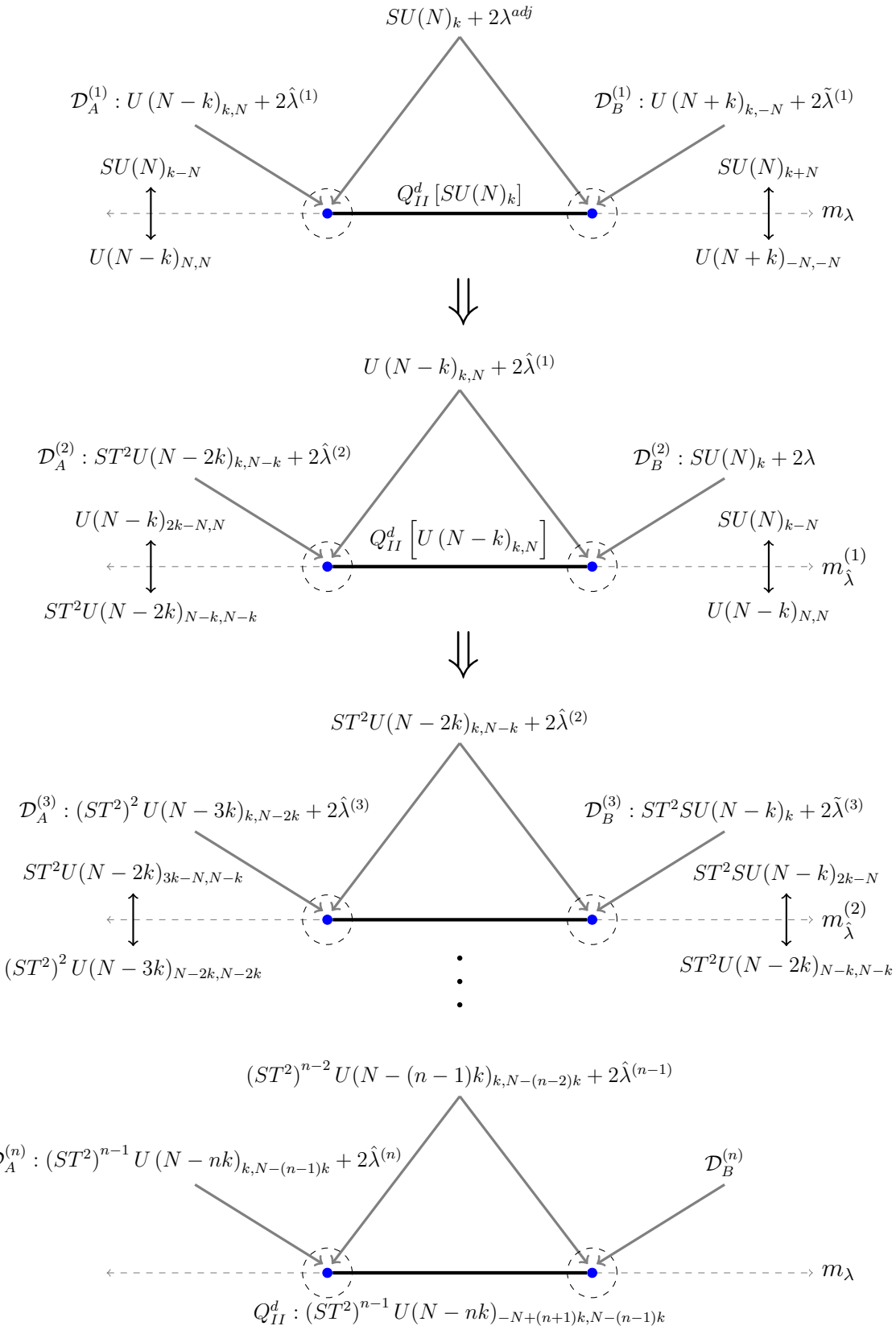

Figure 4.5: Duality chain process for n steps that lead to the phase diagram of the $SU(N)_k + 2\lambda^{adj}$ in the range $0 < k < \frac{N}{2}$.

and $\mathcal{D}_B^{(1)} = U(N+k)_{k,-N} + 2\tilde{\lambda}^{(1)}$, where $\hat{\lambda}^{(1)}$ and $\tilde{\lambda}^{(1)}$ are the dual adjoint fermions associated with the dual theories after the first step. As we mentioned earlier, the two dual theories are strongly coupled since $\hat{k}_A^{(1)} = k < N-k$ and $\tilde{k}_B^{(1)} = k < N+k$. It is also evident that the dual theory $\mathcal{D}_A$ has a lower rank, thus from now on, we will only focus on the dual theory on the left side of the phase diagram.

In the second step, we take $\mathcal{D}_A^{(1)}$ and try to find its phases. This requires introducing the next fermion-fermion dualities. The asymptotic theories for large mass are $U(N-k)_{N,N} \leftrightarrow SU(N)_{k-N}$ for large positive mass and $U(N-k)_{2k-N,N} \leftrightarrow ST^2U(N-2k)_{N-k,N-k}$ (using the generalized level/rank dualities) for large negative mass. The latter allows us to conjecture the next fermion-fermion duality in the duality chain, which is given by $\mathcal{D}_A^{(2)} : ST^2U(N-2k)_{k,N-k} + 2\hat{\lambda}^{(2)}$. We notice that $\mathcal{D}_A^{(2)}$ is still weakly coupled since $k_A^{(2)} = k < N-2k$. The phase diagram for $\mathcal{D}_A^{(1)}$ is described by the second diagram of figure 4.5.

Repeating the same approach results in a new fermion-fermion duality each time. As a result, we identify a pattern in which each step in the duality chain decreases the rank and level of the $U(1)$ part by k. The dual description $\mathcal{D}_A$ will remain strongly coupled until the level $\hat{k}_A$ is larger than or equal to the rank $\hat{N}_A$. Assuming this happens after n steps, we need $k \geq N - nk$. However, in order to assure that n remains an integer, we need $n = \lceil N/k \rceil - 1$. The final dual description is then

$$\mathcal{D}_A^{(n)} : \left(ST^2\right)^{\lceil \frac{N}{k} \rceil - 2} U\left(N - \left\lceil \frac{N}{k} \right\rceil k + k\right)_{k, N - \lceil \frac{N}{k} \rceil k + 2k} + 2\hat{\lambda}^{(n)} \,. \tag{4.19}$$

$\mathcal{D}_A^{(n)}$ is a weakly coupled theory with only two asymptotic phases in the IR. Integrating out $\hat{\lambda}^{(n)}$ for negative mass provides the topological theory that describes the negative mass asymptotic theory, which shares the quantum region of the original theory. Thus, the quantum phase is given by

$$Q_{II}^d \left[SU(N)_k\right] : \left(ST^2\right)^{\lceil \frac{N}{k} \rceil - 2} U\left(N - \left\lceil \frac{N}{k} \right\rceil k + k\right)_{-N + \lceil \frac{N}{k} \rceil k, N - \lceil \frac{N}{k} \rceil k + 2k} . \tag{4.20}$$

4.3 On the possibility of a two dimensional phase diagram

In this section, we discuss some work in progress to construct the two-dimensional phase diagram of QCD_3 with two distinct adjoint fermions λ^{adj} and ψ^{adj} [3]. The phase diagrams of the two adjoints with equal masses become the phases on the diagonal line of the two-dimensional phase diagram.

Following the lead of [2, 61], one may find the asymptotic theories when we send one of the masses to $\pm\infty$ then deal with the theory left as a one-dimensional problem. However, this will only yield asymptotic phases: asymptotic topological theories and quantum areas when only one of the masses is small. The region where the mass of the two fermions are small, for strongly-coupled theory, remains unknown except on the diagonal. The phase diagram of QCD_3 with two adjoints is divided into three cases as before: $k \geq N$, $N/2 \leq k < N$, and $0 < k < N/2$.

For $k \geq N$, the theory is weakly coupled and is described semiclassically via four topological quantum field theories. Hence integrating out the two fermions for various mass sign combinations gives

$$\begin{aligned} &\mathrm{T}_1 : SU(N)_{k+N} \quad \longleftrightarrow \; U(k+N)_{-N,-N}\,, \\ &\mathrm{T}_2 = \mathrm{T}_4 : SU(N)_k \longleftrightarrow U(k)_{-N,-N}\,, \\ &\mathrm{T}_4 : SU(N)_{k-N} \longleftrightarrow U(k-N)_{-N,-N}\,. \end{aligned} \tag{4.21}$$

These topological theories are separated by lines of critical theories at which one of the fermions become massless. The critical theories are given by

$$\begin{aligned} &\mathcal{C}^{\pm}_{\lambda} : SU(N)_{k\pm\frac{N}{2}} + \lambda_0^{adj}\,, \\ &\mathcal{C}^{\pm}_{\psi} : SU(N)_{k\pm\frac{N}{2}} + \psi_0^{adj}\,. \end{aligned} \tag{4.22}$$

The subscript 0 indicates to the fermion being massless. The phase diagram is simple as shown in figure 4.6.

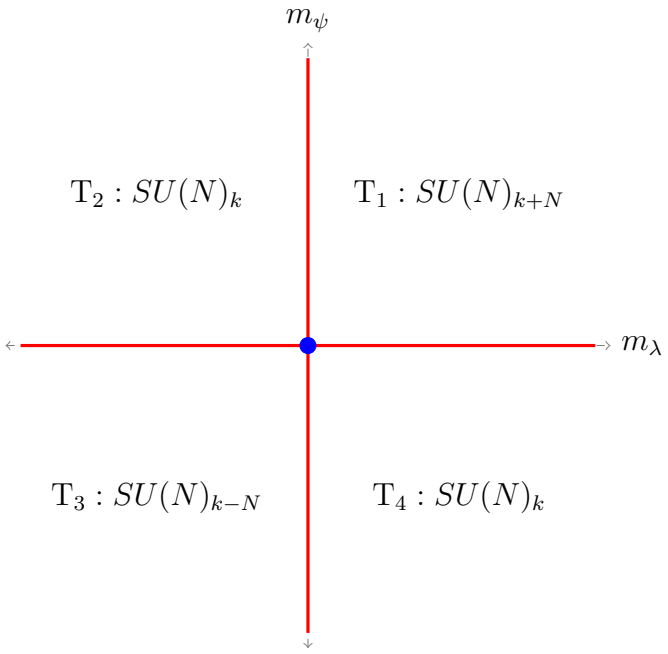

Figure 4.6: Phases of $SU(N)_k + \lambda^{adj} + \psi^{adj}$ with $k \geq N$. The blue point is the point where both fermions are massless. The red lines are the critical lines separating the four asymptotic theories.

For $N/2 \leq k < N$, we expect quantum phases to fill the small mass regions. Integrating out ψ first leads to $SU(N)_{k+N/2}+\lambda^{adj}$ for $m_\psi \to \infty$ and $SU(N)_{k-N/2}+\lambda^{adj}$ for $m_\psi \to -\infty$. Each of the previous theories is a one-dimensional problem, where the first is weakly-coupled with $k + N/2 \geq N/2$ and the second is strongly-coupled with $|k - N/2| < N/2$.

The remaining theory $SU(N)_{k+N/2} + \lambda^{adj}$ has only two topological theories in its phase which are: T_1 for large positive m_λ and T_2 for large negative m_λ. The phase diagram is then represented by a line in the two-dimensional picture. This line describes the phases above the positive critical point of the m_ψ axis (m_ψ^+): T_1 and T_2 separated by a transition point on the red line.

For $SU(N)_{k-N/2} + \lambda^{adj}$, we require a quantum phase to separate the two asymptotic theories: T_4 for large positive m_λ and $\tilde{T}_3 : SU(N)_{k-N} \leftrightarrow U(N-k)_{N,N}$ for large negative m_λ. One may then define dual theories to find the quantum region that separates $\tilde{T}_3$ and T_4. The dual theories for this case are defined by $\mathcal{D}_A : U(N-k)_{\frac{N+k}{2},N} + \hat{\lambda}^{adj}$ near m_λ^- and $\mathcal{D}_B : U(k)_{\frac{k}{2}-N,-N} + \tilde{\lambda}^{adj}$ near m_λ^+. The

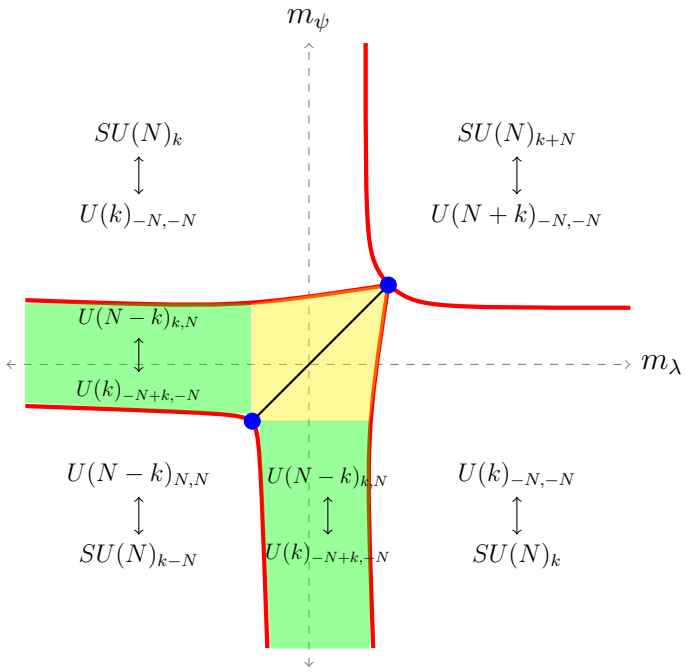

Figure 4.7: Possible phase diagram for $SU(N)_k + \lambda^{adj} + \psi^{adj}$ for $\frac{N}{2} \leq k < N$. The solid black line is represented by equation (4.9). The green regions are the quantum phases Q_{23} and Q_{34}. The shaded yellow regions are unknown areas.

two dual theories are weakly-coupled for this range of k. The quantum phase is now given by $Q_{34} : U(N-k)_{k,N} \leftrightarrow U(k)_{-N+k,-N}$.

The analysis is also similar for other large masses cases when we integrate out λ first. The quantum region separating the asymptotic theories is exactly the same $Q_{23} = Q_{34}$, while the quantum region on the diagonal is given by Q_I^d as in equation (4.9). However, it is not clear which quantum phase covers the regions right off the diagonal. The expected phase diagram for this range of k is shown in figure 4.7.

The same problem arises in the case $k < N/2$, where we are unable to locate the quantum regions off the diagonal line and inside the mass ranges $(m_\psi^\pm, m_\lambda^\pm)$. The following alternative resolutions can be considered:

- We can start from the critical theories with two massless adjoint fermions and perturb these theories via a potential. This is similar to the fundamental QCD_3 case where we get the phases around each critical point. The question now is what type of potential can we use to deform these massless theories? Any suggested potential should recover the quantum regions of the two

degenerate adjoints case, which can be a good exercise towards the phases of the interior region of the two-dimensional diagram.

- We may perturb the quantum region on the diagonal via mass deformation by adding either δm_λ or δm_ψ to the fermion masses. This should give us the theories above and below the diagonal line. The problem with this suggestion is that the two dual theories that describe the critical blue points are significantly different, with one being weakly-coupled and the other strongly-coupled. It becomes significantly more challenging for the $k < N/2$ range when both theories are strongly-coupled.

- One can consider starting from $\mathcal{N} = 1$ supersymmetry as in the single adjoint case. Then couple it to adjoint matter multiplet by adding a scalar ϕ^{adj} in the adjoint representation and another adjoint fermion. The scalar comes from the dimensional reduction of the four-dimensional theory. The theory has $\mathcal{N} = 2$ supersymmetry for the particular choice $m_\lambda = m_\psi = m_\phi = -kg^2/2\pi$. Altering one of the fermion masses breaks supersymmetry to $\mathcal{N} = 1$ supersymmetry whose phase diagram is well established in [66]. Turning on soft breaking symmetry mass for both fermions completely breaks supersymmetry to the theory of interest. A small deformation around the $m_\phi = 0$ point may shed light on the phases off the diagonal. The phase diagram will be slightly different since the transition points will be shifted as a result of the scalar. The phase diagram will include lines representing the phases of $\mathcal{N} = 1$ theory as defined in [66].

Chapter 5

Conclusions and discussions

We studied the IR dynamics of $SU(N)$ gauge theory coupled to a Chern-Simons term of level k and matter in different representations. The general Lagrangian density for our theory is

$$\mathscr{L}_{SU(N)_k} = -\frac{1}{4g^2}\mathrm{Tr}\mathcal{F}^2 + \frac{k}{4\pi}\mathrm{Tr}\left(AdA - \frac{2i}{3}A^3\right) + \mathscr{L}_{\text{matter}}\,, \tag{5.1}$$

where the matter term is given by

$$\mathscr{L}_{\text{matter}} = \begin{cases} \sum_{j=1}^{F}\left(i\bar{\psi}^j \not{D}\psi_j + \frac{m_\psi}{4\pi}\bar{\psi}^j\psi_j\right), & \text{for the fundamental case.} \\ = i\bar{\lambda}\not{D}\lambda + \frac{m}{4\pi}\bar{\lambda}\lambda, & \text{for the adjoint case.} \end{cases} \tag{5.2}$$

The first is a theory coupled to F fermions ψ in the fundamental representation, while the second is a theory coupled to a single Majorana fermion λ in the adjoint representation.

The two theories differ primarily in that the normalisation condition on the Chern-Simons level demands $F/2 + k \in \mathbb{Z}$ for the fundamental case and $N/2 + k \in \mathbb{Z}$ for the adjoint case. Both theories have time-reversal symmetry for $k = m = 0$. The fundamental theory possesses a $U(F)$ global symmetry that

rotates the flavours (m_ψ preserves this symmetry), whereas the adjoint theory lacks this symmetry. The fundamental theory, on the other hand, has no one-form symmetry, whereas the adjoint theory has a $\mathbb{Z}_N$ one-form symmetry [82, 83]. Finally, integrating the matter results in a shift in the Chern-Simons level given by

$$k_{IR} = \begin{cases} k + \text{sgn}(m_\psi)\frac{F}{2}, & \text{for the fundamental case} \\ k + \text{sgn}(m_\lambda)\frac{N}{2}, & \text{for the adjoint case}. \end{cases} \quad . \tag{5.3}$$

These two theories have decoupling limits where they could be described semiclassically

1. **For large** m **(**$|m| \gg g^2$**)**: The fermions decouple even before the interaction starts, and the theory is already weakly-coupled with heavy matter. The Yang-Mills term is also negligible in this limit since it has higher derivatives than the Chern-Simons term. As a result, we integrate the fermion(s) out to get pure topological field theories whose levels are governed by the shifts defined in equation (5.3).

2. **For large** k **(**$k \gg N$ **or** $k \gg 1$**)**: The gauge field is heavy with a mass of $kg^2 \gg g^2N$, and then it decouples before the interaction. The remaining light fields weakly interact, and there is a weakly-coupled conformal field theory if we tune m (Qualitatively, we tune m to zero). To decide the limit of how large k should be to keep the theory as weakly-coupled as possible, we make use of the following: For the fundamental theory, Aharony introduced a dual bosonic description defined in equation (1.34) which holds for $k \geq F/2$. On the other side, there is an $\mathcal{N} = 1$ supersymmetry for the adjoint case when we take the particular choice of $m_\lambda = -kg^2/2\pi$, and Witten argued that it is spontaneously broken for $k < N/2$. The decoupling limits remain valid for $k \geq F/2$ for the fundamental theory and $k \geq N/2$ for the adjoint theory.

To follow the story of the IR dynamics of QCD_3, new phases that do not occur semiclassically have been introduced (for this reason, we call them quantum phases). The presence of the scalar theory that is dual to the fundamental QCD_3 suggests the existence of a non-linear sigma model in the phase diagram, which does not appear semiclassically. The supersymmetry breakdown scenario, on the other hand, implies the presence of a massless Goldstino in the phase diagram, which cannot meet the $\mathbb{Z}_N$ one-form symmetry.

We started the thesis with the phases of the fundamental QCD_3 coupled to F fermions. We reviewed the conjectured quantum phases introduced when the theory is strongly-coupled. For $k \geq F/2$, the phase diagram has only two asymptotic theories described by the topological theories $SU(N)_{k\pm F/2}$ separated by a phase transition. The phase transition could be first or second order, or a series of first-order phase transitions as in the large N limit [67, 68, 70]. For $k < F/2$, the theory has the same asymptotic phases for large mass separated by a quantum phase represented by a non-linear sigma model with a Grassmannian as in equation (2.3). The transition point is split into two, and a boson/fermion duality is introduced near each point.

The next natural step towards the fundamental theory was to split the F fermions into two families with distinct masses [2, 61]. The theory is then $SU(N)_k + p\psi_1 + (F-p)\psi_2$. We covered the details of this theory resulting in a two-dimensional phase diagram with only four topological theories given by equations (2.10), (2.11) and (2.14). The phase diagram has sigma-models with various Grassmannians describing the quantum regions.

As the core of this thesis, we investigated the IR behaviour of $SU(N)$ gauge theory coupled to three families of flavours in the fundamental representation, expanding the prior work for one family [1] and two families [2, 61]. Our description covers the entire phase diagram in all the possible ranges of the Chern-Simons level. Our approach yields a three-dimensional phase diagram that is semiclassically well defined by topological gapped phases for $k \geq F/2$, as in the one and two-family

cases. In addition to topological phases, we come across one-dimensional sigma models, planar sigma models, and cuboid sigma models, all of which are quantum phases. The cuboid sigma models, which occur when one of the fermion masses becomes small, are an inherent feature of the three-dimensional phase diagram.

We also provided consistency checks such as matching the phases of the bosonic dual descriptions with the fermionic ones and perturbing the diagonal sigma-model via mass deformations to match the off-diagonal lines phases. The reduction to the two-family case by describing the various planes when two of the masses are equal reproduces the results of [2, 61].

In chapter 4, we revisited the work of the adjoint QCD_3 with both single and double adjoint fermions. The phase diagram has a quantum phase, in the form of a topological theory, for sufficiently small k values. The quantum phases are conjectured via introducing new fermion-fermion dualities that hold near each critical point. The theory with two degenerate adjoint fermions requires a series of fermion-fermion dualities by applying a process known as the "Duality Chain" defined in [84]. The main task of the duality chain process is to reduce the rank of the new dual theory until we reach a weakly-coupled theory whose asymptotic theory shares the quantum region of the original theory. The possibility of constructing a two-dimensional phase diagram of the two adjoint theory has also been discussed with some possible resolutions to the unknown phases.

One of the most important applications of studying the dynamics of three-dimensional theories is that they are linked to the dynamics of problems in 4d and their domain walls. The Yang-Mills theories in 4d, when coupled to either an adjoint fermion or fundamental Dirac fermions, have degenerate vacua, each of which is gapped and trivial. As a result, three-dimensional theories exist within the domain walls of their four-dimensional equivalents. The symmetries and anomalies of these domain walls are the same as those of the 3d theories. In some circumstances, their phases may be explicitly estimated using techniques in 4d, and the quantum phases can be discovered. For example, the QCD_4 with $F = 2$

heavy quarks and $\theta = \pi$ has two ground states for nonzero positive mass. We have $SU(2)_1$ TQFT on the wall for large m, and the coset $\frac{U(2)}{U(1)\times U(1)} \approx \mathbb{CP}^1$ on the wall for small m [64, 85].

The $2+1$ dimensions techniques has also shed light to some $\mathcal{N} = 1$ supersymmetric theories in 4d with simply connected gauge groups ($SU(N)$, $Sp(N)$, and $Spin(N)$). We notice that the quantum phase for the $SU(N)_k + \lambda^{adj}$ coincides with results from the domain wall theories of four dimensional $\mathcal{N} = 1$ $SU(N)$ SYM defined in [86]. The quantum phase of the same theory with $Spin(N)$ was also identified from the 3d techniques in [79].

We hope to finish the two-dimensional phase diagram for the adjoint case in the near future. The large N computations show that the phase transitions appearing on the phase diagram of theory with fundamental flavours are represented by a series of first-order phase transitions in both the one and two-family case [67–69, 87]. It would be interesting to perform the large N implementation for the three-family case to have a flavour of the critical theories on the three-dimensional picture. We also seek a better understanding of the types of phase transitions that we encountered in the adjoint QCD_3.

References

[1] Zohar Komargodski and Nathan Seiberg. A symmetry breaking scenario for QCD_3. *JHEP*, 01:109, 2018. doi: 10.1007/JHEP01(2018)109.

[2] Riccardo Argurio, Matteo Bertolini, Francesco Mignosa, and Pierluigi Niro. Charting the phase diagram of QCD_3. *JHEP*, 08:153, 2019. doi: 10.1007/JHEP08(2019)153.

[3] Abdullah Khalil and Radu Tatar. Phases of QCD_3 with three families of fundamental flavors. *Eur. Phys. J. C*, 80(9):805, 2020. doi: 10.1140/epjc/s10052-020-8385-9.

[4] Jaume Gomis, Zohar Komargodski, and Nathan Seiberg. Phases Of Adjoint QCD_3 And Dualities. *SciPost Phys.*, 5(1):007, 2018. doi: 10.21468/SciPostPhys.5.1.007.

[5] Abdullah Khalil and Radu Tatar. In preparation.

[6] Changha Choi. Phases of Two Adjoints QCD_3 And a Duality Chain. *JHEP*, 04:006, 2020. doi: 10.1007/JHEP04(2020)006.

[7] N. Seiberg. Electric - magnetic duality in supersymmetric nonAbelian gauge theories. *Nucl. Phys. B*, 435:129–146, 1995. doi: 10.1016/0550-3213(94)00023-8.

[8] N. Seiberg. The Power of duality: Exact results in 4-D SUSY field theory. *Prog. Theor. Phys. Suppl.*, 123:337–347, 1996. doi: 10.1142/S0217751X01005705.

[9] Kenneth A. Intriligator and N. Seiberg. Lectures on supersymmetric gauge theories and electric-magnetic duality. *Nucl. Phys. B Proc. Suppl.*, 45BC: 1–28, 1996. doi: 10.1016/0920-5632(95)00626-5.

[10] Andreas Karch. Seiberg duality in three-dimensions. *Phys. Lett. B*, 405: 79–84, 1997. doi: 10.1016/S0370-2693(97)00598-4.

[11] Vasilis Niarchos. Seiberg dualities and the 3d/4d connection. *JHEP*, 07:075, 2012. doi: 10.1007/JHEP07(2012)075.

[12] Ofer Aharony, Shlomo S. Razamat, Nathan Seiberg, and Brian Willett. 3d dualities from 4d dualities. *JHEP*, 07:149, 2013. doi: 10.1007/JHEP07(2013)149.

[13] Ofer Aharony, Shlomo S. Razamat, Nathan Seiberg, and Brian Willett. $3d$ dualities from $4d$ dualities for orthogonal groups. *JHEP*, 08:099, 2013. doi: 10.1007/JHEP08(2013)099.

[14] Antonio Amariti, Davide Forcella, Claudius Klare, Domenico Orlando, and Susanne Reffert. 4D/3D reduction of dualities: mirrors on the circle. *JHEP*, 10:048, 2015. doi: 10.1007/JHEP10(2015)048.

[15] Antonio Amariti, Csaba Csáki, Mario Martone, and Nicolas Rey-Le Lorier. From 4D to 3D chiral theories: Dressing the monopoles. *Phys. Rev. D*, 93 (10):105027, 2016. doi: 10.1103/PhysRevD.93.105027.

[16] Antonio Amariti. 4d/3d reduction of s-confining theories: the role of the "exotic" D instantons. *JHEP*, 02:139, 2016. doi: 10.1007/JHEP02(2016)139.

[17] Antonio Amariti, Domenico Orlando, and Susanne Reffert. String theory and the 4D/3D reduction of Seiberg duality. A review. *Phys. Rept.*, 705-706:1–53, 2017. doi: 10.1016/j.physrep.2017.08.002.

[18] Antonio Amariti and Marco Fazzi. Dualities for three-dimensional $\mathcal{N} = 2$ $SU(N_c)$ chiral adjoint SQCD. *JHEP*, 11:030, 2020. doi: 10.1007/JHEP11(2020)030.

[19] E. Fradkin and A. Lopez. Fractional Quantum Hall effect and Chern-Simons gauge theories. *Phys. Rev. B*, 44:5246–5261, 1991. doi: 10.1103/PhysRevB.44.5246.

[20] A. Zee. Quantum Hall fluids. *Lect. Notes Phys.*, 456:99–153, 1995. doi: 10.1007/BFb0113369.

[21] Xiao-Gang Wen. Topological orders and edge excitations in FQH states. *Adv. Phys.*, 44(5):405–473, 1995. doi: 10.1080/00018739500101566.

[22] Edward Witten. Three lectures on topological phases of matter. *Riv. Nuovo Cim.*, 39(7):313–370, 2016. doi: 10.1393/ncr/i2016-10125-3.

[23] David Tong. Lectures on the Quantum Hall Effect. 6 2016.

[24] Shiin-Shen Chern and James Simons. Characteristic forms and geometric invariants. *Annals Math.*, 99:48–69, 1974. doi: 10.2307/1971013.

[25] Albert S. Schwarz. The Partition Function of a Degenerate Functional. *Commun. Math. Phys.*, 67:1–16, 1979. doi: 10.1007/BF01223197.

[26] Jonathan F. Schonfeld. A Mass Term for Three-Dimensional Gauge Fields. *Nucl. Phys. B*, 185:157–171, 1981. doi: 10.1016/0550-3213(81)90369-2.

[27] R. Jackiw and S. Templeton. How Superrenormalizable Interactions Cure their Infrared Divergences. *Phys. Rev. D*, 23:2291, 1981. doi: 10.1103/PhysRevD.23.2291.

[28] Stanley Deser, R. Jackiw, and S. Templeton. Three-Dimensional Massive Gauge Theories. *Phys. Rev. Lett.*, 48:975–978, 1982. doi: 10.1103/PhysRevLett.48.975.

[29] Stanley Deser, R. Jackiw, and S. Templeton. Topologically Massive Gauge Theories. *Annals Phys.*, 140:372–411, 1982. doi: 10.1016/0003-4916(82)90164-6. [Erratum: Annals Phys. 185, 406 (1988)].

[30] Edward Witten. Quantum Field Theory and the Jones Polynomial. *Commun. Math. Phys.*, 121:351–399, 1989. doi: 10.1007/BF01217730.

[31] Gerald V. Dunne. Aspects of Chern-Simons theory. In *Les Houches Summer School in Theoretical Physics, Session 69: Topological Aspects of Low-dimensional Systems*, 7 1998.

[32] Sidney R. Coleman. The Uses of Instantons. *Subnucl. Ser.*, 15:805, 1979.

[33] J. Wess and B. Zumino. Consequences of anomalous Ward identities. *Phys. Lett. B*, 37:95–97, 1971. doi: 10.1016/0370-2693(71)90582-X.

[34] Edward Witten. Global Aspects of Current Algebra. *Nucl. Phys. B*, 223: 422–432, 1983. doi: 10.1016/0550-3213(83)90063-9.

[35] Tomoki Nakanishi and Akihiro Tsuchiya. Level rank duality of WZW models in conformal field theory. *Commun. Math. Phys.*, 144:351–372, 1992. doi: 10.1007/BF02101097.

[36] P. Goddard, A. Kent, and David I. Olive. Virasoro Algebras and Coset Space Models. *Phys. Lett. B*, 152:88–92, 1985. doi: 10.1016/0370-2693(85)91145-1.

[37] Po-Shen Hsin and Nathan Seiberg. Level/rank Duality and Chern-Simons-Matter Theories. *JHEP*, 09:095, 2016. doi: 10.1007/JHEP09(2016)095.

[38] Cyril Closset, Thomas T. Dumitrescu, Guido Festuccia, Zohar Komargodski, and Nathan Seiberg. Contact Terms, Unitarity, and F-Maximization in Three-Dimensional Superconformal Theories. *JHEP*, 10:053, 2012. doi: 10.1007/JHEP10(2012)053.

[39] Cyril Closset, Thomas T. Dumitrescu, Guido Festuccia, Zohar Komargodski, and Nathan Seiberg. Comments on Chern-Simons Contact Terms in Three Dimensions. *JHEP*, 09:091, 2012. doi: 10.1007/JHEP09(2012)091.

[40] Sachin Jain, Shiraz Minwalla, and Shuichi Yokoyama. Chern Simons duality with a fundamental boson and fermion. *JHEP*, 11:037, 2013. doi: 10.1007/JHEP11(2013)037.

[41] Guy Gur-Ari and Ran Yacoby. Three Dimensional Bosonization From Supersymmetry. *JHEP*, 11:013, 2015. doi: 10.1007/JHEP11(2015)013.

[42] Simone Giombi and Xi Yin. On Higher Spin Gauge Theory and the Critical O(N) Model. *Phys. Rev. D*, 85:086005, 2012. doi: 10.1103/PhysRevD.85.086005.

[43] Simone Giombi, Shiraz Minwalla, Shiroman Prakash, Sandip P. Trivedi, Spenta R. Wadia, and Xi Yin. Chern-Simons Theory with Vector Fermion Matter. *Eur. Phys. J. C*, 72:2112, 2012. doi: 10.1140/epjc/s10052-012-2112-0.

[44] Ofer Aharony, Guy Gur-Ari, and Ran Yacoby. Correlation Functions of Large N Chern-Simons-Matter Theories and Bosonization in Three Dimensions. *JHEP*, 12:028, 2012. doi: 10.1007/JHEP12(2012)028.

[45] Juan Maldacena and Alexander Zhiboedov. Constraining conformal field theories with a slightly broken higher spin symmetry. *Class. Quant. Grav.*, 30:104003, 2013. doi: 10.1088/0264-9381/30/10/104003.

[46] Simone Giombi and Xi Yin. The Higher Spin/Vector Model Duality. *J. Phys. A*, 46:214003, 2013. doi: 10.1088/1751-8113/46/21/214003.

[47] Ofer Aharony, Simone Giombi, Guy Gur-Ari, Juan Maldacena, and Ran Yacoby. The Thermal Free Energy in Large N Chern-Simons-Matter Theories. *JHEP*, 03:121, 2013. doi: 10.1007/JHEP03(2013)121.

[48] Sachin Jain, Shiraz Minwalla, Tarun Sharma, Tomohisa Takimi, Spenta R. Wadia, and Shuichi Yokoyama. Phases of large N vector Chern-Simons theories on $S^2 \times S^1$. *JHEP*, 09:009, 2013. doi: 10.1007/JHEP09(2013)009.

[49] Sachin Jain, Mangesh Mandlik, Shiraz Minwalla, Tomohisa Takimi, Spenta R. Wadia, and Shuichi Yokoyama. Unitarity, Crossing Symmetry and Duality of the S-matrix in large N Chern-Simons theories with fundamental matter. *JHEP*, 04:129, 2015. doi: 10.1007/JHEP04(2015)129.

[50] Shiraz Minwalla and Shuichi Yokoyama. Chern Simons Bosonization along RG Flows. *JHEP*, 02:103, 2016. doi: 10.1007/JHEP02(2016)103.

[51] Guy Gur-Ari, Sean A. Hartnoll, and Raghu Mahajan. Transport in Chern-Simons-Matter Theories. *JHEP*, 07:090, 2016. doi: 10.1007/JHEP07(2016)090.

[52] Indranil Halder and Shiraz Minwalla. Matter Chern Simons Theories in a Background Magnetic Field. *JHEP*, 11:089, 2019. doi: 10.1007/JHEP11(2019)089.

[53] Ofer Aharony and Adar Sharon. Large N renormalization group flows in 3d $\mathcal{N} = 1$ Chern-Simons-Matter theories. *JHEP*, 07:160, 2019. doi: 10.1007/JHEP07(2019)160.

[54] Ofer Aharony. Baryons, monopoles and dualities in Chern-Simons-matter theories. *JHEP*, 02:093, 2016. doi: 10.1007/JHEP02(2016)093.

[55] Đorđe Radičević. Disorder Operators in Chern-Simons-Fermion Theories. *JHEP*, 03:131, 2016. doi: 10.1007/JHEP03(2016)131.

[56] Nathan Seiberg, T. Senthil, Chong Wang, and Edward Witten. A Duality Web in 2+1 Dimensions and Condensed Matter Physics. *Annals Phys.*, 374:395–433, 2016. doi: 10.1016/j.aop.2016.08.007.

[57] Andreas Karch and David Tong. Particle-Vortex Duality from 3d Bosonization. *Phys. Rev.*, X6(3):031043, 2016. doi: 10.1103/PhysRevX.6.031043.

[58] Jeff Murugan and Horatiu Nastase. Particle-vortex duality in topological insulators and superconductors. *JHEP*, 05:159, 2017. doi: 10.1007/JHEP05(2017)159.

[59] Francesco Benini. Three-dimensional dualities with bosons and fermions. *JHEP*, 02:068, 2018. doi: 10.1007/JHEP02(2018)068.

[60] Kristan Jensen. A master bosonization duality. *JHEP*, 01:031, 2018. doi: 10.1007/JHEP01(2018)031.

[61] Andrew Baumgartner. Phases of flavor broken QCD_3. *JHEP*, 10:288, 2019. doi: 10.1007/JHEP10(2019)288.

[62] Edward Witten. Fermion Path Integrals And Topological Phases. *Rev. Mod. Phys.*, 88(3):035001, 2016. doi: 10.1103/RevModPhys.88.035001.

[63] Thomas Appelquist and Daniel Nash. Critical Behavior in (2+1)-dimensional QCD. *Phys. Rev. Lett.*, 64:721, 1990. doi: 10.1103/PhysRevLett.64.721.

[64] Davide Gaiotto, Zohar Komargodski, and Nathan Seiberg. Time-reversal breaking in QCD_4, walls, and dualities in $2 + 1$ dimensions. *JHEP*, 01:110, 2018. doi: 10.1007/JHEP01(2018)110.

[65] Davide Gaiotto, Anton Kapustin, Zohar Komargodski, and Nathan Seiberg. Theta, Time Reversal, and Temperature. *JHEP*, 05:091, 2017. doi: 10.1007/JHEP05(2017)091.

[66] Vladimir Bashmakov, Jaume Gomis, Zohar Komargodski, and Adar Sharon. Phases of $\mathcal{N} = 1$ theories in $2 + 1$ dimensions. *JHEP*, 07:123, 2018. doi: 10.1007/JHEP07(2018)123.

[67] Adi Armoni, Thomas T. Dumitrescu, Guido Festuccia, and Zohar Komargodski. Metastable vacua in large-N QCD_3. *JHEP*, 01:004, 2020. doi: 10.1007/JHEP01(2020)004.

[68] Riccardo Argurio, Adi Armoni, Matteo Bertolini, Francesco Mignosa, and Pierluigi Niro. Vacuum structure of large N QCD_3 from holography. *JHEP*, 07:134, 2020. doi: 10.1007/JHEP07(2020)134.

[69] Andrew Baumgartner. Flavor broken QCD_3 at large N. *JHEP*, 08:145, 2020. doi: 10.1007/JHEP08(2020)145.

[70] Takuya Kanazawa, Mario Kieburg, and Jacobus J. M. Verbaarschot. Cascade of phase transitions in a planar Dirac material. *JHEP*, 21:015, 2020. doi: 10.1007/JHEP06(2021)015.

[71] Cumrun Vafa and Edward Witten. Eigenvalue Inequalities for Fermions in Gauge Theories. *Commun. Math. Phys.*, 95:257, 1984. doi: 10.1007/BF01212397.

[72] Deog Ki Hong and Ho-Ung Yee. Holographic aspects of three dimensional QCD from string theory. *JHEP*, 05:036, 2010. doi: 10.1007/JHEP05(2010)036. [Erratum: JHEP 08, 120 (2010)].

[73] Edward Witten. Supersymmetric index of three-dimensional gauge theory. pages 156–184, 1999. doi: 10.1142/9789812793850_0013.

[74] Hsein-Chung Kao, Ki-Myeong Lee, and Taejin Lee. The Chern-Simons coefficient in supersymmetric Yang-Mills Chern-Simons theories. *Phys. Lett.*, B373:94–99, 1996. doi: 10.1016/0370-2693(96)00119-0.

[75] Edward Witten. The "Parity" Anomaly On An Unorientable Manifold. *Phys. Rev. B*, 94(19):195150, 2016. doi: 10.1103/PhysRevB.94.195150.

[76] Yuji Tachikawa and Kazuya Yonekura. On time-reversal anomaly of 2+1d topological phases. *PTEP*, 2017(3):033B04, 2017. doi: 10.1093/ptep/ptx010.

[77] Yuji Tachikawa and Kazuya Yonekura. More on time-reversal anomaly of 2+1d topological phases. *Phys. Rev. Lett.*, 119(11):111603, 2017. doi: 10.1103/PhysRevLett.119.111603.

[78] Francesco Benini, Po-Shen Hsin, and Nathan Seiberg. Comments on global symmetries, anomalies, and duality in $(2 + 1)$d. *JHEP*, 04:135, 2017. doi: 10.1007/JHEP04(2017)135.

[79] Clay Córdova, Po-Shen Hsin, and Nathan Seiberg. Time-Reversal Symmetry, Anomalies, and Dualities in (2+1)d. *SciPost Phys.*, 5(1):006, 2018. doi: 10.21468/SciPostPhys.5.1.006.

[80] Clay Cordova, Po-Shen Hsin, and Nathan Seiberg. Global Symmetries, Counterterms, and Duality in Chern-Simons Matter Theories with Orthogonal Gauge Groups. *SciPost Phys.*, 4(4):021, 2018. doi: 10.21468/SciPostPhys.4.4.021.

[81] Edward Witten. SL(2,Z) action on three-dimensional conformal field theories with Abelian symmetry. In *From Fields to Strings: Circumnavigating Theoretical Physics: A Conference in Tribute to Ian Kogan*, pages 1173–1200, 7 2003.

[82] Anton Kapustin and Nathan Seiberg. Coupling a QFT to a TQFT and Duality. *JHEP*, 04:001, 2014. doi: 10.1007/JHEP04(2014)001.

[83] Davide Gaiotto, Anton Kapustin, Nathan Seiberg, and Brian Willett. Generalized Global Symmetries. *JHEP*, 02:172, 2015. doi: 10.1007/JHEP02(2015)172.

[84] Changha Choi, Martin Roček, and Adar Sharon. Dualities and Phases of $3DN = 1$ SQCD. *JHEP*, 10:105, 2018. doi: 10.1007/JHEP10(2018)105.

[85] Riccardo Argurio, Matteo Bertolini, Francesco Bigazzi, Aldo L. Cotrone, and Pierluigi Niro. QCD domain walls, Chern-Simons theories and holography. *JHEP*, 09:090, 2018. doi: 10.1007/JHEP09(2018)090.

[86] Bobby Samir Acharya and Cumrun Vafa. On domain walls of N=1 supersymmetric Yang-Mills in four-dimensions. 3 2001.

[87] Kristan Jensen and Priti Patil. Chern-Simons dualities with multiple flavors at large N. *JHEP*, 12:043, 2019. doi: 10.1007/JHEP12(2019)043.